A functional analysis of the Nup188-Nup93 complex in the Nuclear Pore Complex

der Fakultät für Biologie

der **E**BERHARD **K**ARLS **U**NIVERSITÄT **T**ÜBINGEN

zur Erlangung des Grades eines Doktors
der Naturwissenschaften

von

Boopathy Gandhi Theerthagiri Kuppusamy

aus Dharmapuri, Tamil Nadu, India

vorgelegte

Dissertation

2010

Tag der mündlichen Prüfung: 14. 10. 2010

Dekan:	Prof. Dr. W. Rosenstiel
1. Berichterstatter:	Prof. Dr. Andrei N. Lupas
2. Berichterstatter:	Prof. Dr. Alfred Nordheim

Dedicated to my Mom and Dad

Acknowledgements

I am heartily thankful to my supervisor, Dr. Wolfram Antonin for his patience, motivation, enthusiasm. He supported during good and bad times of my PhD through with his personal and professional advice for which I am always grateful. I could not have imagined having a better advisor and mentor for my Ph.D study. It has been an honor to be his first Ph.D student.

I am very grateful to Prof. Dr. Alfred Nordheim, Prof. Dr. Andrei Lupas, and Dr. Dmitri Ivanov for having been my Ph.D advisory committee (PAC) members. All of their encouragement, suggestions and discussions during the PAC meeting greatly helped me to complete this study.

I thank Dr. Adriana Magalska, Nathalie Eisenhardt, Ruchika Sachdev, Benjamin Vollmer, Cornelia Sieverding, Allana Schooley, Philipp Wild, and Josef Redolfi for their immense contribution to my time at the lab. The group has been a source of friendships as well as good advice and support. I will surely miss this very supportive and talented group.

I thank the Max-Planck-Society for the scholarship throughout my Ph.D study.

FML is a fantastic place to work as there are many people that contribute to making all kinds of experiments efficient. I thank the technical staffs for their cooperation and for being very kind. I thank Nadine Weiss for her love on maintaining frogs and rabbits. I thank Dr. Antonio Virgilio Failla for his helpful suggestions concerning confocal microscopy.

I thank my friends Khaleel and Pratheep for their time and personal support. I also would like to thank Max-Planck-Indian group for the 'Friday dinners,' every single dinner was memorable and I will miss them.

I am forever indebted to my parents, brother, sister and my wife Kavitha for their love, constant support and encouragement. Despite a long distance, their support was highly instrumental and I really cannot thank them enough.

Summary

The determining property of eukaryotes is the compartmentalization of genetic information inside the cell nucleus. This compartmentalization by the nuclear envelope (NE) enables the eukaryotic cell to separate transcription and translation in space and time. The NE is composed of two membranes, the outer (ONM) and inner nuclear membrane (INM). The ONM is an extension of the endoplasmic reticulum whereas the INM contacts chromatin and the nuclear lamina, and is connected to the ONM via the pore membrane, the region where nuclear pore complexes (NPCs) are localized. Although, these membranes are continuous with each other, the INM contains a distinct set of proteins and the mechanism of INM protein targeting is not yet completely understood. NPCs are the gateway to the nucleus; they are embedded on the NE where INM and ONM are fused. They are about 60 MDa in vertebrates, and, are comprised of around 30 distinct proteins called nucleoporins or nups many which nucleoporins form subcomplexes that act as building blocks for NPC assembly.

This thesis aims to characterize the Nup188-Nup93 complex during NPC assembly and function. One of the evolutionarily conserved subcomplexes is the Nup93 complex. It is a major structural component of the NPC which is thought to be positioned at the region where the NPC and nuclear membranes interact. In *Xenopus*, the core of the Nup93 complex has been understood to be formed by three proteins: Nup205, Nup188 and Nup93. Using biochemical and cell biological assays we show that Nup93 is not part of a single complex but is in fact a component of two distinct subcomplexes, Nup188-Nup93 and Nup205-Nup93. Using *in vitro* nuclear assembly reactions, we find that neither Nup188-Nup93 nor Nup205-Nup93 is required for NPC or NE formation at the end of mitosis. However, nuclei lacking Nup188-Nup93 increased dramatically in size compared to normal nuclei. Our analysis of Nup188-Nup93 depleted nuclei demonstrates that the DNA content and nucleocytoplasmic transport of soluble proteins, mRNA and small molecules are similar to normal nuclei. We show, through a novel assay, that the enlarged nuclear phenotype observed in the absence of Nup188-Nup93 correlates with an increase in translocation of integral membrane proteins to the INM through NPCs. The phenotype is rescued with recombinant Nup188-Nup93 confirming the specificity of the depletion effect. This work establishes the idea that Nup188-Nup93 limits the passage of membrane proteins through the NPC and is thus crucial for the

homeostasis of nuclear membranes. In addition, our results also strengthen the view that integral membrane proteins of INM reach to the interior of nuclei by passage from the ONM through the NPC in the plane of membrane.

Zusammenfassung

Ein zentrales Charakteristikum in Eukaryonten ist die Kompartimentierung der Erbinformation im Zellkern. Diese Kompartimentierung durch die Kernhülle erlaubt es der eukaryontischen Zelle, Transkription und Translation räumlich und zeitlich voneinander zu trennen. Die Kernhülle besteht aus zwei Membranen, der äußeren und inneren Kernmembran. Die äußere Kernmembran ist ein Ausläufer des endoplasmatischen Reticulums, wohingegen die innere Kernmembran mit Chromatin und der Kernlamina verknüpft ist und mit der äußeren Kernmembran über die Porenmembran, die Region, an der Kernporenkomplexe sitzen, verbunden ist. Obwohl alle diese Membranen miteinander verbunden sind, besitzt die innere Kernmembran eine spezifische Proteinzusammensetzung, wobei noch nicht vollständig verstanden ist, wie diese Proteine dorthin gelangen. Der Zugang zum Zellkern wird durch Kernporenkomplexe ermöglicht. Diese sind an den Punkten, wo die innere mit der äußeren Kernmembran verbunden ist, in die Kernhülle eingebettet. In Vertebraten haben Kernporenkomplexe eine Masse von ca. 60 MDa und sind aus rund 30 verschiedenen Proteinen, sogenannten Nukleoporinen oder Nups, aufgebaut. Viele dieser Nukleoporine sind Teile größerer Unterkomplexe, die die Bausteine für den Aufbau der Kernporenkomplexe bilden.

Diese Arbeit hat zum Ziel, die Bedeutung des Nup188-Nup93-Komplexes für den Aufbau und die Funktion des Kernporenkomplexes zu charakterisieren. Einer der evoluntionär konservierten Unterkomplexe ist der Nup93-Komplex. Er stellt eine bedeutende strukturelle Einheit der Kernpore dar, von der man annimmt, dass sie an der Interaktionsfläche von Kernpore und Kernmembranen lokalisiert ist. In *Xenopus* ging man ursprünglich davon aus, dass die drei Proteine Nup205, Nup188 und Nup93 die Grundeinheit dieses Komplexes bilden. Mittels biochemischer und zellbiologischer Versuche wird hier gezeigt, dass Nup93 nicht nur Teil eines Komplexes, sondern Bestandteil von zwei verschiedenen Unterkomplexen, Nup188-Nup93 und Nup205-Nup93, ist. Mithilfe von *in vitro* Reaktionen zum Kernaufbau wird hier nachgewiesen, dass weder Nup188-Nup93 noch Nup205-Nup93 für den Aufbau von Kernporen und der Kernhülle am Ende der Mitose notwendig sind. Allerdings werden Kerne, denen Nup188-Nup93 fehlt, um ein vielfaches größer als normale

Zellkerne. Unsere Analyse der Nup188-Nup93 depletierten Zellkerne zeigt, dass der DNA-Gehalt sowie der Transport von löslichen Proteinen, mRNA und kleinen Molekülen zwischen Zytosol und Kerninnerem im Vergleich zu Kontrollkernen unverändert bleiben. Mittels eines neuen Versuchssystems wird gezeigt, dass der Phenotyp der vergrösserten Kerne mit einen erhöhten Durchtritt von integralen Membraneproteinen durch die Kernpore zur inneren Kernmembran korreliert. Dieser Phänotyp kann durch die Zugabe von rekombinanten Nup188-Nup93 aufgehoben werden, was die Spezifität der Depletion unterstreicht. Diese Arbeit belegt, dass Nup188-Nup93 den Durchgang von Membranproteinen durch die Kernpore begrenzt und damit maßgeblich für die Homöostase der Kernmembranen ist. Die Ergebnisse untermauern außerdem die Annahme, dass integrale Membranproteine der inneren Kernmembran diese mittels Transport entlang der äußeren Kernmembran und den Durchtritt durch die Kernpore in der Membranebene erreichen.

Table of contents

ACKNOWLEDGEMENTS I

SUMMARY II

ZUSAMMENFASSUNG IV

TABLE OF CONTENTS VI

ABBREVIATIONS VIII

1. INTRODUCTION 10

1.1 The nuclear architecture 2

1.2 The nuclear envelope 3

1.3 The Nuclear pore complex (NPC) 5
1.3.1 Structure and composition of the NPC 6
1.3.2. Structural features of nucleoporins 7
1.3.3. Molecular composition of the nuclear pore complex 10

1.4. Nucleocytoplasmic transport 13
1.4.1. Transport of soluble cargos 14
1.4.2. Transport of integral membrane proteins to the inner nuclear membrane 16

1.5. Experimental systems to study the NE and NPCs 16

1.6. Aims of the project 19

2. RESULTS 20

2.1. Nup188 controls passage of membrane proteins across the nuclear pore complex 21
2.1.1. Generating the tools 21
2.1.2. Nup93 is part of two distinct sub-complexes 21
2.1.3. Depletion of Nup188-Nup93 enlarges the nuclear size and they contain NPCs. 25
2.1.4. Nup188-Nup93 depleted nuclei recruits other nucleoporins and proteins. 29
2.1.5. The Nup188-Nup93 depleted nuclei grow only after the NE is formed. 31
2.1.6. DNA content is not increased in Nup188-Nup93 depleted nuclei: 33
2.1.7. Diffusion barrier of the NPCs on Nup188-Nup93 depleted nuclei is not altered: 34
2.1.8. The rate of nuclear import is not affected during Nup188-Nup93 depletion. 35
2.1.9. Nuclear export of proteins is not affected during Nup188-Nup93 depletion. 38
2.1.10. Nuclear export of mRNA is not affected during Nup188-Nup93 depletion. 39
2.1.11. Blocking of NPCs make Nup188-Nup93 depleted nuclei smaller. 40
2.1.12. ER fragmentation leads to a decrease in the size of Nup188-Nup93 depleted nuclei. 41

2.1.13. Finding a cause for the bigger nuclei 42
2.1.14. An assay to follow the transport of INM proteins 43
2.1.15. Nup188-Nup93 restricts transport of integral membrane proteins through the NPC 46
2.1.16. Only INM proteins could travel into the Nup188-Nup93 depleted nuclei 51
2.1.17. Size limitation of the INM proteins to travel into the Nup188-Nup93 depleted nuclei is still valid 52
2.1.18. Faster transport of proteins to INM is not caused by the increased number of NPCs. 53
2.1.19. INM reporters are not targeted in the nuclei that do not contain NPCs 56

2.2. Nup98 is required for the maintenance of the diffusion barrier of NPCs. 58
2.2.1. Functional investigation of Nup98 in nuclear assembly 58
2.2.2. Immunodepletion of Nup98 58
2.2.3. The size exclusion limit of Nup98 depleted nuclei is altered 60
2.2.4. Immunofluorescence on Nup98 depleted nuclei reveals that levels of the p62 complex and other complexes are reduced 61

3. DISCUSSIONS 63

3.1. Nup188 controls passage of membrane proteins across the NPC 64
3.1.1. Nup93 exists in two distinct complexes 64
3.1.2. Nup188 and Nup205 are not essential for NE and NPC assembly 64
3.1.3. Transport of soluble cargos in Nup188-Nup93 depleted nuclei is normal 65
3.1.4. Nup188-Nup93 controls the passage of membrane proteins through NPC 66

3.2. Nup98 is an essential component for the establishment of diffusion barrier of NPC 71
3.2.1. Depletion of Nup98 alters the size exclusion limit of NPCs 71

4. MATERIALS AND METHODS 73

4.1. Materials 74
4.1.1. Chemicals 74
4.1.2. Commonly used buffers and solutions 75
4.1.3. Commonly used material 76
4.1.4. Instrumental Equipments 77
4.1.5. Plasmids 77
4.1.6. Antibodies 82

4.2. Methods 85
4.2.1. Microbiological methods and molecular cloning 85
4.2.2. Biochemical standard methods 87
4.2.3. Biochemical methods related to the *X. laevis* egg extract system 91
4.2.4. Light microscopy 98

REFERENCES 99

PUBLICATION 110

CURRICULUM VITAE 130

Abbreviations

µm	Micrometre
3D	Three - dimensional
aa	Amino acid
BSA	Bovine serum albumin
C. elegans	Caenorhabditis elegans
Crm1	Chromosome region maintenance 1
DAPI	4’,6-Diamidino-2-phenyindole
DiIC18	1,1'-Dioctadecyl-3,3,3',3' tetramethylindocarbocyanine perchlorate
DNA	Deoxyribonucleic acid
DRB	5,6-dichloro-1-ß-D-ribobenzimidazole
E. coli	*Escherichia coli*
EDTA	1-(4-Aminobenzyl)ethylenediamine-N,N,N’,N’-tetraacetic acid
EGFP	Enhanced green fluorescent protein
EM	Electron microscopy
ER	Endoplasmic reticulum
EST	Expressed sequence tag
FG	Phenylalanine glycine dipeptide
GFP	Green fluorescent protein
GST	Glutathione-S-transferase
GTP	Guanosine triphosphate
GTPase	Guanosine triphosphatase
hCG	Human chorionic gonadotropin
INM	Inner nuclear membrane
IPTG	Isopropyl-β-D-thiogalactopyranoside
Kb	Kilo base
kDa	Kilo Dalton
LBR	Lamin B receptor
mAb	Monoclonal antibody
MISTIC	Membrane-integrating sequence for translation of integral membrane protein constructs
mRNA	Messenger RNA
NE	Nuclear envelope
NES	Nuclear export sequence
Ni-NTA	Nickel-nitrilotriacetic acid
NLS	Nuclear localization signal
NPC	Nuclear pore complex
Nup	Nucleoporin
ONM	Outer nuclear membrane

ORF	Open reading frame
PCR	Polymerase chain reaction
PFA	Paraformaldehyde
PMSG	Pregnant mare serum gonadotropin
Ran	Ras-related nuclear protein
RanGAP	Ran GTPase activating protein
RanGEF	Ran guanine nucleotide exchange factor
RCC1	Regulator of chromatin condensation 1
RNA	Ribonucleic acid
RNAi	RNA interference
S. cerevisiae	*Saccharomyces cerevisiae*
SDS-PAGE	Sodium dodecylsulfate - polyacrylamid gel electrophoresis
TEV	Tobacco etch virus
WGA	Wheat germ agglutinin
X. laevis/Xenopus	*Xenopus laevis*

1. Introduction

1.1 The nuclear architecture

Cell is the fundamental unit of life. One of the basic features of a living unit is the phenomenon of heredity. A cell is the transport device for the heritable information. For the maintenance of life, cell division takes place after the genome is doubled – resulting in a mother and a daughter cell. In contrast to prokaryotes, the genome of eukaryotes is compartmentalized in the cell nucleus by the nuclear envelope (NE), the structure that demarcates the nucleus in a cell (Alberts et al., 2002). The NE is comprised of two phospholipid bilayers, the outer nuclear membrane (ONM) and inner nuclear membranes (INM). The ONM is exposed to the cytoplasm, whereas the INM faces the nucleoplasm (Fernandez-Martinez and Rout, 2009). They are separated by a lumenal space. The ONM is continuous with endoplasmic reticulum (ER) and both are believed to have the similar protein composition (Lusk et al., 2007; Mattaj, 2004) (Fig. 1.1). Conversely, the INM shelters a unique set of proteins (Holmer and Worman, 2001). The ONM and INM are fused at the pore membrane where nuclear pore complexes (NPCs) are incorporated (Antonin et al., 2008).

Genetic material is packaged inside the nucleus in the form of euchromatin and heterochromatin. Previously, it was shown that chromosomes are maintained in distinct nuclear territories according to transcriptional state (Cremer and Cremer, 2001; Williams, 2003). Generally, inactive genes are packaged into heterochromatin and reside at the nuclear periphery while active genes are found as euchromatin and localized in the nuclear interior. These eu- and heterochromatin structures therefore occupy distinct fractions of nuclear space during the interphase. Regions of interphasic nuclei that do not contain chromatin are supposed to contain transcription machinery, RNA processing components and other nuclear bodies such as the PML bodies (Cremer and Cremer, 2001; Williams, 2003). The nucleus consists of many distinct substructures which are characterized by the absence of delineating membranes and which have been implicated in specific functions of gene expression (Dundr and Misteli, 2001). The site of ribosomal RNA transcription and ribosomal subunit assembly are nucleoli, the most prominent structures in the nucleus. The rRNA genes are transcribed as precursors, processed and assembled into ribosomal subunits, and subsequently exported to cytoplasm where they translate mRNAs. Other sub-structures that are organized inside the

nucleus include speckles, paraspeckles, Cajal bodies, GEMS and coiled-coiled bodies (Lamond and Sleeman, 2003). Nuclear speckles contain large quantities of SR proteins, serine/arginine-rich proteins that are involved in mRNA pre-processing (Sanford et al., 2005). Cajal bodies, also called coiled bodies, have shown to contain factors required for U snRNP assembly and PML bodies (Gall, 2000).

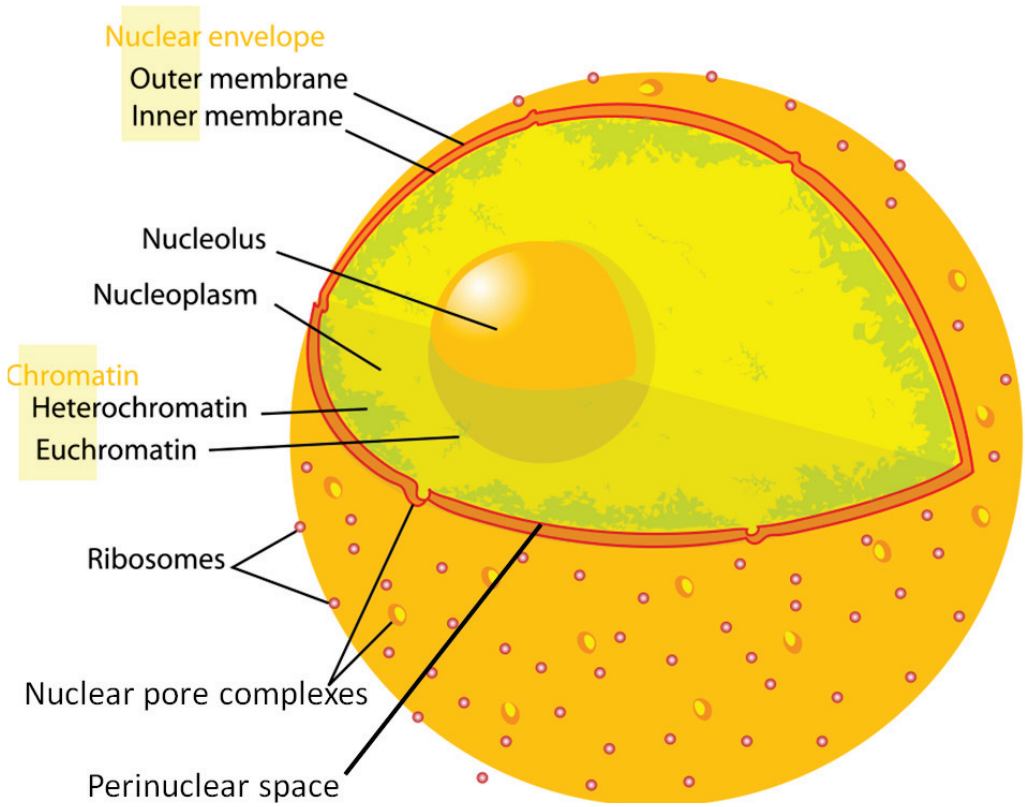

Fig. 1.1. *A schematic overview of a eukaryotic celluar nucleus*. Schema of the nucleus shows that nucleus is coveded by nuclear envelope (NE), that consists of the outer (ONM) and inner nuclear membrane (INM). Ribosomes (red dots) are embeded on the ONM, the nuclear pore complex (nuclear pore) are embedded on the NE. The nucleoplasm consists of heterochromatin (green), euchromatin (yellow) and the nucleolus. (modified from Wikipedia:Cell_nucleus; courtesy: Mariana Ruiz).

1.2 The nuclear envelope

The NE functionally separates DNA replication, transcription and RNA processing from cytoplasmic processes such as translation and other metabolic activities. The nuclear compartmentalization provided by the NE provides a plethora of possibilities for the regulation of gene expression. For example, a variety of extracellular signaling pathways use

the translocation across the NE as an important step in gene activation. As mentioned earlier, while the ONM and ER share similar protein composition the INM is distinguished by the presence of unique transmembrane proteins. These INM proteins either interact with the lamina and/or with chromatin (Holmer and Worman, 2001). The nuclear lamina is a thick fibrillar network composed of intermediate filaments which structurally stabilizes the NE (Fig. 1.2). More than eighty transmembrane proteins have been found to be localized at the INM but only a few have been well characterized. These include Emerin, which is mutated in X-linked Emery-Dreifuss muscular dystrophy, LAP2, MAN1 and the Lamin B receptor (LBR) (Worman, 2005). Many proteins that decorate the INM are implicated in a variety of diseases (Worman, 2005), implying their importance. LBR is an eight transmembrane domain-containing protein that interacts with B-type lamins in order to link the lamin intermediate filament network and the INM (Worman et al., 1988). LBR also interacts with HP1 (heterochromatin protein 1) and contributes to the organization of heterochromatin at peripheral localizations inside the nucleus (Ye and Worman, 1996).

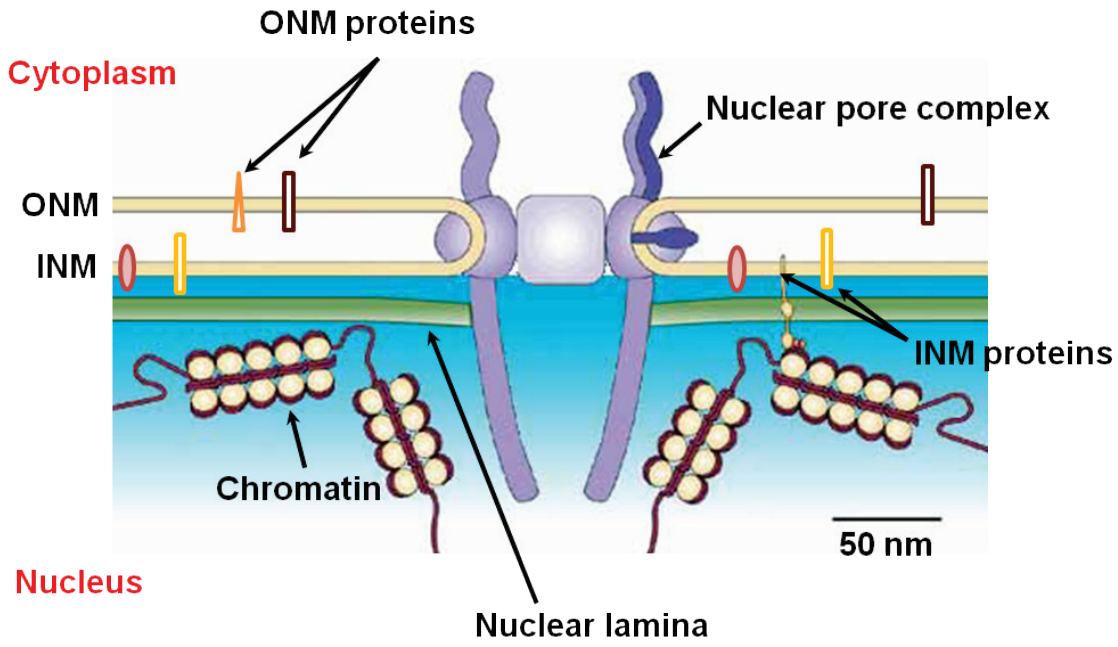

Fig. 1.2. *Composition of the metazoan nuclear envelope (NE)*. The NE consists of an outer (ONM) and inner nuclear membrane (INM). The nuclear pore complex (purple) is embeded in the NE, where the ONM and INM join. The nuclear lamina (green) is shown adjecent to the INM. The integral membrane proteins of INM and ONM are embeded on their respective membranes. Nucleoporins with transmembrane domains link NPCs to the nuclear membrane (indicated by dark purple component of the NPC which is inserted into the NE membrane at the right side). (Modified from (Burke and Ellenberg, 2002)).

The equal distribution of genetic material to two new daughter cells is an important step in mitotic cell division. In some single-celled eukaryotes, such as *Saccharomyces cerevisiae* (*S. cerevisiae*), the NE remains intact during cell division (Hetzer et al., 2005). In such cases, tubulin is imported into the nucleus and the mitotic spindle is assembled within the NE to segregate the chromosomes to opposite sides of the dividing cell (De Souza et al., 2004). This process is called 'closed mitosis' because the NE is not disassembled. Metazoa undergo open mitosis where the NE breaks down (NEBD) and reforms during each cell division. Open mitosis has striking consequences for the dividing cell as the components of nucleoplasm and the cytoplasm are mixed when the NE breaks down. This allows the establishment of mitotic spindle to capture and segregate the duplicated chromosomes (Hetzer et al., 2005). One of the earliest events during prometaphase is the disassembly of the nuclear lamina. This disassembly is mediated by the cdc2/cyclin B complex (Gerace and Blobel, 1980; Ottaviano and Gerace, 1985). The destabilization of NPCs may also occur early during NEBD and could trigger later steps in membrane disassembly (Kiseleva et al., 2001). It was previously demonstrated that upon NEBD the INM proteins are redistributed throughout the ER, indicative of the absorption of the NE into the ER (Ellenberg et al., 1997; Yang et al., 1997). At the end of mitosis, separation of the nucleoplasmic and cytoplasmic components by the reformation of the nuclear compartment around the segregated chromosomes occurs. This process of NE formation is tightly regulated. The GTPase Ran, the major regulator of nucleocytoplasmic transport, is required both for NE membrane fusion and NPC assembly steps (Hetzer et al., 2002).

1.3 The Nuclear pore complex (NPC)

The transport of heterogeneous cargos such as small molecules, proteins, RNAs or combinations thereof both into and out of the nucleus occurs through the NPC. NPCs are large proteinaceous assemblies, each with a calculated mass of 40 and 66 MDa in yeast and vertebrates, respectively (Cronshaw et al., 2002; Rout et al., 2000) (for review see also (Brohawn et al., 2008)). The present study explores the possibility of the transport of integral membrane components to the INM which to date represents a poorly understood transport

function of NPC. In order to put this idea in context, the structure and composition of NPCs, and the nucleocytoplasmic transport of diverse substrates will first be discussed. Following this, the function of nucleoporins in NE assembly will be summarized.

1.3.1 Structure and composition of the NPC

The NPC's huge structure is composed of only 30 different nuclear pore proteins jargoned as nucleoporins or Nups. Most of the nucleoporins, if not all, have been identified and characterized. But how this huge structure is assembled with only a relatively small number of proteins is not very well understood (Antonin et al., 2008; D'Angelo and Hetzer, 2008). The structure of this massive assembly was studied using many different methods including cryo-electron microscopy (Akey, 1989; Akey and Radermacher, 1993; Yang et al., 1998), scanning electron microscopy (Goldberg and Allen, 1993, 1996; Jarnik and Aebi, 1991; Ris, 1991; Ris, 1997; Ris and Malecki, 1993), atomic force microscopy (Rakowska et al., 1998; Stoffler et al., 1999) and cryo-electro tomography (Beck et al., 2007). Fig 1.3 shows the latest model of the NPC from *Dictyostelium discoideum* with a resolution below 6 nm (Beck et al., 2004; Beck et al., 2007).

State-of-the-art structural studies have confirmed that NPCs have an eight fold rotational symetry. Mainly, the structure of NPCs can be divided into three parts; The central core, cytoplasmic filaments and the nuclear basket (Fig. 1.3). The central core of the NPC is formed of three distinct rings and contact the membranes at the NE. The spoke ring is composed of clamp shaped structures that are attached to the NE. This spoke ring is sandwiched between a cytoplasmic and nuclear ring. The central core consists of the eight extended filaments on the cytoplasmic and a basket-like structure extending from the nuclear ring on the nuclear side. The attached cytoplasmic filaments are ~50 nm in length, whereas the nuclear basket is ~100 nm. The overall dimensions of a *D. discoideum* NPC is 125 nm in diameter at its cytoplasmic face, 40 nm diameter at the distal nucleoplasmic ring and ~110 nm in total length. The narrowest point in the channel, measuring 45nm, lies within the central pore and allows translocation of cargo complexes with a diameter of 35-40 nm. An important understanding of

the attachment of NPCs to the NE was derived from the visualization of luminal connector element that spans between the ONM and INM (Fig 1.3). In comparision to the vertebrate NPCs, the yeast NPCs are smaller having roughly half the mass.

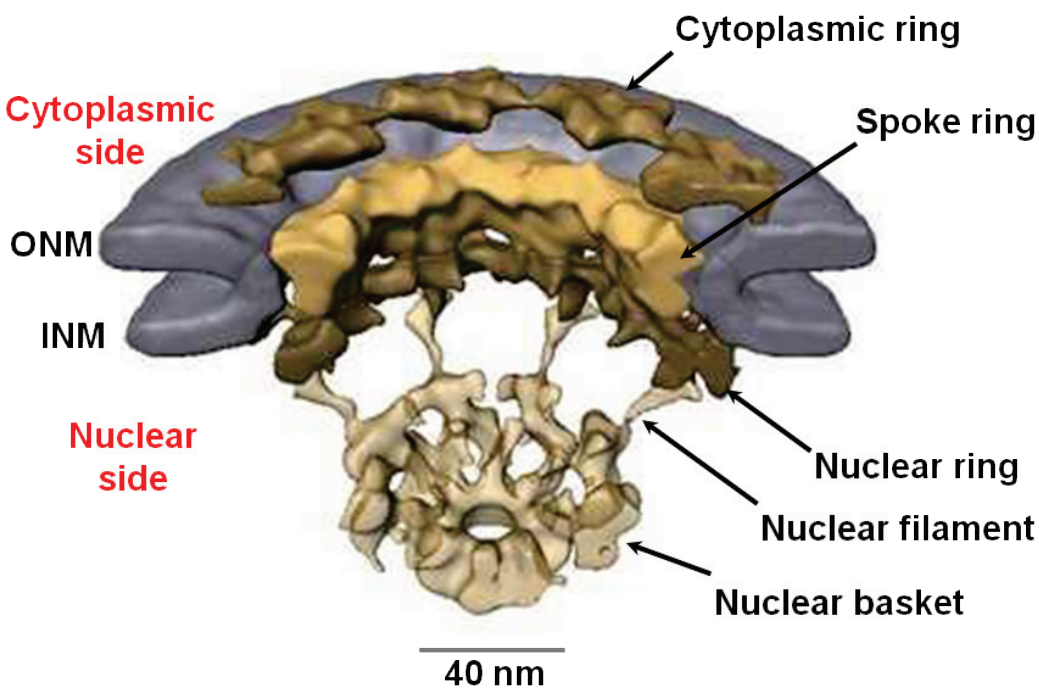

Fig. 1.3. *Structure of the NPC*. A cutaway view of the density map of the *Dictyostelium discoideum* NPC using cryo-electron tomography at 5.8 nm resolution. The cytoplasmic and spoke ring of NPC were represented in brown and yellow, respectively. The inner nuclear membrane (INM) and outer nuclear membrane (ONM) are represented in grey. (modified from (Beck et al., 2007)).

1.3.2. Structural features of nucleoporins

Nucleoporins are mainly composed of four distinct domain structural elements: FG repeat regions, coiled-coil domains, β-propellers and α-helical repeats (Fig. 1.4) (Mans et al., 2004; Schwartz, 2005). Many nucleoporins contain FG repeats; natively unfolded domains with phenylalanine–glycine repeats. FG repeat nucleoporins are localized at both the cytoplasmic and nuclear periphery as well as in the central channel of the NPC and mediate interactions between nucleoporins and soluble transport receptors (Fahrenkrog et al., 2004). It was previously demonstrated that FG-repeats of yeast nucleoporins constitute regions that lack an

ordered secondary structure. Within the NPC, they may constitute an amorphous mesh of filaments that form a mechanical barrier for non-cargo proteins. The unfolded and flexible features of FG-repeats could enable multiple, simultaneous, and transient contacts with a variety of interaction partners (Denning et al., 2003). The second structural feature of nucleoporins are coiled-coil domains that are commonly found to mediate protein-protein interactions (Cronshaw et al., 2002). Thirdly, WD-repeats present in some nucleoporins are predicted to be organized into β-propellers (Schwartz, 2005). The fourth structural element is α-helical repeats arranged to higher order structures in many nucleoporins. The Nup107-Nup160 complex members, for example, contain the structural elements of β-propeller folds, α-solenoid folds, or a defined combination of both (Schwartz, 2005).

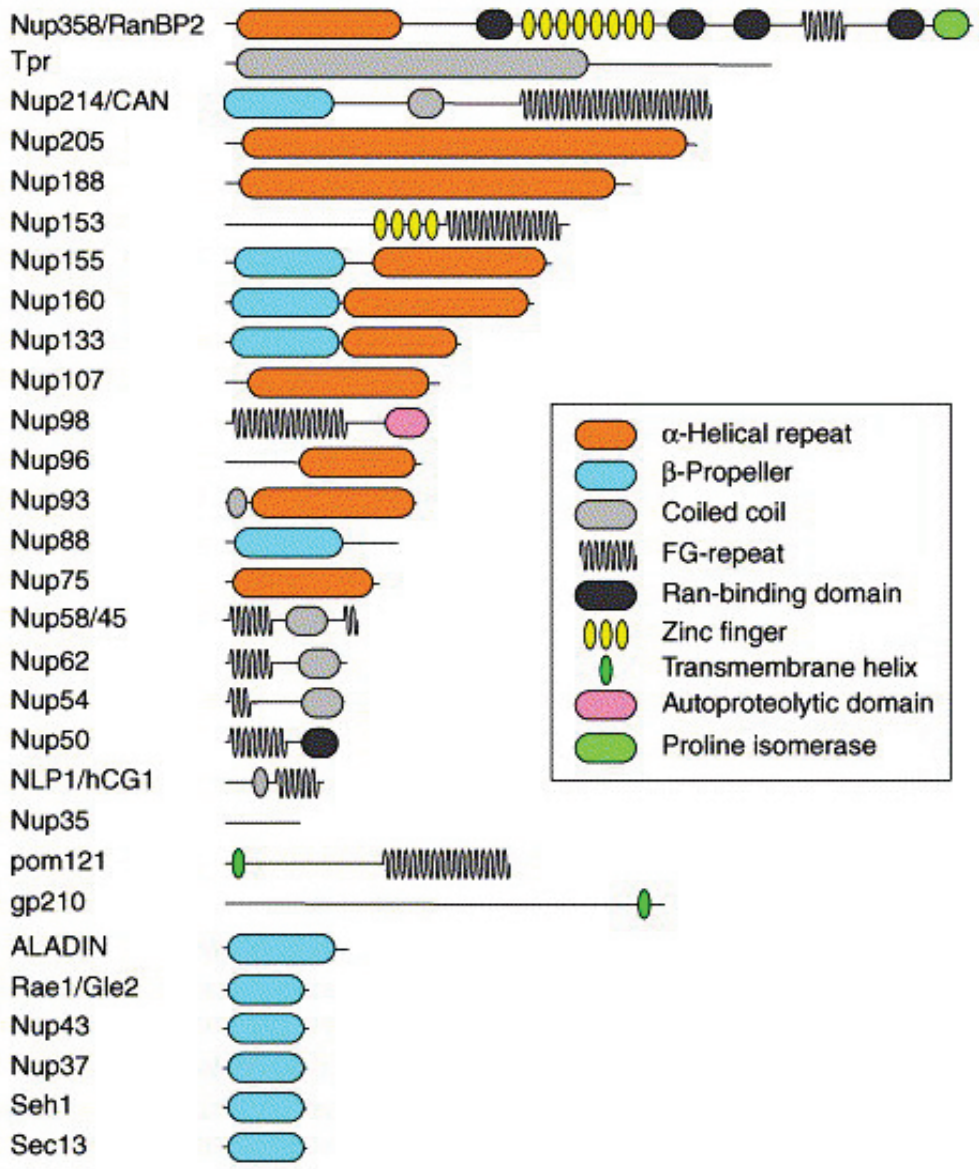

Figure. 1.4. *Schematic view of the domain architecture of nucleoporins*. Structural elements and domains of the nucleoporins are shown. Four distinct domain structural elements, FG repeat regions, coiled-coil domains, β-propellers and α-helical repeats are represented as zig-zag marks, grey, cyan and orange colored rounded boxes, respectively. Source of the most structural elements mentioned are based on the published data and the α-helical repeat regions are predicted using bioinformatic tools (Modified from (Schwartz, 2005) and the references therein).

1.3.3. Molecular composition of the nuclear pore complex

It will be very interesting to understand how the enormous NPC structure is built from approximately 30 nucleoporins. Nuclear pore complexes can be biochemically dissected into discrete subcomplexes both in yeast and higher eukaryotes (Alber et al., 2007) (for review see (Schwartz, 2005)). In vertebrates, at least three major subcomplexes were found to make up the major part of the NPC: the Nup107-Nup160, Nup93 and Nup62 complexes (Fig 1.5) (Antonin et al., 2008). These complexes are believed to function as building modules of the NPC upon which several peripheral nucleoporins are assembled from an existing free pool (Rabut et al., 2004). Of these three complexes, the Nup107-Nup160 subcomplex is the best studied (Devos et al., 2004; Glavy et al., 2007; Walther et al., 2003).

The vertebrate Nup107-Nup160 complex consists of nine components: Nup107, Nup133, Nup160, Nup96, Nup75, Nup37, Nup43, Seh1 and the coatomer II protein (COPII) Sec13 (Loiodice et al., 2004) See also Fig. 1.5. In yeast, the Nup84 complex is homologous to the vertebrate Nup107 complex. The Nup84 complex has been reconstituted from seven known subunits in vitro and the structure determined by EM showed a Y-shaped multiprotein complex (Lutzmann et al., 2002). This complex constitutes a major part of the octagonal spoke-ring complex (Fig. 1.3) as sixteen copies localize symeterically around the cytoplasmic and nuclear ring (Krull et al., 2004). Peripheral membrane proteins represent an important way to bend the membrane structures. It has been proposed that as the yeast Nup84 complex and the vesicle coating complexes are composed of α-solenoids and β-propeller folds and have a similar overall structure they may have a common ancestor (Devos et al., 2004) and therefore share some membrane bending function. A fraction of the vertebrate Nup107-Nup160 complex also localizes to kinetochores during mitosis (Loiodice et al., 2004) and the complex binds to chromatin as a stable anchoring point for the assembly of NPCs at a very early stage in nuclear reassembly (Walther et al., 2003).

The second major structural unit of the NPC and the main subject of our study in this thesis is the Nup93 subcomplex. In vertebrates, it is comprised of five nucleoporins: Nup205, Nup188,

Nup155, Nup93 and Nup53. Both Nup155 and Nup53 have been found to be essential for NE and NPC assembly (Franz et al., 2005; Hawryluk-Gara et al., 2008). The yeast orthologue of vertebrate Nup93 complex is the Nic96 complex. Nup155 has two orthologues in yeast, Nup170p and Nup157p, the loss of which blocks NPC assembly (Makio et al., 2009). Both of these orthologues bind to Nup53p and Nup59p, similarly to the corresponding vertebrate Nup53, which in turn interact with the transmembrane nucleoporin Ndc1p (Mansfeld et al., 2006; Onischenko et al., 2007). Potentially, these interactions might anchor NPCs in the membrane of the NE. Vertebrate Nup53 is shown to be tightly associated with both the nuclear membranes and the lamina through Lamin B. Additionally, Nup53 was shown to interact with Nup93 and Nup205 within the complex members (Hawryluk-Gara et al., 2005). In vertebrates, Nup188, Nup205 and Nup93 are believed to exist in a complex (Meier et al., 1995). Initially, the yeast homologue of Nup93 was showed to be essential for NPC assembly and was also shown to interact with Nup188p and Nup192p, yeast homologues of Nup188 and Nup205, respectively (Gomez-Ospina et al., 2000; Nehrbass et al., 1996; Zabel et al., 1996). Immunodepletion of vertebrate Nup93 in *Xenopus* egg extracts followed by *in vitro* nuclear assembly resulted a reduction in NPCs in those nuclei (Grandi et al., 1997), demonstrating the importance of the Nup93 complex in NPC assembly. In *C. elegans*, depletion of Nup93 or Nup205 by RNAi resulted in close to complete embryonic lethality and initially slightly smaller nuclei than in control embryos. Strong and abnormal peripheral condensation of chromosomes was also observed. NPCs aggregated in the NE and allowed passive diffusion of a 70 kDa dextran unlike control NPCs, despite the nuclei being enclosed by intact NEs and containing NPCs. In addition, protein import was not impaired (Galy et al., 2003). The worm ortholog of vertebrate Nup188 has not yet been identified. In yeast the vertebrate Nup188 orthologue, Nup188p, is not essential for the cell growth (Zabel et al., 1996), and its disruption resulted in structural abnormalities of the NE without any affect on the nuclear transport (Nehrbass et al., 1996; Zabel et al., 1996).

The Nup62 complex is one of the key subcomplexes of the NPC. The nucleoporin p62 (Nup62) is one of the first characterized vertebrate nucleoporins and was found to form a subcomplex with the nucleoporins p54, as well as p58 and its splice variant p45 (Finlay et al., 1991; Hu et al., 1996). Immunodepletion of the p62 complex from *Xenopus* egg extracts and

produced assembled nuclei which were deficient for nucleocytoplasmic transport (Finlay et al., 1991).

All the above mentioned subcomplexes have been shown to be important for structural and functional feautures of the NPC. However, some nucleoporins which have not been shown to be part of distinct subcomplexes have also been found to be important for the maintainence and function of NPCs. One of such nucleoporin is Nup98. Nup98 is the only vertebrate nucleoporin with containing a substantial number of GLFG-type repeats (Powers et al., 1995). The functional importance of Nup98 is emphasized by the finding that Nup98 knockout mice die early in embryonic development (Wu et al., 2001). Nup98 depleted nuclei remain small and fail to replicate DNA, indicating an essential nuclear role for Nup98 (Powers et al., 1995). However, given the importance of Nup98, its complete functional significance is still not understood.

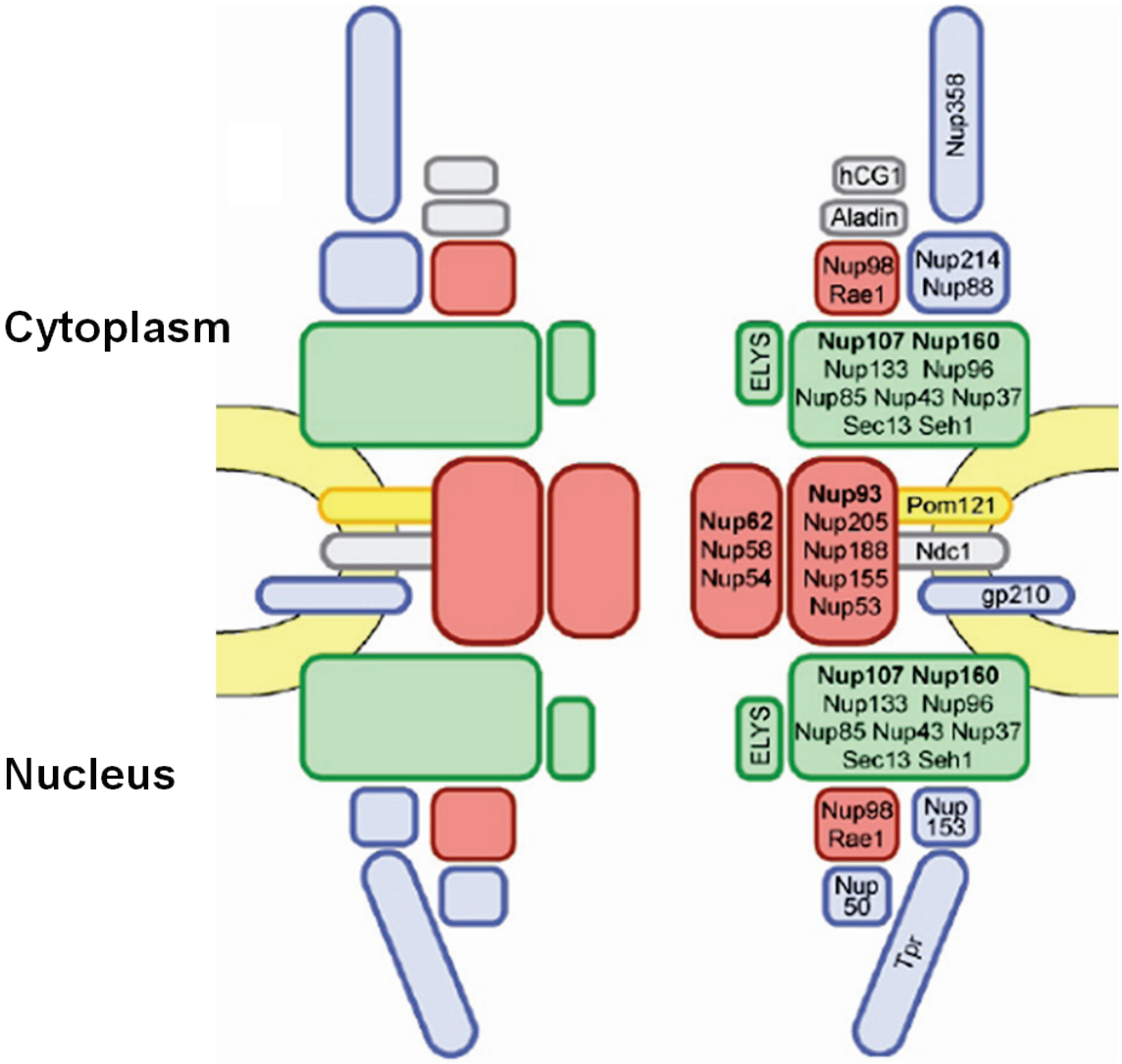

Figure. 1.5. *Schematic view of the modular structure of the NPC*. The schema shows the modular view of a metazoan NPC with different biochemically characterized subcomplexes. The NPC is embedded in the NE (yellow), the transmembrane nucleoporins (pom121, Ndc1 and gp210) are also shown. Green, yellow, red and blue colors of the nucleoporins and subcomplexes represent their recruting time during the NPC assembly mentioned in the respective order. (Modified from (Antonin et al., 2008)).

1.4. Nucleocytoplasmic transport

The compartmentalization of the eukaryotic cells requires an exchange of macromolecules between the cytoplasm and the nucleus. Nuclear proteins such as histones and transcription factors must be imported from the cytoplasm where they are synthesized. In contrast, tRNA, rRNA and mRNA, which are synthesized in the nucleus upon transcription need to be

exported to cytoplasm, their point of function. Integral membrane proteins of INM are synthesized in ER and must therefore be transported from the ER/ONM to the INM. Each of these transport schemes involves the regulated transport of soluble cargos through the NPC and has been comprehensively studied (for review see (Suntharalingam and Wente, 2003)).

1.4.1. Transport of soluble cargos

There are two basic mechanisms by which soluble cargoes reach the nucleus through the NPC: passive diffusion and transporter mediated active transport. Passive diffusion is only possible for ions, metabolites, and small macromolecules and becomes limiting for cargos greater than 40 kDa in size (Fried and Kutay, 2003). The active transport of macromolecules across the NE is determined by signals. These signals consist of short amino acid sequences, termed nuclear localization signal (NLS) and the nuclear export signal (NES) for nuclear import and nuclear export, respectively (Fried and Kutay, 2003). Transport receptors release their loads at their destinations and recycle back to the opposite site of the NPC where they are reloaded with new cargo. Nucleocytoplasmic transport is best understood for the family of importin β transport receptors that require the small Ran GTPase (Kuersten et al., 2001; Weis, 2003). The regulatory functions of Ran are not only limited to the nucleocytoplasmic transport, as Ran is also involved in the formation of the mitotic spindle as well as NE and NPC assembly (Hetzer et al., 2005). As a GTPase, Ran mediates energy consuming processes. Ran function requires a guanine nucleotide exchange factor, RanGEF, which promotes GDP dissociation from Ran and subsequent binding of GTP. The GTPase activating protein (RanGAP) catalyzes the hydrolysis of Ran bound GTP to GDP with the help of RanBP1 and RanBP2 (Kuersten et al., 2001). The key characteristic of the Ran cycle is that RanGEF (RCC1) and RanGAP are spatially separated. RCC1 binds to chromatin through an interaction with core histones and resides in the nucleus, whereas RanGAP and RanBP1/BP2 are restricted to the cytoplasmic side of the NE. The local separation of RanGEF and RanGAP generates a RanGTP gradient across the NE, with a high RanGTP concentration in the nucleus. This gradient is coupled to nucleocytoplasmic transport.

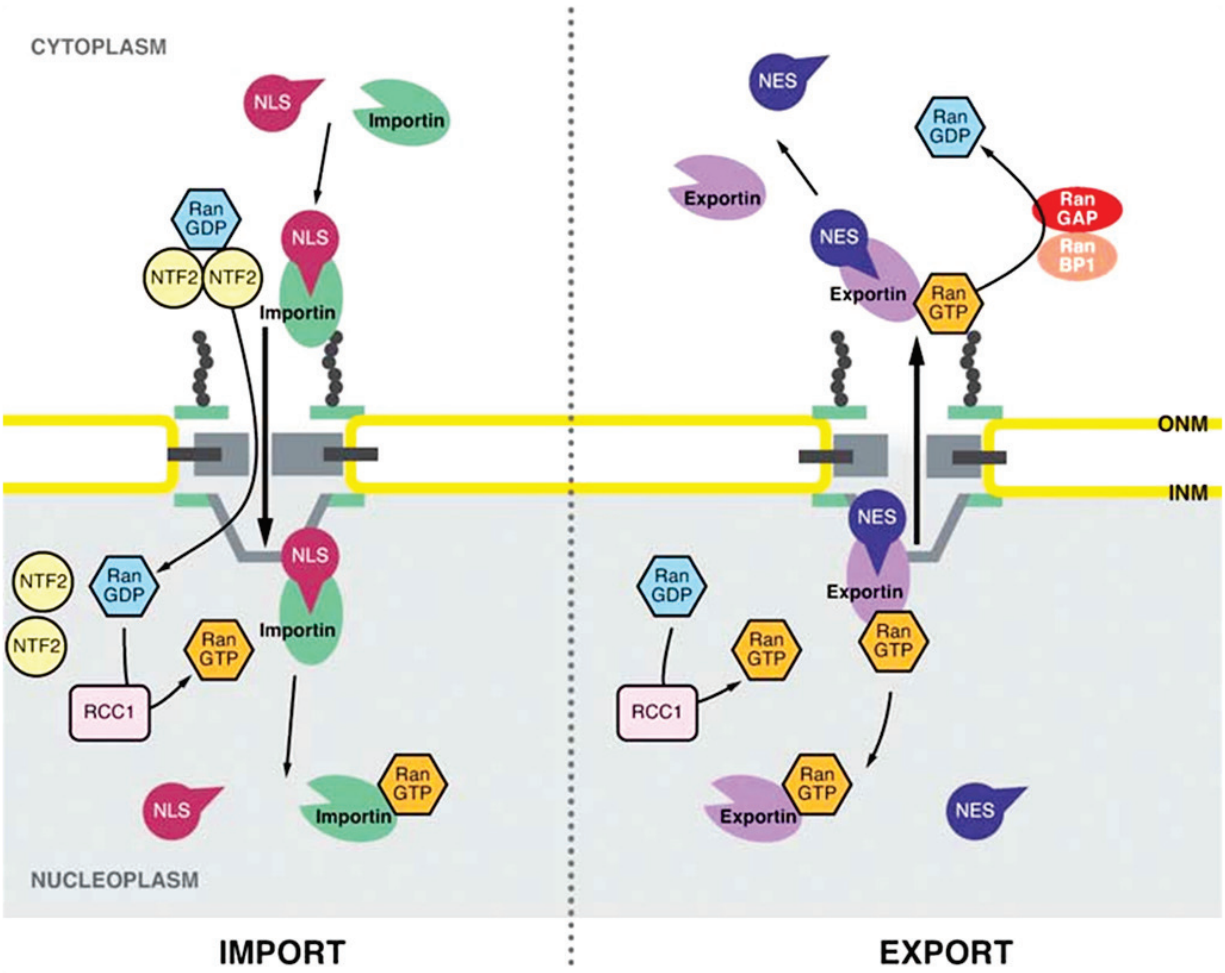

Figure. 1.6. *Schematic view of the nucleocytoplasmic transport cycle*. Import and export cycles mediated by karyopherins; Importins (right) and Exportins (left). Importins (green) bind to cargo molecules through nuclear localization signals (NLS) in the cytoplasm and mediate interactions with the NPC to translocate into the nucleus (left). RanGTP in the nucleus binds to Importin and induces cargo release. The Importin-RanGTP complex is then recycled to the cytoplasm. The export cycle is similar to the import cycle with the important difference that in the nucleus RanGTP induces cargo binding to an export receptor (right). Chromatin bound RCC1 mediates nucleotide exchange of GDP with GTP on Ran. (Adapted from (Hetzer et al., 2005)).

Importins bind their substrate in the cytosol either directly or via an adaptor molecule. Importin α is an adaptor that recognizes cargo carrying a NLS (Fig 1.6). Importin α acts as a bridge between cargo and the import receptor importin β (Fried and Kutay, 2003). Inside the nucleus, RanGTP binds to importin β and displaces importin α along with the imported substrate. Importin β-RanGTP leaves the nucleus and the transport receptor is recycled after RanGTP hydrolysis upon interaction with RanGAP and RanBP1/BP2 at the cytoplasmic NPC filaments. In contrast to importin β-cargo complexes that are destabilized by RanGTP, export complexes are stabilized by RanGTP binding. The exported substrate is released as described

above when GTP hydrolysis occurs and the export complex disassembles. The empty exportin recycles back into the nucleus. Importin α is guided back to the cytoplasm by the export receptor CAS and RanGTP. Equivalent to importin β, CRM1 is a multivalent export receptor which makes use of a variety of cofactors to shuttle a diverse group of cargos. A major class of CRM1 substrates are proteins with a leucine-rich NES (Wen et al., 1995). To complete a cycle, RanGDP is imported back into the nucleus by the small nuclear transport factor 2 (NTF2) (Ribbeck et al., 1998).

1.4.2. Transport of integral membrane proteins to the inner nuclear membrane

The ER is continuous with ONM which is in turn continuous with INM. Although these membranes are continuous, the INM contains specific set of proteins that are exclusively found in the INM. The transport of soluble factors in and out of the NPCs across the NE is thoroughly studied (Suntharalingam and Wente, 2003). The mechanism of INM protein sorting is not entirely elucidated but many models have been proposed. One such model is based on vesicle fusion events; The ONM and INM could fuse and transfer membrane proteins to the INM. Another model is based on the reversal of how Herpes virus comes out of nuclei by budding of INM vesicles and fusion with the ONM (Mettenleiter et al., 2009). A third and interesting model proposes that these transmembrane proteins could easily diffused from the ONM through the NPC in the plane of membrane (Ohba et al., 2004). Please see the discussion for more details on these models.

1.5. Experimental systems to study the NE and NPCs

Several methodologies in a variety of model organisms have been used to study the translocation of molecules across the NE. Genetic screens in *S cerevisiae* have been successfully employed to identify proteins involved in different transport pathways. Synthetic lethality screens in yeast have been an important tool for the essentiality and identification subcomplexes (Fabre and Hurt, 1997). However, yeast cannot be employed for studying the

candidates that participate in postmitotic NE assembly as they undergo a closed mitosis (Chen et al., 2010; Straube et al., 2005). Only a few nucleoporins have been studied using the mouse system due to the amount of time and the resources required to generate mouse strains (van Deursen et al., 1996; Wu et al., 2001). In *C.elegans*, genome wide systematic RNAi knock down studies have described and grouped candidates leading to defects in pronuclear/nuclear appearance that require further biochemical investigation (Colaiacovo et al., 2002; Sonnichsen et al., 2005; Zipperlen et al., 2001). However, the process of NE assembly is very hard to manipulate experimentally in intact cells.

In the early 1980s, using cell-free extracts from eggs of *R.pipiens*, Lohka and Masui established the first in vitro nuclear assembly system (Lohka and Masui, 1983). Stockpiles of NE precursors and other nuclear proteins that permit rapid mitotic divisions upon fertilization are stored in eggs of many species. This egg extract system provides an enormous amount of material required for NE and NPC assembly, producing nuclei that can reliably complete one or more full cell division cycles in the test tube. The cell cycle state of the egg extracts can be manipulated (interphasic to mitotic and vice versa) and proteins in the extracts can be depleted through specific antibodies to verify functions. These qualities make the egg extracts a rich and therefore biochemically valuable source of study for in vitro NE formation.

When demembranated sperm nuclei were incubated with egg extract, an intact NE formed, chromatin decondensed, and DNA synthesis was initiated (Lohka and Masui, 1983). Cell-free extracts with similar qualities could also be prepared from *X. laevis* eggs (Lohka and Maller, 1985) and are employed in our studies. *Xenopus* egg extracts collected in the mitotic or interphase state can be prepared depending on how the eggs are manipulated. Natively, progesterone secretion by follicle cells induces completion of meiosis I. The oocyte next enters meiosis II, which primes it for ovulation. This process can also be induced by injecting frogs with pregnant mare serum gonadotropin (PMSG). Next, the oocytes are arrested at metaphase of meiosis II, ovulate and are ready for fertilization. Human chorionic gonadotropin (hCG) stimulates the ovulation of mature oocytes. Penetration of the egg by a sperm induces a transient cytoplasmic Ca^{2+} increase, which is the signal for release of the metaphase arrest. The oocyte completes meiosis II, enters interphase, and starts early

embryogenesis by a series of rapid mitotic cell divisions. This fertilization can be mimicked *in vitro* by applying an electric shock or adding a calcium ionophore. In our system we use calcium ionophore (A23187). These treatments release the eggs from metaphase arrest. Egg extracts of these activated eggs will complete the meiosis II and would be able to assemble the nucleus (Murray, 1991). These *in vitro* assembled nuclei are similar to the physiological cell nuclei and are capable of performing nucleocytoplasmic transport and DNA replication (Blow and Laskey, 1986; Newmeyer et al., 1986).

Xenopus eggs can be kept arrested in metaphase II and used to generate the egg extracts that mimic mitotic events. In this case, the eggs are not activated by imitation of fertilization and release of Calcium. Instead, EGTA (a Calcuim chelator) and phosphatase inhibitors are added to prevent dephosphorylation of cell cycle regulators. Together, the cell-free *Xenopus* egg extract system is very well suited for manipulation and allows the investigation of very complex and multi stepped cellular processes. As mentioned earlier, these components can be depleted from the *Xenopus* egg extracts to understand their importance through their respective phenotypes. The specificity of the observed phenotypes can also be understood by the addition of recombinant components to the egg extracts (Antonin et al., 2005; Grandi et al., 1997; Harel et al., 2003; Walther et al., 2003; Walther et al., 2001; Walther et al., 2002).

1.6. Aims of the project

My PhD project aims to understand and characterize the functions of Nup93 complex in NPC and NE assembly. There are two main reasons for choosing the Nup93 complex. First, Nup93 is one of the major structural subcomplexs of the NPC. Second, the Nup93 complex is thought to be positioned at the core region where the NPC and NE interact. In *Xenopus*, the Nup93 complex was understood to comprise a core of three proteins, Nup205, Nup188 and Nup93 (Miller et al., 2000) with the other two nucleoprins Nup155 and Nup53 rather weakly interacting. However, given the importance of this complex, it is not very well characterized. We therefore set out to characterize the function of Nup93 complex in NPC and NE assembly.

For the analyses of the Nup93 complex, we initially used immunoprecipitations of the individual complex members to understand the interaction network. Subsequently, a nuclear reconstitution system was employed. In the nuclear reconstitution system, we depleted the individual complex members for a genuine loss-of-function situation. The reconstituted nuclei lacking the nucleoporins and respective interaction partners were analyzed using a variety of light microscopic, biochemical and cell biological techniques to gain an understanding about the function of the depleted nucleoporin in NPC and NE assembly and nucleocytoplasmic transport.

2. Results

2.1. Nup188 controls passage of membrane proteins across the nuclear pore complex

2.1.1. Generating the tools

To study the protein interaction network of the Nup93 complex, we raised antibodies against the individual complex members. In order to generate these antibodies, fragments of *Xenopus* Nup188, Nup205, Nup93, Nup53, Nup98, or full length Nup155 were expressed and purified as mentioned in materials and methods (4.2.2.1). The polyclonal antibodies for the each antigen were generated in two rabbits (4.2.2.7). Antisera were tested for their recognition of respective antigens in *Xenopus* egg cytosol by Western blot analysis. Antisera successfullyprecipitated the intended antigens which were detectable as single bands of expected molecular weights (data not shown) with the exception of Nup93. Both antisera produced against Nup93 recognized a double band at 95 kDa, the top one of which was not observed in immunoprecipitation experiments and could therefore be considered the result of cross-reactivity with another protein in the total egg extract (Fig. 2.2).

2.1.2. Nup93 is part of two distinct sub-complexes

In order to understand the protein interaction network of the Nup93 complex, we performed immunoprecipitations (4.2.3.7) using polyclonal antibodies raised against each of the five members of the complex and *Xenopus* egg extract cytosol (Fig. 2.1). Starting material and Nup188, Nup93, Nup205, Nup155, Nup53 or Nup98 immunoprecipitates were analysed by SDS-PAGE and Western blot. Cytosol is loaded in the first lane to identify the respective nups on the blot; the antibodies against Nup188 are from two different rabbits are loaded next to each other. Two separate antibodies against Nup188 precipitated Nup188 and Nup93 but not Nup205 (lane 2 and 3). Antibodies against Nup155 and Nup53 precipitated only their respective antigens (lane 6 and 7) and no other complex members as reported previously by (Franz et al., 2005) and (Hawryluk-Gara et al., 2008), respectively. Antibodies against Nup205 precipitated Nup205 and Nup93 but not Nup188 (lane 5). Consistent with previous

immunoprecipitations, Nup93 antibodies precipitated Nup188, Nup205 and its own antigen Nup93 (lane 4). Surprisingly, Nup93, Nup188 and Nup205 did not exist in a trimeric complex although they were previously were reported to be found in a single complex (Meier et al., 1995) and (Miller et al., 2000). The Nup98 immunoprecipitation serves as a negative control and did not precipitate any member of the Nup93 complex as expected (lane 8).

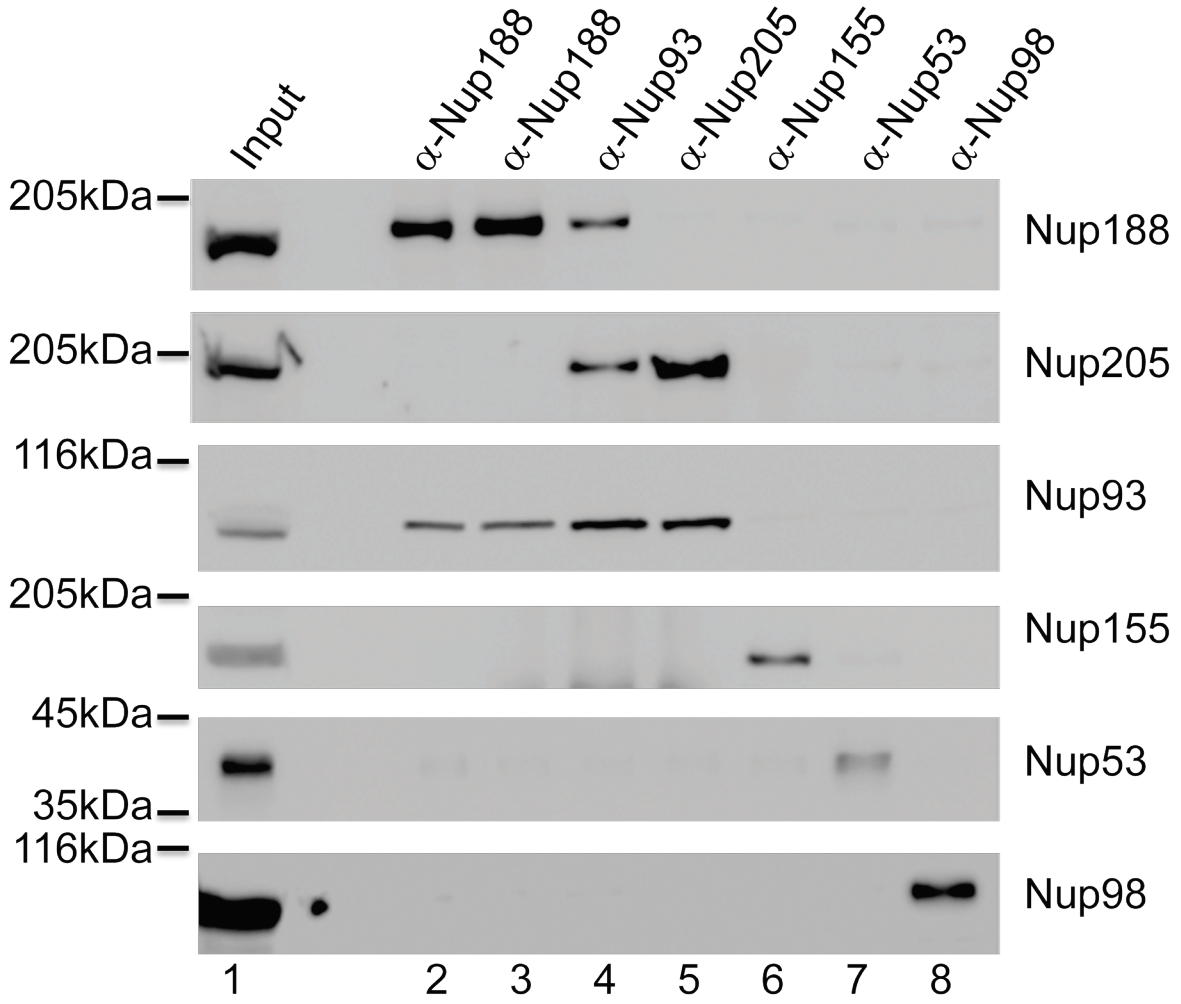

Figure 2.1: *Nup93 exists in two distinct complexes*. Nup188, Nup93, Nup205, Nup155, Nup53 and Nup98 were immunoprecipitated from *Xenopus* egg cytosol with their respective antibodies. Two different antibodies for Nup188 were raised in two different rabbits. Proteins detected by Western blot are indicated at right. Input representing 10% of the starting material is loaded in the first lane.

We excluded the possibility that Nup188 and Nup205 antibodies precipitated only a subpopulation present in the egg cytosol by performing immunoprecipitations in a

quantitative manner (Fig. 2.2). Even when all of the Nup188 was precipitated (removed from unbound; lane 9 and 10), Nup205 was not co- immunoprecipitated (lane 4 and 5) and vice versa (lane 7 and 12). Our results demonstrate that Nup93 does not exist in a trimeric complex but rather exists in two distinct sub complexes, one with Nup188 and one with Nup205.

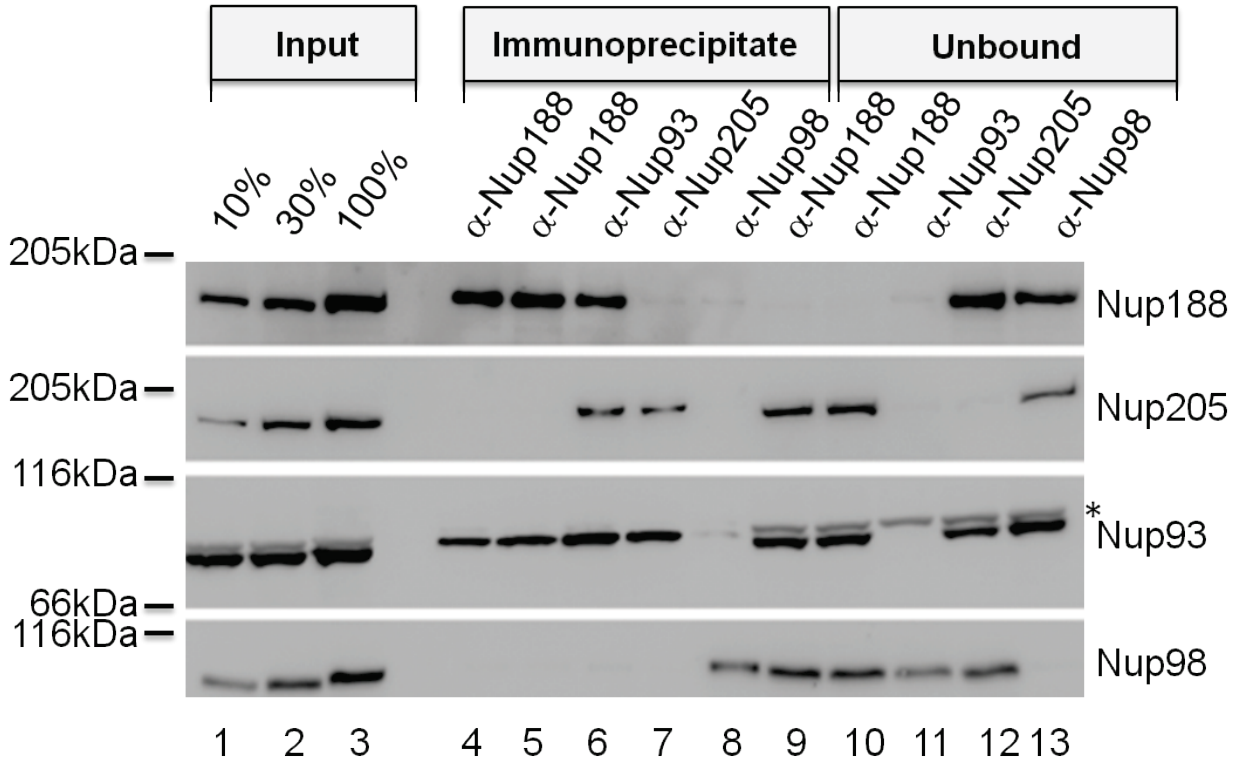

Figure 2.2: *Quantitative immunoprecipitations of the Nup93 complex*. Immunoprecipitations for Nup188, Nup93, Nup205 and Nup98 (as a control) from limited amounts of *Xenopus* egg cytosol were performed. Increasing fractions of the starting material (input), immunoprecipitate and unbound material from the immunoprecipitations were analyzed on a blot with the antibodies mentioned at the right side. Asterisk indicates a cross-reactivity recognized by the Nup93 antibody in the egg cytosol (input and unbound material) seen just above the Nup93 band.

To understand more about the Nup188-Nup93 and Nup205-Nup93 complexes, we investigated the amount of total Nup93 interacting with either Nup188 or Nup205. To this end, we quantified the amount of Nup93 present in Nup188 depleted, Nup205 depleted and Nup188-Nup205 co-depleted extracts (Fig. 2.3). Both Nup188 and Nup205 individually precipitated around 45% of total the total Nup93 present. This shows that the amount of Nup93 interacting with either Nup188 or Nup205 in *Xenopus* egg extracts is approximately equal.

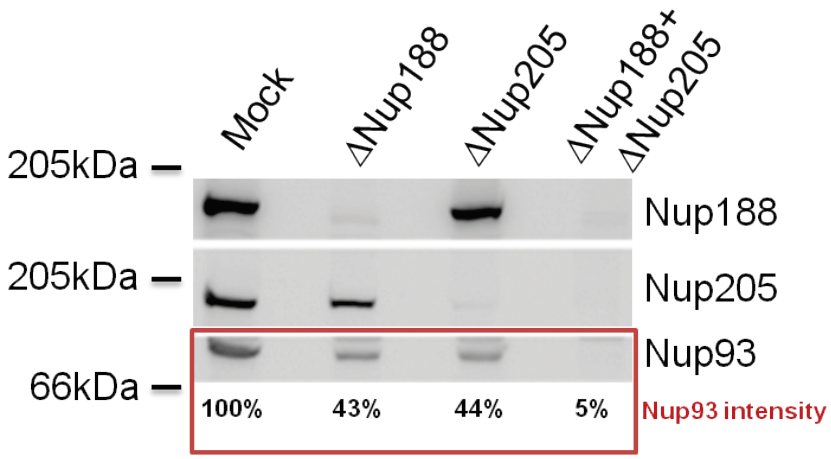

Figure 2.3: *Quantitation of the Nup93 interacting with Nup188 and Nup205*. *Xenopus* egg cytosol were immunodepleted with control IgG (mock), αNup188, αNup205 or a mixture of αNup188 – αNup205 antibody beads. The immunodepleted cytosols were analyzed by Western blot for Nup93, Nup188 and Nup205. Signal intensity of Nup93 on the blot was quantified and normalized to the mock.

As we had found that Nup205 and Nup188 exist in different subcomplexes we wanted to determine their point of recruitment during NPC assembly. Nuclear assembly time course experiments were therefore performed in which recruitment of Nup188, Nup205 and Nup93 was monitored by immunofluorescence (Fig. 2.4). Briefly, demembranated sperm chromatin was incubated with *Xenopus* egg extracts for 10 min at 20 °C, at which time (t = 0 min) unlabeled membranes were added together with an energy mix. Nuclear assembly was stopped at the indicated time points. To summarize, these results demonstrate that Nup188, Nup205 and Nup93 were each recruited by around 10 min and that there was no difference in their recruitment at any of the time points tested. Antibody staining of all three nucleoporins reveals an overall increase in signal intensity with increasingly continuous, smoother staining around the decondensed chromatin over time.

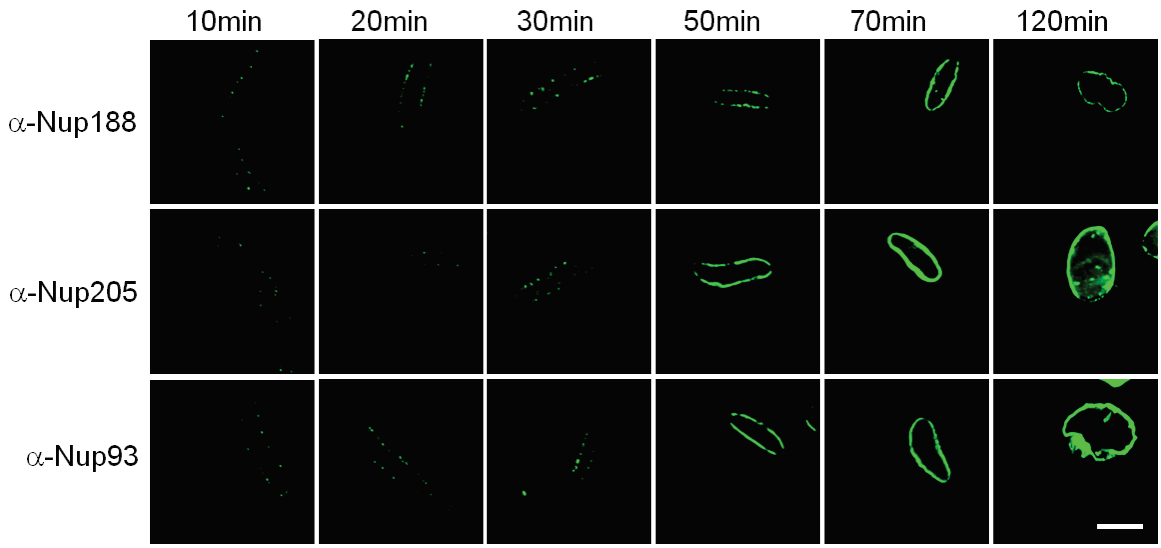

Figure 2.4. *Recruitment of Nup188-Nup93 and Nup205-Nup93 happens at the same time during NPC assembly.* Nuclear assembly was performed and the reaction was stopped by fixing nuclei with 4% PFA at the indicated time points. Immunofluorescence of Nup188, Nup205 and Nup93 was done on the fixed nuclei using specific antibodies. Scale bar: 20 µm.

2.1.3. Depletion of Nup188-Nup93 enlarges the nuclear size and they contain NPCs.

To understand the functional importance of the two Nup93 complexes, we planned to immunodeplete the complexes separately from *Xenopus* egg cytosol and use the cytosol for *in vitro* nuclear assembly (4.2.3.5). Nuclear proteins and disassembled NE components are stockpiled in *Xenopus* eggs (Murray, 1991), which contain a very biologically active cytosol and can each gives rise to numerous nuclei. This implies that proteins are often present in large quantities in *Xenopus* egg cytosol and may therefore require very harsh depletion conditions for their complete removal. For this reason, an excessive amount of affinity purified antibodies specific for Nup205 and Nup188 were made (4.2.2.8) and coupled to protein A sepharose (4.2.2.9). The column was first blocked with bovine serum albumin (BSA) to prevent binding of nonspecific proteins. Cytosol was then incubated with Nup205 and Nup188 antibody beads for two rounds to efficiently deplete Nup205-Nup93 and Nup188-Nup93, respectively. The ratios of cytosol to antibody beads were approximately

1:1.5 and 1:1.2 for Nup205 and Nup188 depletions, respectively. Mock-depleted cytosol was obtained by incubating rabbit IgG beads in the same ratio as the nucleoporin immunodepletion. Indeed, efficient depletion of Nup205 and Nup188 was seen by western blot analysis (Fig. 2.5A and 2.8A, respectively) and immunofluorescence (Fig. 2.6 and 2.9, respectively). Depletion of Nup205 and Nup188 seemed to be specific as Nup98 was not depleted in the same extract. *In vitro* nuclear assembly reactions were performed (4.2.3.5) immediately following immunodepletion because freezing of the depleted cytosol impaired its activity.

Nuclei assembled in egg cytosol depleted of the Nup205-Nup93 complex for 90 min looked normal in appearance compared to controls according to membrane and chromatin staining (Fig. 2.5B). Immunofluorescence for mAb414, a widely used mouse monoclonal antibody for staining NPCs which recognizes four different nucleoporins, indicated that NPC staining in mock and Nup205 depleted nuclei was not different (Fig. 2.6). We were also, able to detect the presence of other nucleoporins such as Nup93, Nup188, Nup53 and Nup155 by immunofluorescence (Fig. 2.7).

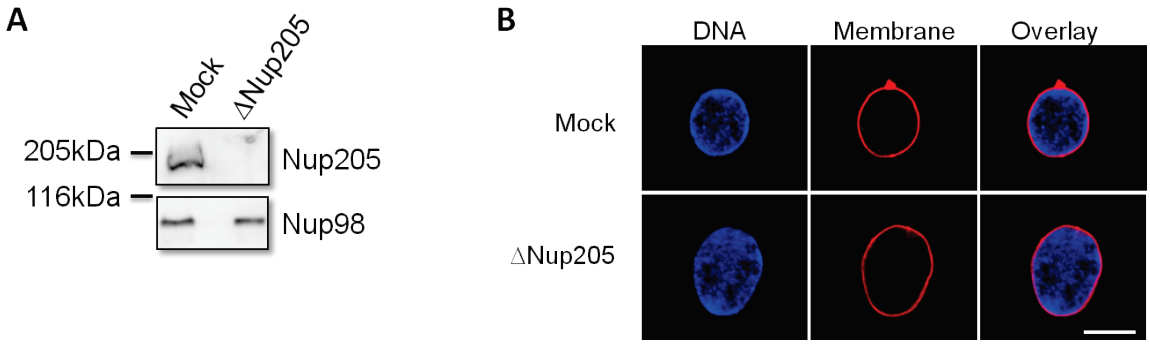

Figure 2.5: *Immunodepletion of Nup205*. (A) Western blot analysis of mock and Nup205 depleted *Xenopus* egg extracts. (B). Nuclei were assembled for 90 min using mock and Nup205 depleted egg extracts and fixed with 4% PFA + 0.5% glutaraldehyde. Nuclei stained with DAPI:chromatin (blue) and DiIC18:membranes (red) , were analyzed using confocal microscopy. (blue: DAPI, red: DiIC18). Scale bar: 20 µm.

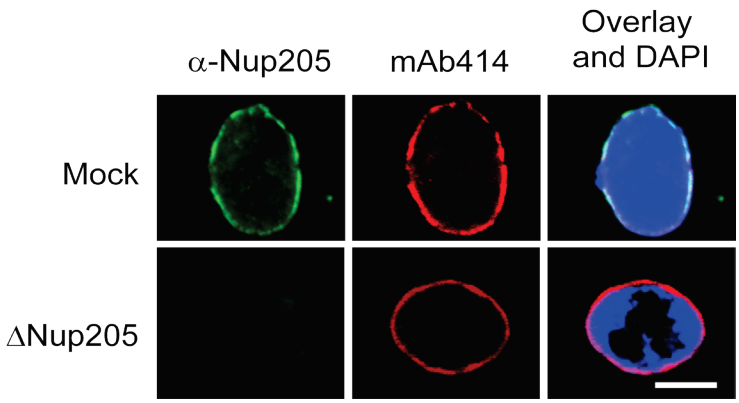

Figure 2.6. *Nup205-Nup93 depleted nuclei contain NPCs*. Nuclei were assembled in mock and Nup205-Nup93 depleted extracts for 90 min and fixed with 4% PFA. Imunofluoresence was done using Nup205 antibodies (green) and the mouse monoclonal antibody mAb414 (red). Nuclei were scanned for chromatin (blue) and antibody staining using aconfocal microscope. Scale bar: 20 µm.

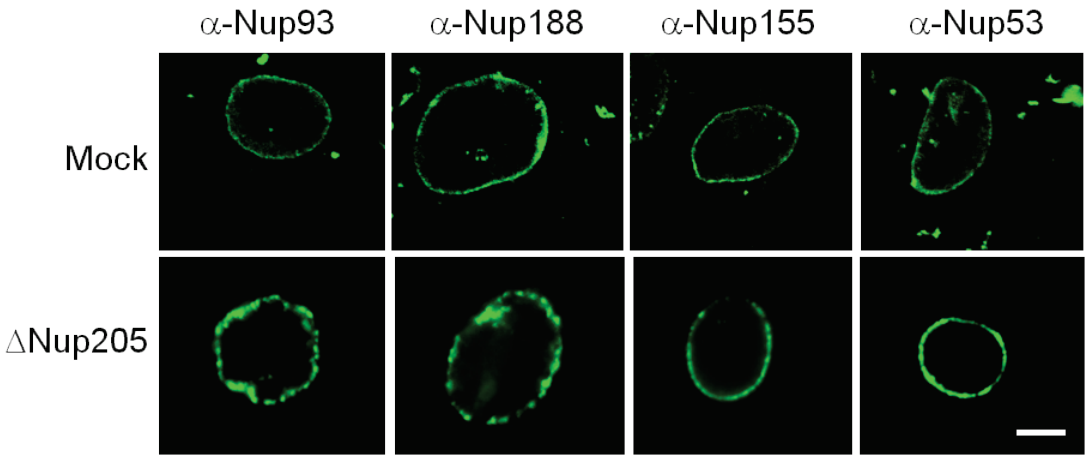

Figure 2.7. *Immunofluorescence of nucleoporins on Nup205-Nup93 depleted nuclei.* Immunofluorescence of Nup93, Nup188, Nup155 and Nup53 on the mock and Nup205-Nup93 depleted nuclei. Nucleoporin staining was analysed using confocal microscopy. Scale bar: 20 µm.

Interestingly, nuclei lacking Nup188-Nup93 were much bigger than control nuclei based on membrane and chromatin staining (Fig. 2.8B). Immunofluorescence for mAb414 indicated that the Nup188-Nup93 depleted nuclei contained NPCs (Fig. 2.9). Since these nuclei increase in size by several fold, we checked whether mock and Nup188-Nup93 depleted nuclei contain the same number of NPCs. The number of NPCs in individual nuclei was counted by staining them with mAb414, a method adopted from an earlier study (D'Angelo et al., 2006). To avoid

background signal, the nuclei were fixed with Vikifix without gluteraldehyde. The slides were analyzed using confocal microscopy. Nuclei with evenly punctuate NPC staining were identified and scanned along the z-axis using maximum intensity projections of optical sections of whole nuclei. Imaris 6.1.5® from Bitplane Scientific Solutions was used for to produce 3D reconstructions of the scanned nuclei in order to count the number of pores as mentioned in section 4.2.3.12. We found threefold more NPCs in the Nup188-Nup93 depleted nuclei compared to the mock control after 2 hours of nuclear assembly (green bars; Fig. 2.10). However, the number of NPCs per sq. micrometer (density of NPCs) for both mock and Nup188-Nup93 depleted nuclei was calculated and no difference in NPC density was found (red bars; Fig. 2.10).

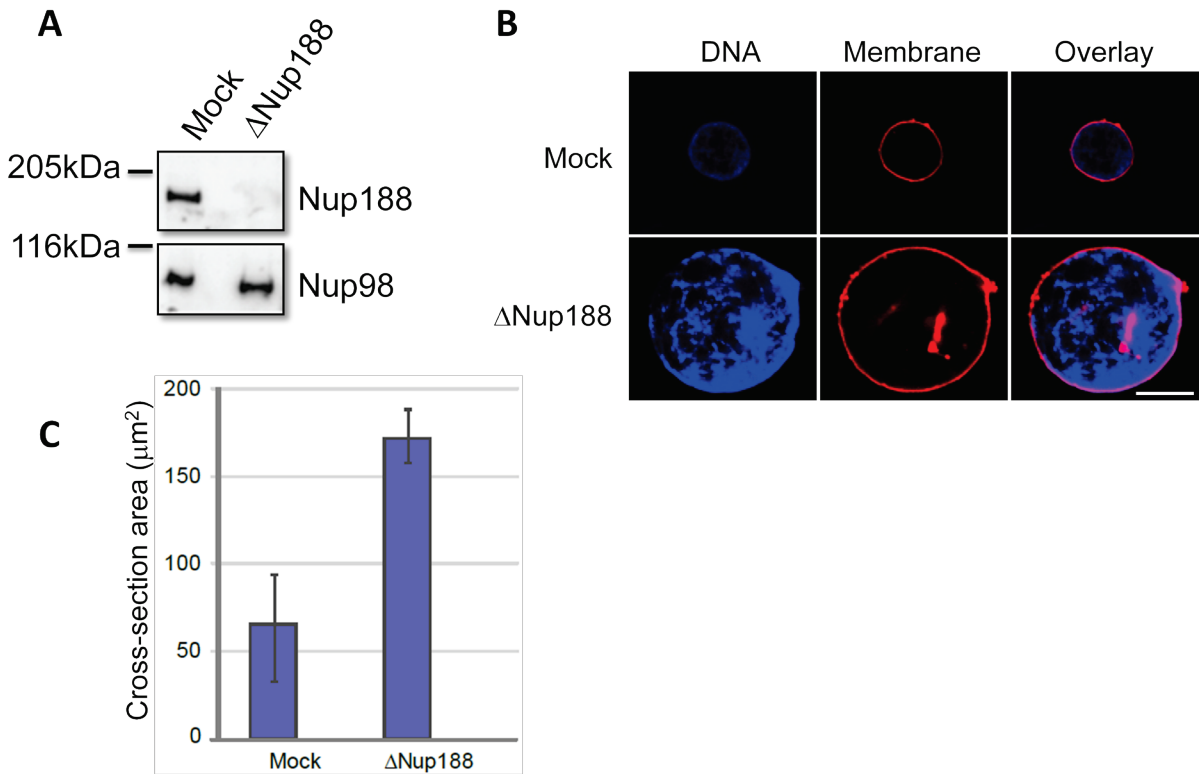

Figure 2.8: *Immunodepletion of Nup188-93 enlarges nuclei*. (A) Mock and Nup188-93 depleted *Xenopus* egg extracts were analyzed by western blot (B). Nuclear assembly using mock and Nup188-93 depleted extracts for 90 min, assembled nuclei are fixed with 4% PFA and 0.5% glutaraldehyde. Confocal microscopy was used to visualize chromatin and membrane staining (blue: DAPI, red: DiIC18). Scale bar: 20 µm. (C). Cross sectional area of mock and Nup188-93 depleted nuclei were measured More than 100 nuclei were selected from the same experiment as in B. Data from an average of three independent experiments is represented, error bars show the total variation.

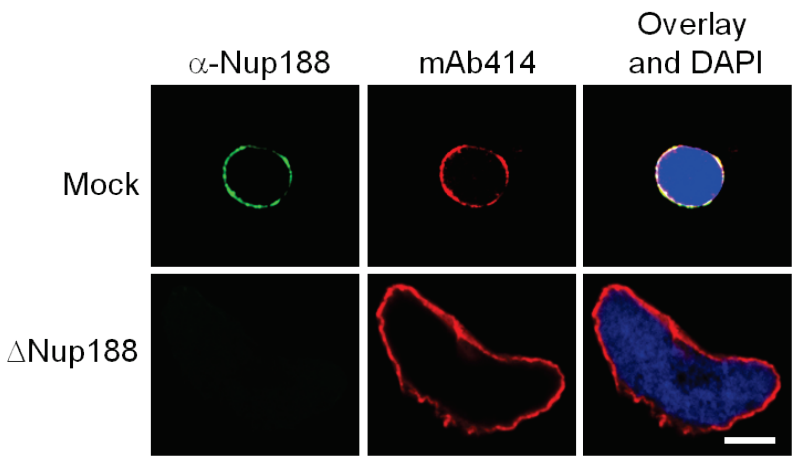

Figure 2.9. *Nup188-Nup93 depleted nuclei contain NPCs*. Immunofluorescence using a Nup188 antibody (green) and the mouse monoclonal antibody mAb414 (red) was done for nuclei assembled using mock and Nup188-Nup93 depleted extracts for 90 min and fixed with 4% PFA. These nuclei were scanned for chromatin (blue) and antibody staining using a confocal microscope. Scale bar: 20 µm.

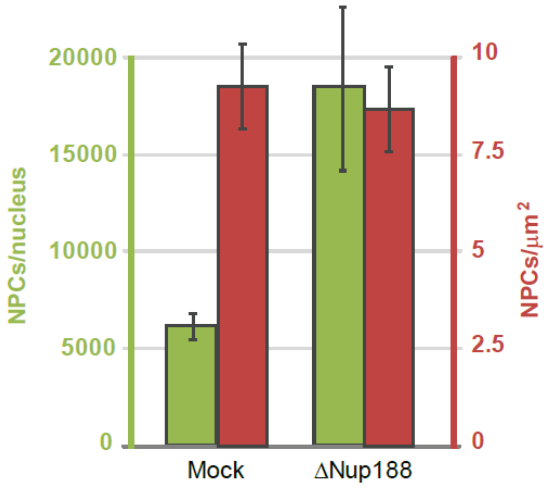

Figure 2.10. *Nup188-Nup93 depleted nuclei contain more NPCs*. Immunofluorescence using Nup188 antibody (green) and the mouse monoclonal antibody mAb414 (red) was done on the nuclei assembled using mock and Nup188-Nup93 depleted extracts for 90 min and fixed with 4% PFA. These nuclei were scanned for chromatin (blue) and antibodies staining using confocal microscopy. The number of NPCs and their density are counted based on the mAb414 as mentioned in sections 4.2.3.12 and 4.2.3.13, respectively. Error bars represent the standard deviation.

2.1.4. Nup188-Nup93 depleted nuclei recruits other nucleoporins and proteins.

The Nup188-Nup93 depleted nuclei were also stained for the presence of other soluble nucleoporins such as Nup93, Nup205, Nup53 and Nup155 using immunofluorescence (Fig. 2.11). All of the tested nucleoporins were present in the depleted nuclei. In addition to soluble

nucleoprins, we tested two transmembrane nucleoporins, gp210 and NDC1 for their presence in the Nup188-Nup93 depleted nuclei. Fig. 2.12A shows that gp210 and NDC1 are present in Nup188-Nup93 depleted nuclei. We also checked whether there was a change in the normal recruitment of the inner nuclear membrane proteins, Lamin B and Lamin B receptor (LBR) in the depleted nuclei. We did immunofluorescence for Lamin B and LBR in depleted nuclei and found that there was no reduction or absence of the tested inner nuclear membrane proteins (Fig. 2.12B). Using the transmission electron microscopy, the morphology of Nup188-Nup93 depleted nuclei further compared with the mock control. Aside from the increase in size of depleted nuclei no morphological alterations were detected (Fig. 2.13).

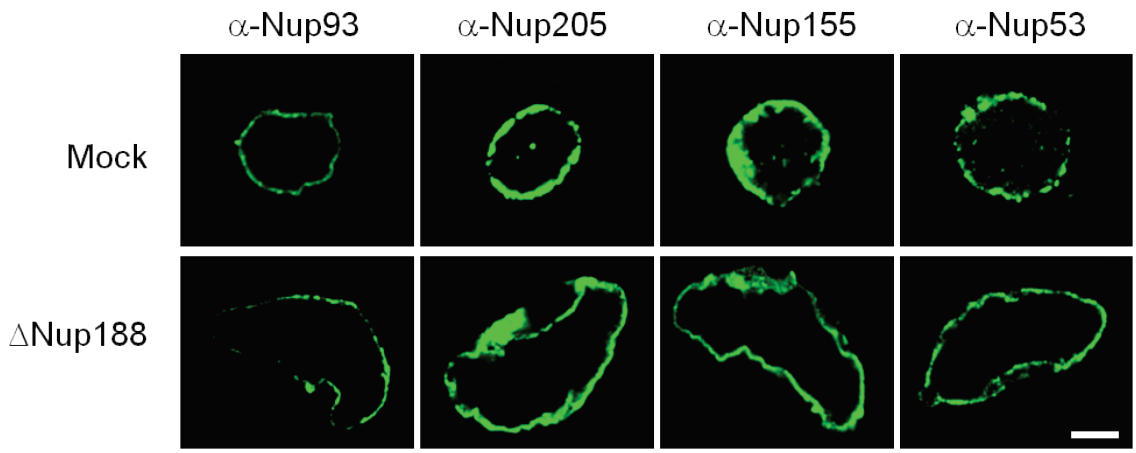

Figure 2.11. *Immunofluorescence of nucleoporins on Nup188-Nup93 depleted nuclei.* Nup93, Nup205, Nup155 and Nup53 were stained using respective antibodies and immunofluorescence in mock and Nup188-Nup93 depleted nuclei. The antibody staining was visualized using confocal microscopy. Scale bar: 20 µm.

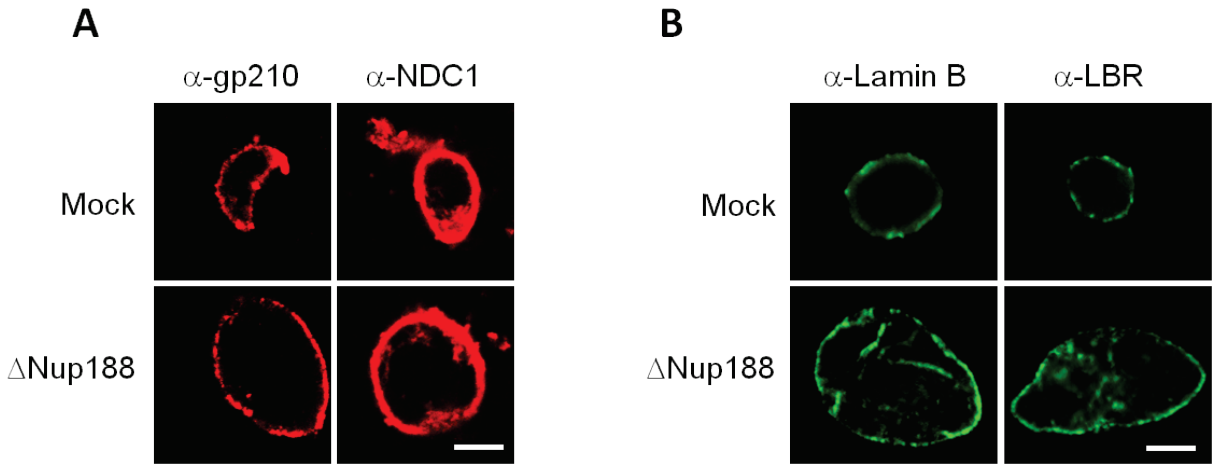

Figure 2.12. *Transmembrane nucleoporins and INM proteins are present in Nup188-Nup93 depleted nuclei.* The mock and Nup188-Nup93 depleted nuclei were assembled, and stained for immunofluorescence using specific antibodies to the transmembrane nucleoporins, gp210 and NDC1 (A) and INM proteins, Lamin-B and Lamin B receptor (LBR). Scale bar: 20 µm.

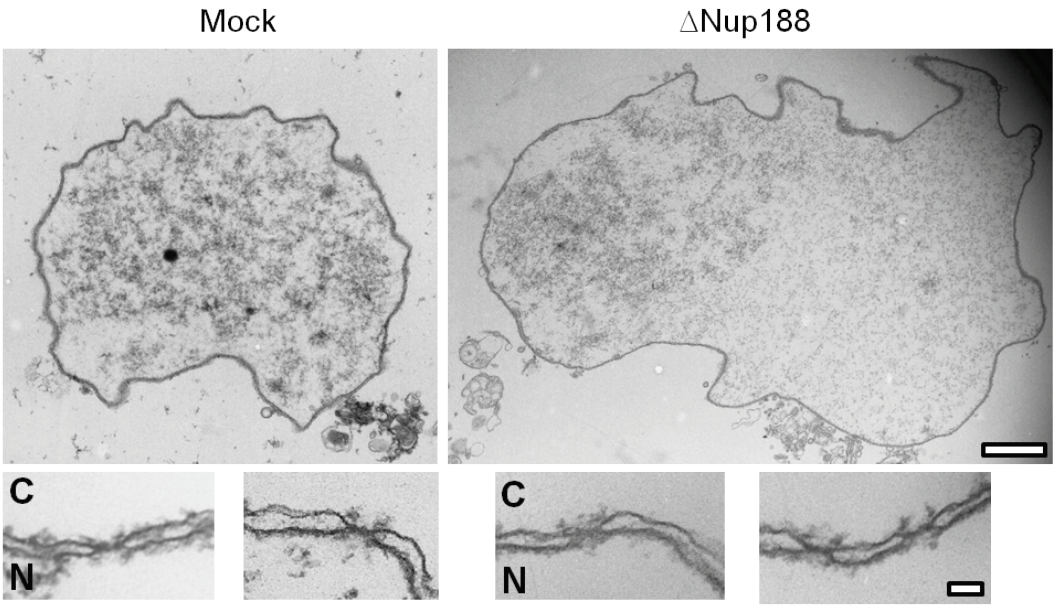

Figure 2.13. *Transmission electron microscopic view of Nup188-Nup93 depleted nuclei.* The nuclei assembled using mock and Nup188-Nup93 depleted extracts were fixed and analyzed in a transmission electron microscope. (C: cytosplasmic side and N: nucleoplasmic side of the NE). Scale bar in the upper row is 1 µm and 100 nm in the lower row.

2.1.5. The Nup188-Nup93 depleted nuclei grow only after the NE is formed.

Until reentry into the mitosis, *in vitro* assembled nuclei grow continuously, but slowly once the NE is formed; however this assembly rate is quite slow. To understand more about the nuclear growth Nup188-Nup93 depleted nuclei, we fixed the assembling nuclei at different time points (Fig. 2.14). In the time course, the size of the mock and Nup188-Nup93 depleted nuclei were similar until 50 min. The rapid growth of Nup188-Nup93 depleted nuclei occurs only after 50 min, meaning that the growth occurs after the NE is completely formed.

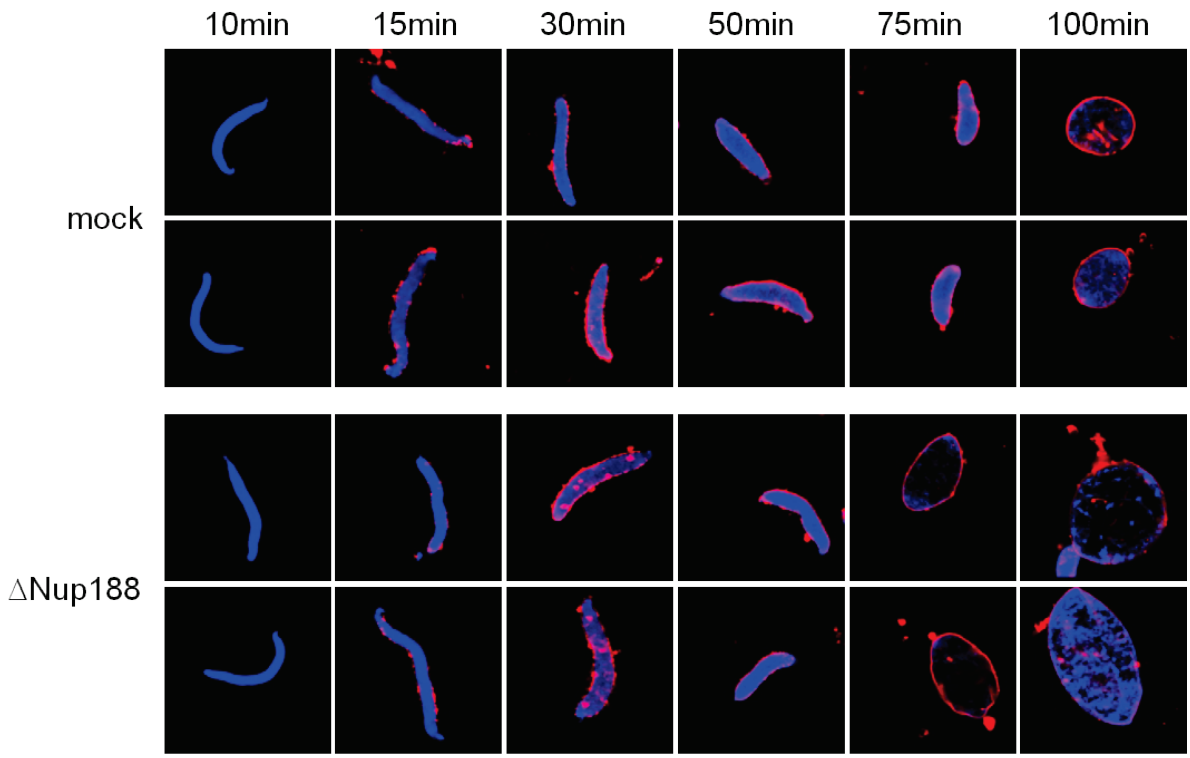

Figure 2.14. *Enlargement of Nup188-Nup93 depleted nuclei happens only after the NE is formed.* The mock and Nup188-Nup93 depleted egg extracts were incubated with demembranated sperm chromatin for 10 min at 20 °C, then prelabeled membranes were added. The nuclear assembly reaction was stopped by fixing the nuclei with 4% PFA and 0.5% gluteraldehyde at the indicated time points (blue: DAPI, red: DiIC18). Scale bar: 20 µm.

After we realized that the growth of Nup188-Nup93 depleted nuclei occurs only after the NE closed we sought to find out the reason for the nuclear enlargement. We could imagine a variety of reasons for this enormous nuclear growth of Nup188-Nup93 depleted nuclei. Some of the reasons are follows. Based on the increase in the volume of Nup188-Nup93 depleted nuclei, we could suspect any impairment in the DNA replication control and resulting an increase in the amount of DNA in turn making it bigger. Another scenario is that the removal of Nup188-Nup93 could increase the exclusion limit for the passive diffusion of NPCs, causing a diffusion of larger molecules into the nuclei. Other scenario could be impairment in the protein import pathways leading to an import of large amount of proteins making the nuclei bigger. Also, in Nup188-Nup93 depleted NPCs, protein or mRNA export pathways might have been deteriorated. This might cause retention of the cargos and accumulation of which might cause an increase in volume of the nuclei. We could also imagine that the amount of increase in membrane components may increase in the volume of the Nup188-

Nup93 depleted nuclei. In this thesis, we planned to systematically study these scenarios in Nup188-Nup93 depleted nuclei in comparison with mock depleted nuclei for the understanding the cause of enlarged nuclei.

2.1.6. DNA content is not increased in Nup188-Nup93 depleted nuclei:

In *Xenopus* egg extracts, after the nuclear assembly the decondensed chromatin can undergo one round of replication. DNA replication licensing ensures that DNA replication happens only once per cycle (Blow and Sleeman, 1990). We wanted to check whether the depletion of the Nup188-Nup93 complex deteriorates the DNA replication licensing machinery. If the licensing of DNA does not occur DNA replication happens multiple times inside the assembled nuclei, this could increase the nuclear size. To test this, we assembled the mock and Nup188-Nup93 depleted nuclei in the presence of 16 µM aphidicolin (a drug that blocks DNA polymerases (Marheineke and Hyrien, 2001)). To check for the DNA replication we added fluorescently labeled nucleotide analogs (dUTPs). During DNA replication, the fluorescent dUTPs would be incorporated on the newly synthesized strands and if the drug aphidicolin blocks the DNA replication, the fluorescent dUTPs would not be incorporated (Fig. 2.15). Although when the DNA replication is blocked, the size of Nup188-Nup93 depleted nuclei did not reduce. This result shows that the amount of DNA is not the reason for the enormous size of Nup188-Nup93 depleted nuclei.

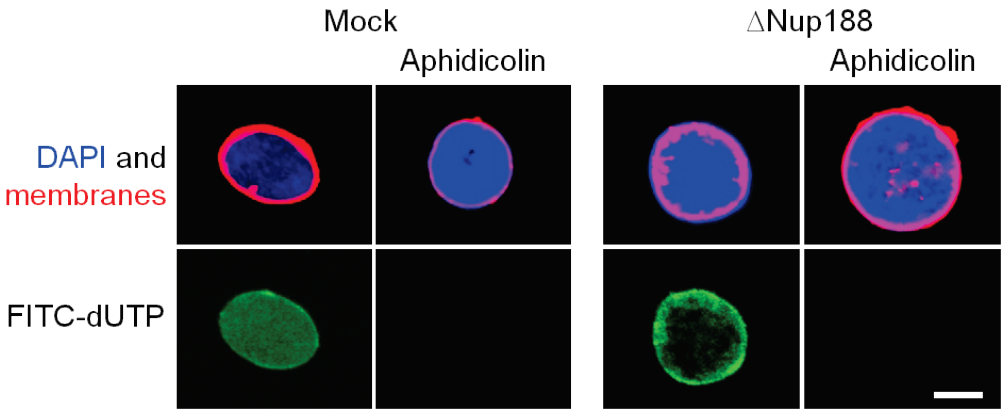

Figure 2.15. *Increase in volume of Nup188-Nup93 depleted nuclei is not caused by higher DNA content.* Nuclei were assembled for 50 min with the mock and Nup188-Nup93 depleted egg extracts. After 50 min, fluorescently labelled dUTP (green) and aphidicolin were added to the indicated nuclei.

The nuclear assembly was stopped at 90 min with 4% PFA and 0.5% gluteraldehyde and analyzed using confocal microscopy (blue: DAPI, red: DiIC18). Scale bar: 20 µm.

2.1.7. Diffusion barrier of the NPCs on Nup188-Nup93 depleted nuclei is not altered:

NPC constitute a diffusion barrier across the cytoplasm and nucleus. The central pore channel of NPC forms a hydrogel like sieve (Frey et al., 2006) that allows the molecules less than 30 kDa to diffuse across the barrier (Mohr et al., 2009). Molecules larger than 30 kDa requires a signal mediated transport machinery. We suspected whether the depletion of Nup188-Nup93 complex would loosen the hydrogel like sieve and this loosening might have allowed uncontrolled flow of larger molecules inside the nucleus, resulting in increased nuclear size. Previously, it was shown that the yeast homologue of Nup188 (Shulga et al., 2000) and the *C. elegans* homologue of Nup205 (Galy et al., 2003) are essential factors for the diffusion barrier to function normally. To test the functionality of the diffusion barrier of the NPCs on Nup205-Nup93 and Nup188-Nup93 depleted nuclei, we treated them with fluorescently labeled dextrans of different size (Fig. 2.16). We have also included mock and Nup98 depleted nuclei as controls, dextrans treated are of sizes 10 kDa, 70 kDa and 2 million Da (mio Da). Two million Da dextran is bigger in size and cannot diffuse inside the nuclei, the intact NPC could also be assumed by the exclusion of two mio Da. Ten kDa dextrans were inside and 2 mio Da dextrans excluded on all conditions. Both the Nup205-Nup93 and Nup188-Nup93 depleted nuclei excluded 70 kDa dextrans indicating that the diffusion barrier in these nuclei was not impaired. As a control, the Nup98 depleted nuclei did not exclude the 70 kDa dextran indicating the diffusion barrier is impaired. The nuclear exclusion of dextrans was quantified on many nuclei on different experiments. It shows the vast majority of Nup188-Nup93 and Nup205-Nup93 nuclei exclude 70 kDa dextrans (Fig. 2.16). These results show that the diffusion barrier of NPCs in Nup188-Nup93 depleted nuclei is not impaired.

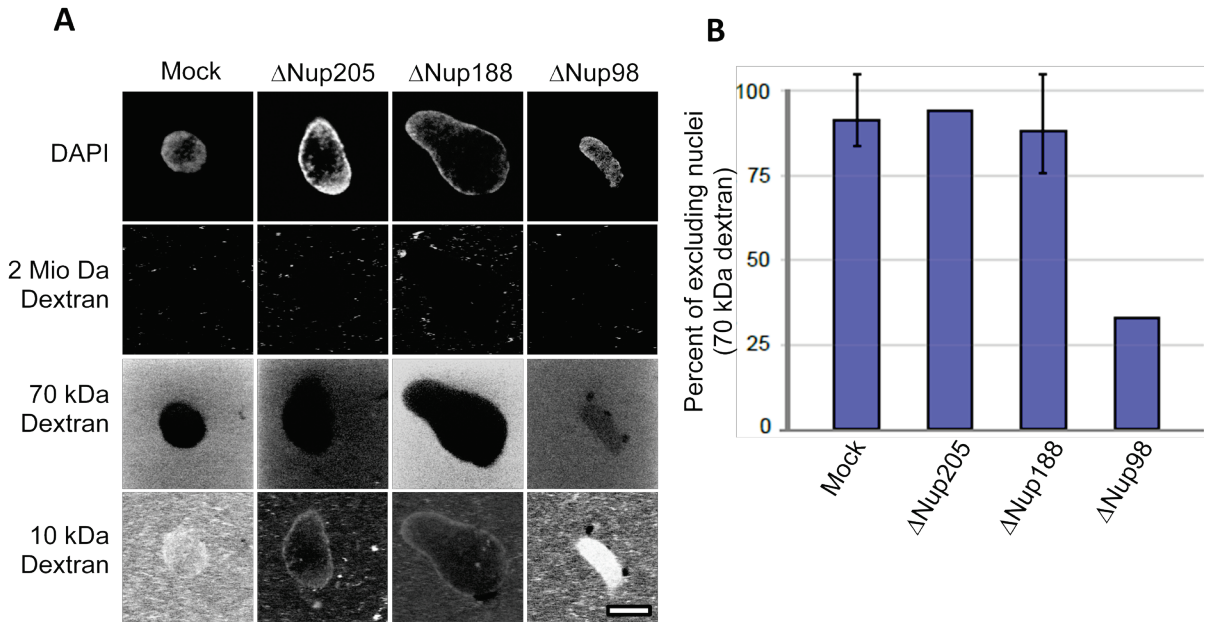

Figure 2.16. *Size exclusion limit of the Nup188-Nup93 is not altered.* (A) Nuclei were assembled with the mock, Nup205-Nup93, Nup188-Nup93 and Nup98 depleted egg extracts. After 90 min, fluorescently dextrans of size 2 million Da (Mio Da) (second row), 70 kDa (third row) and 10 kDa (bottom row) were added to the nuclei and incubated for 5 min and immediately analyzed using confocal microscope. All the nuclei that excluded 2 mio Da, referring the NE is intact, were considered for the analysis. Scale bar: 20 µm. (B). The size exclusion results for 70 kDa from (A) were quantified. Samples from seven independent experiments of mock and Nup188-Nup93, two independent experiments of Nup205-Nup93 and Nup98 were analyzed. Error bars represent the standard deviation.

2.1.8. The rate of nuclear import is not affected during Nup188-Nup93 depletion.

NPCs mediate the signal dependent import and export of molecules across the NE. Initially, we tested the protein import capabilities of both mock and Nup188-Nup93 depleted nuclei using importin α/β dependent substrate (4.2.3.10), we found that both the nuclei were able to import the import substrate with similar intensity based on the staining of EGFP (Fig. 2.17). Then we tested whether the impaired import rate of substrates would cause the increase in the volume of the enlarged nuclei. To understand this we tested the nuclear accumulation protein import by two major import receptor pathways, either importin α/β or transportin dependant, respectively. Protein substrates for both the pathways are tagged to an N-terminal EGFP and

linked to a TEV protease recognition site. These substrates are separately added to the nuclear assembly reactions at 50 min, when the mock and Nup188-Nup93 depleted nuclei are similar size (Fig. 2.18) and contain similar amount of NPCs (2737 +/- 1160 NPCs in a mock depleted nucleus versus 2739 +/- 1437 in Nup188-Nup93 depleted nuclei; Fig. 2.31B). TEV protease fused with a bacterial protein NusA (generally used as a solubility tag for protein expression) was added at the specified time points in the graphs. The fusion of NusA to the TEV protease increases the total size to 90 kDa, this would prevent its diffusion into the nucleus. The import substrates entered into the nuclei were protease protected. This protease protection was then quantified by western blot. The graphs show that both the importin α/β and transportin dependant substrate were able to be imported at the similar rates into the nuclei.

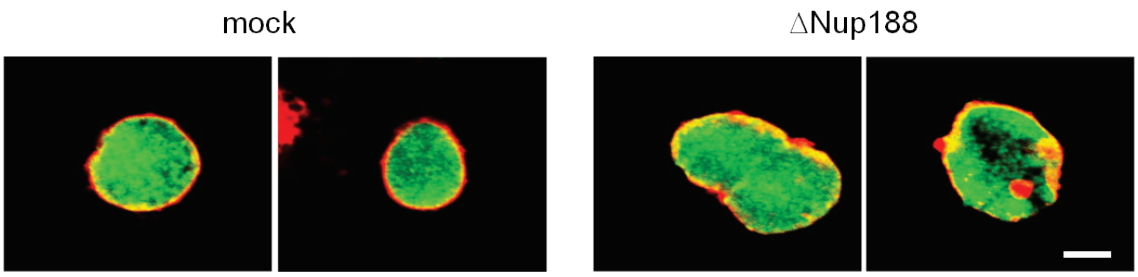

Figure 2.17. *Nuclear import of proteins in Nup188-Nup93 depleted nuclei.* Nuclear assembly was done using the mock and Nup188-Nup93 depleted *Xenopus* egg extracts. During 90 min, nuclei were incubated with nuclear import substrates (green) for 5 min fixed with 4% PFA and 0.5% gluteraldehyde and analyzed using confocal microscopy (red: DiIC18). Scale bar: 20 µm

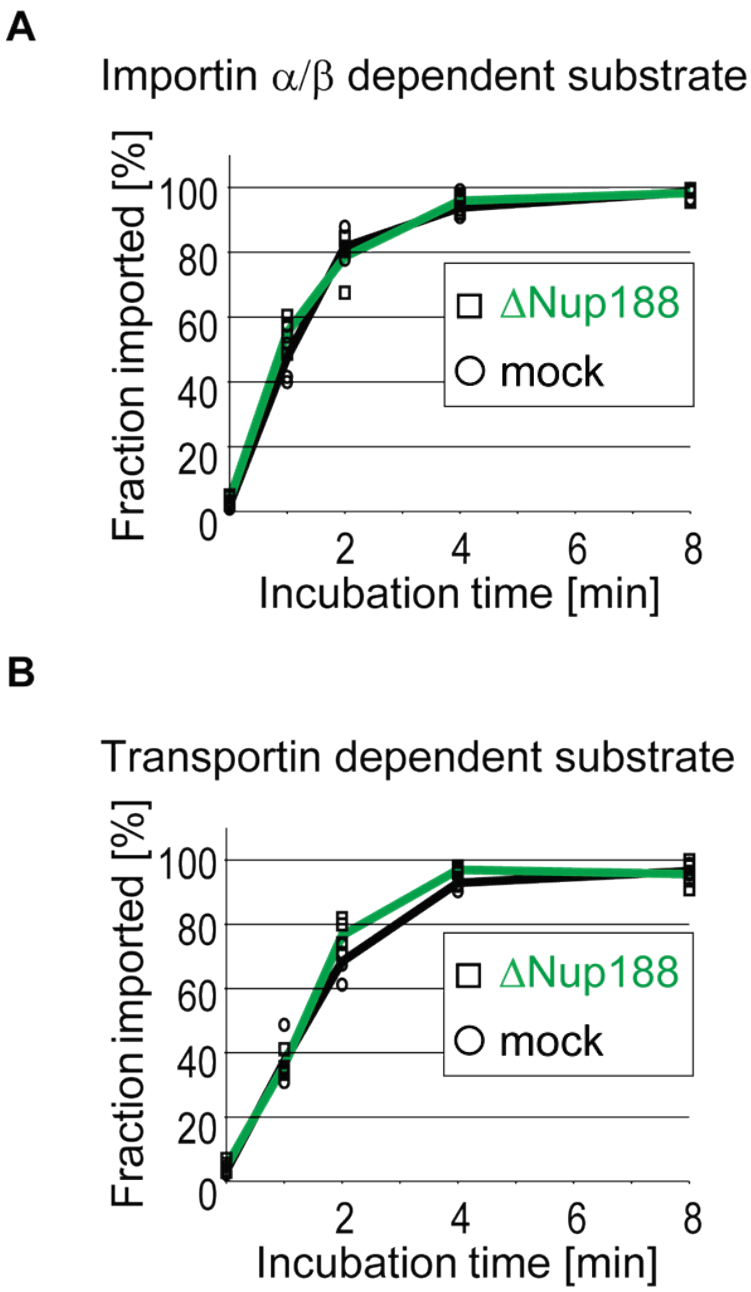

Figure 2.18. *Import kinetics of Nup188-Nup93 depleted nuclei is not changed.* At the 50 min of nuclear assembly using the mock and Nup188-Nup93 depleted *Xenopus* egg extracts, importin α/β (A) or transportin (B) dependent reporter substrates containing a TEV protease cleavage site were added. To check for the nuclear import kinetics, NusA fused TEV protease was added at the indicated time for a min and stopped by the addition of SDS sample buffer and boiling. The samples from different time points were run on a gel, analyzed in a western blot, quantified and plotted on a graph (Circles for mock and squares for Nup188-Nup93 depleted nuclei). The lines indicate the average of four independent experiments (Black for mock and green for Nup188-Nup93 depleted nuclei).

2.1.9. Nuclear export of proteins is not affected during Nup188-Nup93 depletion.

Next, we doubted whether the proteins are to be exported from the nucleus are clogged inside because of any defect in nuclear export machinery during Nup188-Nup93 depletion. To test the nuclear export of proteins we employed a shuttling substrate, containing EGFP, nuclear import and export signals (Englmeier et al., 1999). The shuttling substrate can get inside and get out of the nuclei as it has both the import and export signals, the reporter can be traced by the EGFP fusion protein (4.2.3.11). When the shuttling substrate was added to the mock and Nup188-Nup93 depleted nuclei we did not see the accumulation of the substrate inside the nuclei, meaning the nuclear export was not impaired (Fig. 2.19). To check for the functionality of the shuttling substrate we treated the nuclei with Leptomycin B, a drug that blocks the crm1 mediated nuclear export (Englmeier et al., 1999). The shuttling substrates were accumulated inside the nuclei showing that the substrate is functional. Interestingly, we found that the Leptomycin B treated mock depleted nuclei did not increase its size, this shows that if we block the nuclear export the size of the nuclei does not grow as in the Nup188-Nup93 depleted nuclei. This result, together with the nuclear import shows that the nuclear transport works normally.

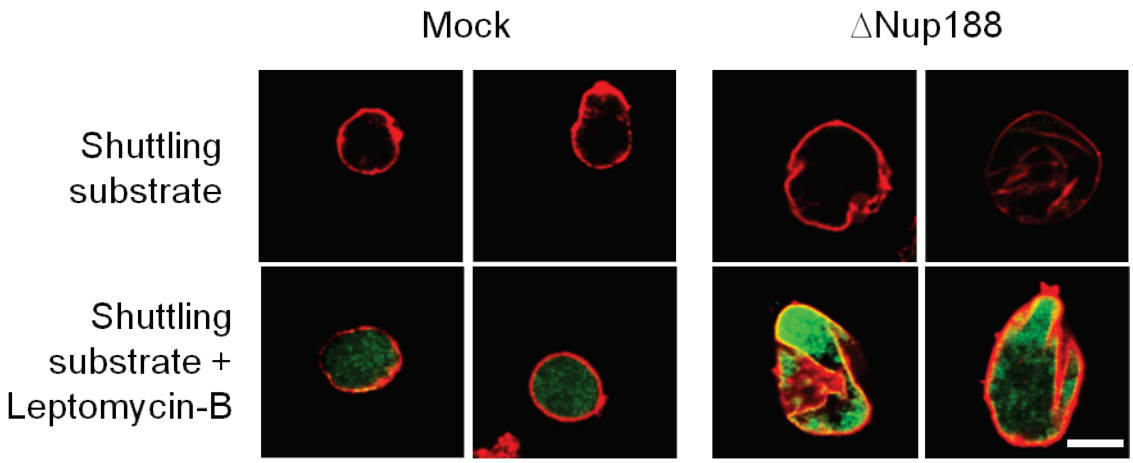

Figure 2.19. *Nuclear export of proteins in Nup188-Nup93 depleted nuclei.* Nuclei were assembled with the mock and Nup188-Nup93 depleted *Xenopus* egg extracts. At 90 min, GFP tagged shuttling substrates (green) with/without 200nM leptomycin-B were incubated for 5 min, fixed with 4% PFA and 0.5% gluteraldehyde and analyzed using confocal microscopy (red: DiIC18). Scale bar: 20 µm

2.1.10. Nuclear export of mRNA is not affected during Nup188-Nup93 depletion.

Since there was no impairment in the export of proteins from the nuclei we then decided to test the export of mRNA although *Xenopus* egg extracts generally are inactive in transcription. We treated these nuclei with the transcriptional inhibitors such as 5, 6-dichloro-1-ß-D-ribobenzimidazole (DRB) or actinomycin D. In the figure 2.20, the results show that even after the treatment of transcriptional inhibitors we found the Nup188-Nup93 depleted nuclei being bigger. This result also shows that an export of mRNA from the nucleus is also not the reason for the larger size of Nup188-Nup93 depleted nuclei.

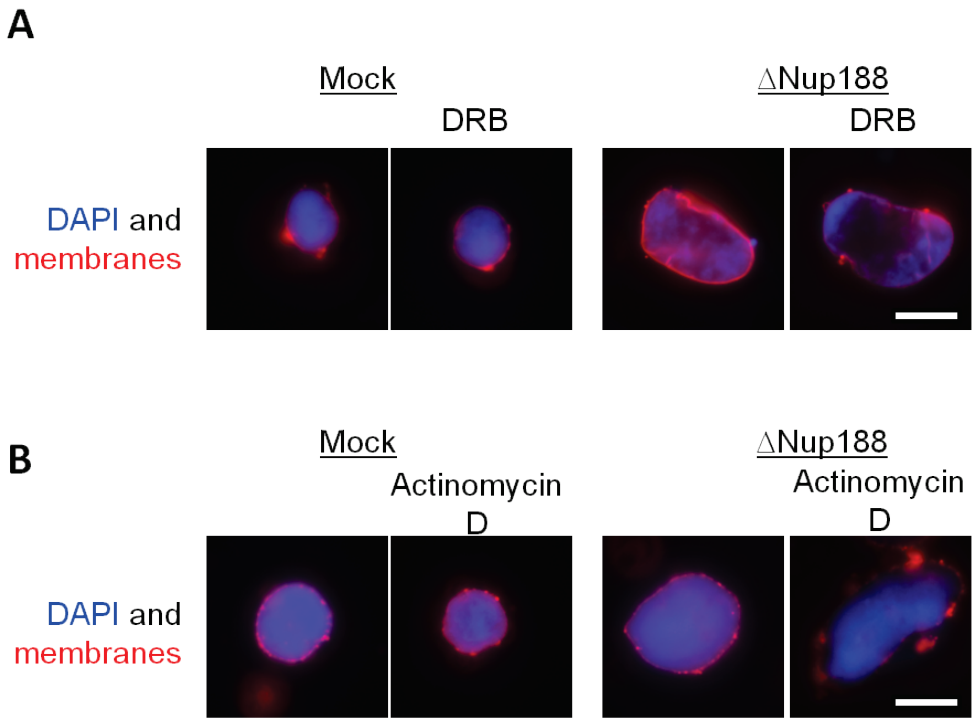

Figure 2.20. *Nuclear export of mRNA in Nup188-Nup93 depleted nuclei.* Nuclei were assembled on mock and Nup188-Nup93 depleted extracts treated with (A) 5, 6-dichloro-1-ß-D-ribobenzimidazole (DRB; 20 µM) or (B) actinomycin D (final concentration of 0.5 µg/ml) where ever mentioned. After 90 min, the nuclei were fixed with 4% PFA and 0.5% gluteraldehyde. The nuclei were analyzed using fluorescence microscopy (red: DiIC18; blue: DAPI). Scale bar: 20 µm.

2.1.11. Blocking of NPCs make Nup188-Nup93 depleted nuclei smaller.

We next tested whether there is any difference in the size of Nup188-Nup93 depleted nuclei when we block the NPCs with wheat germ agglutinin (WGA). WGA is a tetravalent lectin that targets N-acetyl glucosamine moieties in several FG repeat nucleoporins of higher eukaryotes, particularly the Nup62 complex in the central channel (Rutherford et al., 1997) and blocks the transport across NPCs (Finlay et al., 1991). The WGA treated mock and Nup188-Nup93 depleted extracts assembled nuclei *in vitro*. Interestingly, we observed that the size of Nup188-Nup93 depleted nuclei did not grow enormous in size and they were similar in size with mock depleted nuclei (Fig. 2.21). Although, our experiments show that the passive and active transport across the NPCs of Nup188-Nup93 depleted nuclei is working normally, it is interesting to note that the WGA treatment reduces the size of Nup188-Nup93 depleted nuclei.

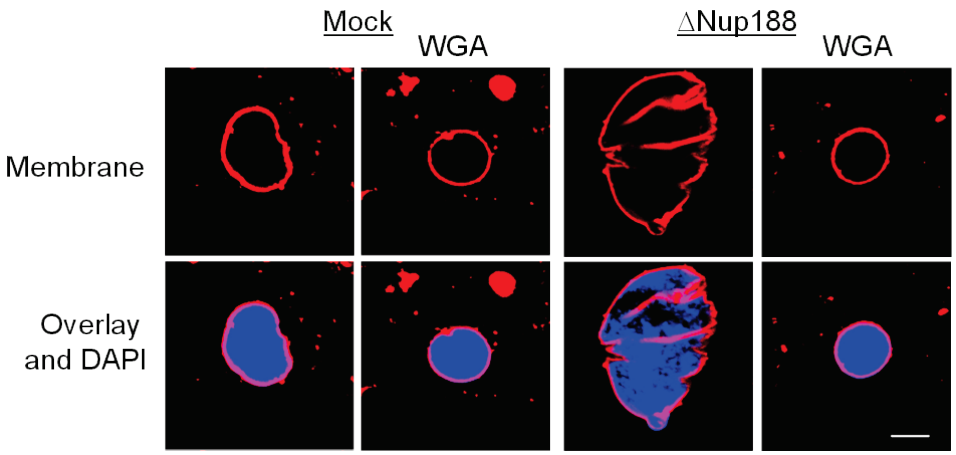

Figure 2.21. *WGA treatment reduces the size of Nup188-Nup93 depleted nuclei.* Demembranated sperm chromatin was incubated with Mock and Nup188-Nup93 depleted *Xenopus* egg extracts for 10 min at 20 °C. WGA (1 mg/ml; final concentration) was added together with labeled membranes (DiIC18) and energy mix. After the nuclear assembly for 90 min, they were fixed with 4% PFA and 0.5% gluteraldehyde and analyzed using confocal microscopy (blue: DAPI and red: DiIC18). Scale bar: 20 µm.

2.1.12. ER fragmentation leads to a decrease in the size of Nup188-Nup93 depleted nuclei.

Above experiments show that the transport across the NPCs in most means is normal in Nup188-Nup93 depleted nuclei. For the enlargement of a nucleus, a lot of membrane is required to keep up the expansion of the nuclei. As the INM and ONM are continuous with the ER, ER might serve as a membrane reservoir and utilized for the nuclear growth of the Nup188-Nup93 depleted nuclei. To test this, during the *in vitro* nuclear assembly, after 50 min (when the NE is completely formed around the chromatin and both mock and Nup188-Nup93 depleted nuclei were of same size), we fragmented the ER network by shaking the nuclei at 800 rpm while the nuclei were assembling. Anderson et. al., (Anderson and Hetzer, 2007) showed that shaking nuclei at this speed cause a fragmentation of the ER network. Interestingly, we find that when the ER is fragmented the Nup188-Nup93 depleted nuclei halted to grow and stay the same size as the mock depleted nuclei (Fig. 2.22). This experiment shows that the membrane is required for the growth of Nup188-Nup93 depleted nuclei.

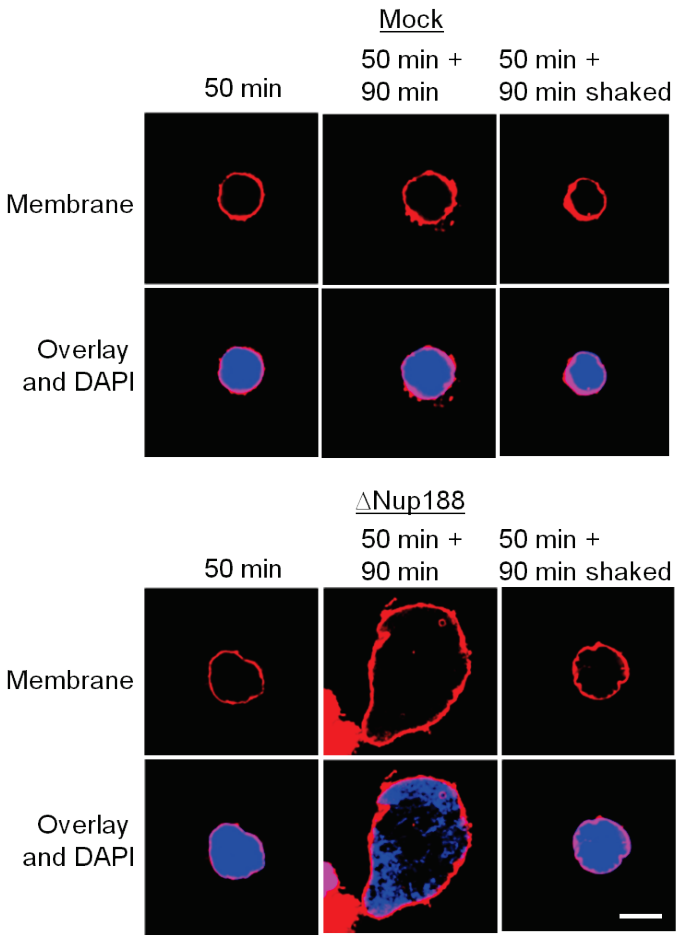

Figure 2.22. *ER fragmentation reduces the size of Nup188-Nup93 depleted nuclei.* Nuclei were assembled with the Mock and Nup188-Nup93 depleted egg extracts for 50 min. Nuclei were either allowed to grow continuously or agitated at 800 rpm at 20 °C. After 90 min, nuclei were fixed with 4% PFA and 0.5% gluteraldehyde. Micrographs are obtained using a confocal microscopy (blue: DAPI and red: DiIC18). Scale bar: 20 µm.

2.1.13. Finding a cause for the bigger nuclei

Both the passive diffusion and active receptor mediated transport of cargos in Nup188-Nup93 depleted nuclei and mock depleted nuclei are similar. We also found that the ER fragmentation during the *in vitro* nuclear assembly of Nup188-Nup93 depleted egg extracts resulted nuclei of similar size with mock depleted nuclei. This indicates that the connection between the NE and the ER is essential for the accelerated growth phenotype seen upon Nup188-Nup93 depletion. If the nuclei grow an expansion of the nuclear membrane is required. For the ONM membrane growth is easy to envision as it is continuous with the ER: Additional membrane components (lipids and proteins) could simply reach the ONM from the

ER by diffusion. However, the INM is only connected to the ONM (and by that indirectly to the ER) via the pore membrane, the region where NPCs localize and where INM and ONM are fused. If a closed NE is formed all membrane components, which are integrated into the INM, need to pass this pore membrane. We speculated that in the wild type situation the passage of membrane components along the pore membrane is limited and could be restricted by the NPC. Upon depletion of Nup188-Nup93 this restriction might be relieved leading to the observed phenotype of accelerated nuclear growth caused by a faster delivery of membrane components to the INM. To test this hypothesis we needed to measure the transport rate of membrane components through the NPC in the wild type situation and upon Nup188-Nup93 depletion. For that we had to develop a experimental system allowing to quantify the passage of integral membrane as a marker for membrane components in *in vitro* assembled nuclei.

2.1.14. An assay to follow the transport of INM proteins

BC08, a single C-terminal transmembrane spanning INM protein (Ulbert et al., 2006) was fused to a EGFP followed by a TEV protease cleavage site at the N-terminus (4.1.5). This reporter protein was expressed and purified in E.coli. The purified recombinant protein was then reconstituted in liposomes. The reporter proteins those are incorporated into the liposomes (proteoliposomes) are added to the nuclear assembly reactions at 50 min, when the NE is complete around the chromatin. The added proteoliposomes readily fuse with ER and the ONM (Fig. 2.23). Immediately after the treatment of proteoliposomes to the nuclear assembly the reporters were distributed throughout ER and ONM that is evident in the immunofluorescence (Fig. 2.24A). The reporters were migrated and enriched only at the NE after 30 min. TEV protease fused with NusA was added to distinguish between the enrichment of the reporters at the INM and ONM. TEV protease together with NusA increases the size of TEV protease and cannot enter into the nucleus because of the absence of NLS. After 30 min, the reporters were protease protected indicating that they are localized in the INM. To ensure that the reporters are at the INM, TEV protease was tagged with NLS were treated at 30 min, the TEV protease were imported inside the nuclei and could cleave the reporters (Fig. 2.23) showing the reporters are indeed at the INM. The protease protection and the reporter cleavage were followed by western blotting of these nuclei over time. A western

blot analysis of the protease protection and the reporter cleavage (Fig. 2.24B) showed that half of the reporters were protease protected at 10 min and completely protease protected at 30 min. Also, the TEV proteases tagged with NLS treatment at 30 min cleaved the reporters at the INM and were not protease protected. These results show that the amount of reporters accumulating at INM based on time could be assayed.

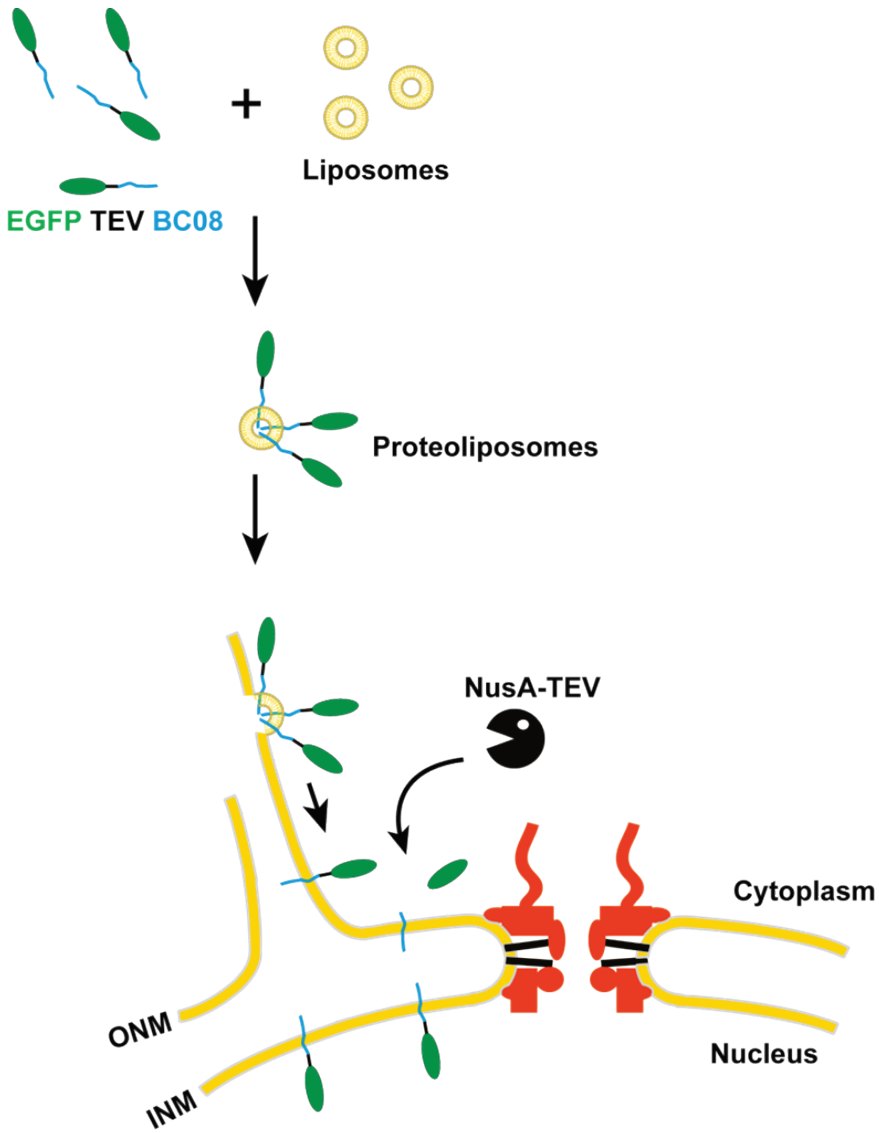

Figure 2.23. *A schematic view of an assay to study the transport of integral membrane proteins to INM.* A fusion protein of EGFP, TEV protease cleavage site and transmembrane domain containing the INM protein BC08 were reconstituted in liposomes. These proteoliposomes immediately fuse with the endoplasmic reticulum (ER) and outer nuclear membrane (ONM) to the *in vitro* assembled nuclei. The inner nuclear membrane localization of the reporter can be distinguished from the ONM and ER by the treatment of TEV protease fused with NusA protein, which could cleave only the reporters at

ER and ONM but not the reporters at the INM because of the absence nuclear localization signal in the fusion protein that contains TEV protease and NusA.

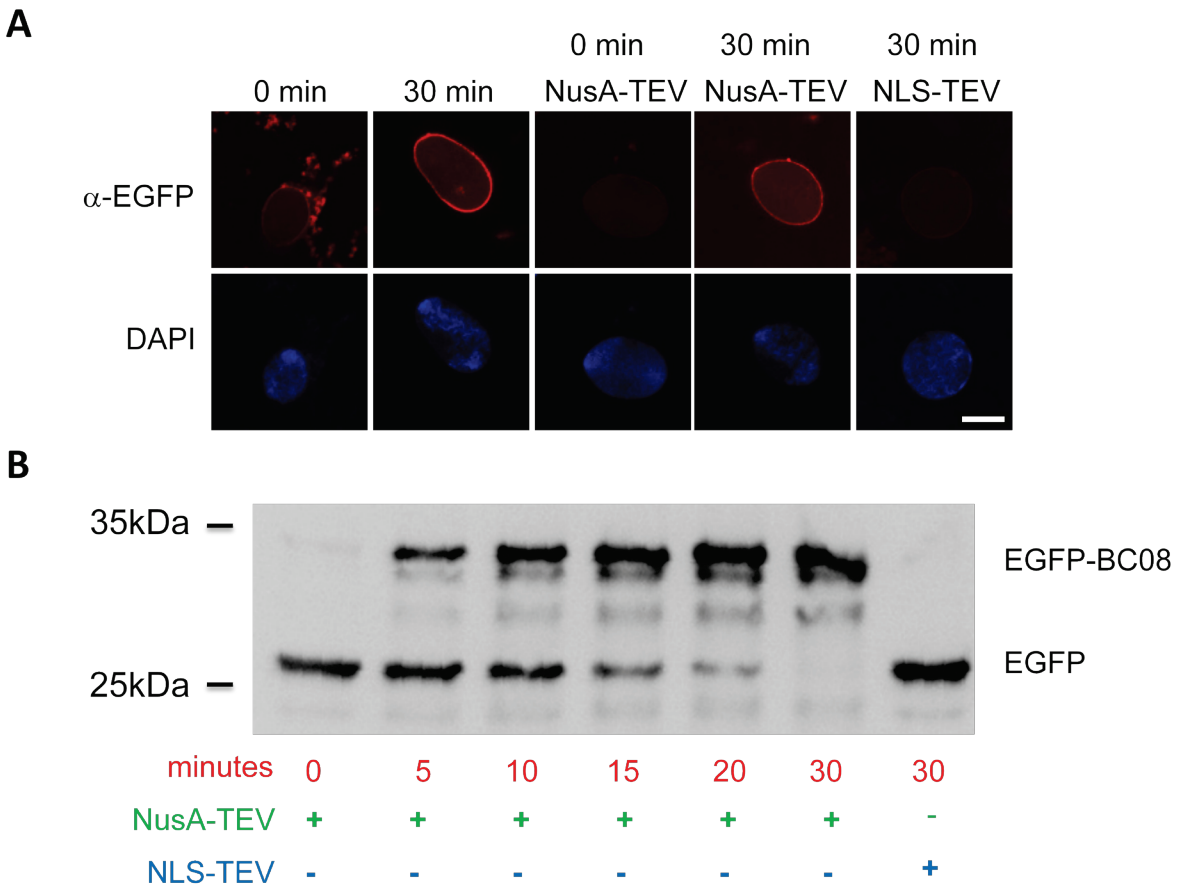

Figure 2.24. *An assay to follow the transport of INM proteins*. (A). After 50 min of the nuclear assembly with the mock and Nup188-Nup93 depleted egg extracts, proteoliposomes containing reporters were added. At the time points mentioned, buffer, TEV protease fused with NusA or TEV protease linked to a nuclear localization signal were added. TEV protease was allowed to function for 5 min and stopped by fixing the nuclei and the samples were processed for immunofluorescence with α-EGFP antibodies (red). Micrographs were obtained using a confocal microscopy (blue: DAPI). Scale bar: 20 µm. (B). The reactions were done as (A), for the western blot analysis the TEV protease cleavage was stopped using the addition of SDS sample buffer and boiling at 95 °C. The samples were loaded on a gel and transferred to a nitrocellulose membrane. The membrane was probed with EGFP antibodies, the position of protease protected (EGFP-BC08) and the EGFP part of cleaved reporters (EGFP) were indicated.

2.1.15. Nup188-Nup93 restricts transport of integral membrane proteins through the NPC

We used the above mentioned assay to check whether the enormous size of Nup188-Nup93 depleted nuclei is due to the increase in rate of transport of membrane components to the INM. After the nuclear assembly for 50 min, when both mock and Nup188-Nup93 depleted nuclei are similar in size and the NE is complete around the chromatin, the proteoliposomes containing the reporter were added. Proteoliposome added nuclei were then treated with TEV protease fused with NusA at different times; the protease protection and the cleavage of reporters were analyzed in a western blot (Fig. 2.25A). Approximately 50% of the protease protection of Nup188-Nup93 depleted nuclei happens at 5 min, much faster than the mock depleted nuclei (Fig 2.25A and B). To confirm the faster protease protection in Nup188-Nup93 depleted nuclei was specific, we co-translated *Xenopus* Nup93 and mouse Nup188 in vitro and added back (Fig. 2.26A). The add-back resulted a decreased rate of protease protection in Nup188-Nup93 depleted nuclei which is similar to the mock depleted nuclei (Fig. 2.25B) showing that the faster delivery of the reporters to the INM in Nup188-Nup93 is specific. We also tested the nuclear assembly of Nup188-Nup93 depleted nuclei reduces in size when we treat the in vitro co-translated *Xenopus* Nup93 and mouse Nup188. Fig. 2.26B shows that after the add-back, the Nup188-Nup93 depleted nuclei reduces in size and looks similar to the mock depleted nuclei. A quantification of the cross sectional area of mock, Nup188-Nup93 depleted nuclei and Nup188-Nup93 depleted nuclei with add-back confirms the reduction in size after the add-back (Fig. 2.26C). A note worth mentioning here is the add-back using the *Xenopus* Nup93 and mouse Nup188 alone could not rescue the enlarged nuclear phenotype. The antibodies against *Xenopus* Nup188 and the anti-His antibodies (from various resources) using immunofluorescence were not able to detect the mouse Nup188 and the His tag fused with the mouse Nup188, respectively. After the nuclear assembly using mock, Nup188-Nup93 depleted and Nup188-Nup93 depleted with add-back *Xenopus* egg extracts, the nuclei were isolated and analyzed in a western blot (Fig. 2.26D) to show the incorporation of recombinant co-translated Nup188 and Nup93 on the Nup188-Nup93 depleted nuclei. The western blot using anti-His antibodies shows the incorporation of recombinant Nup188-Nup93 to the Nup188-Nup93 depleted nuclei and the other western blots show either the depletion of Nup188-Nup93 or equal loading of the samples. Taken together, the above data show that the enormous size of Nup188-Nup93 depleted nuclei is due

to the increased flow of integral membrane proteins to the INM is specific for the Nup188-Nup93 depletion.

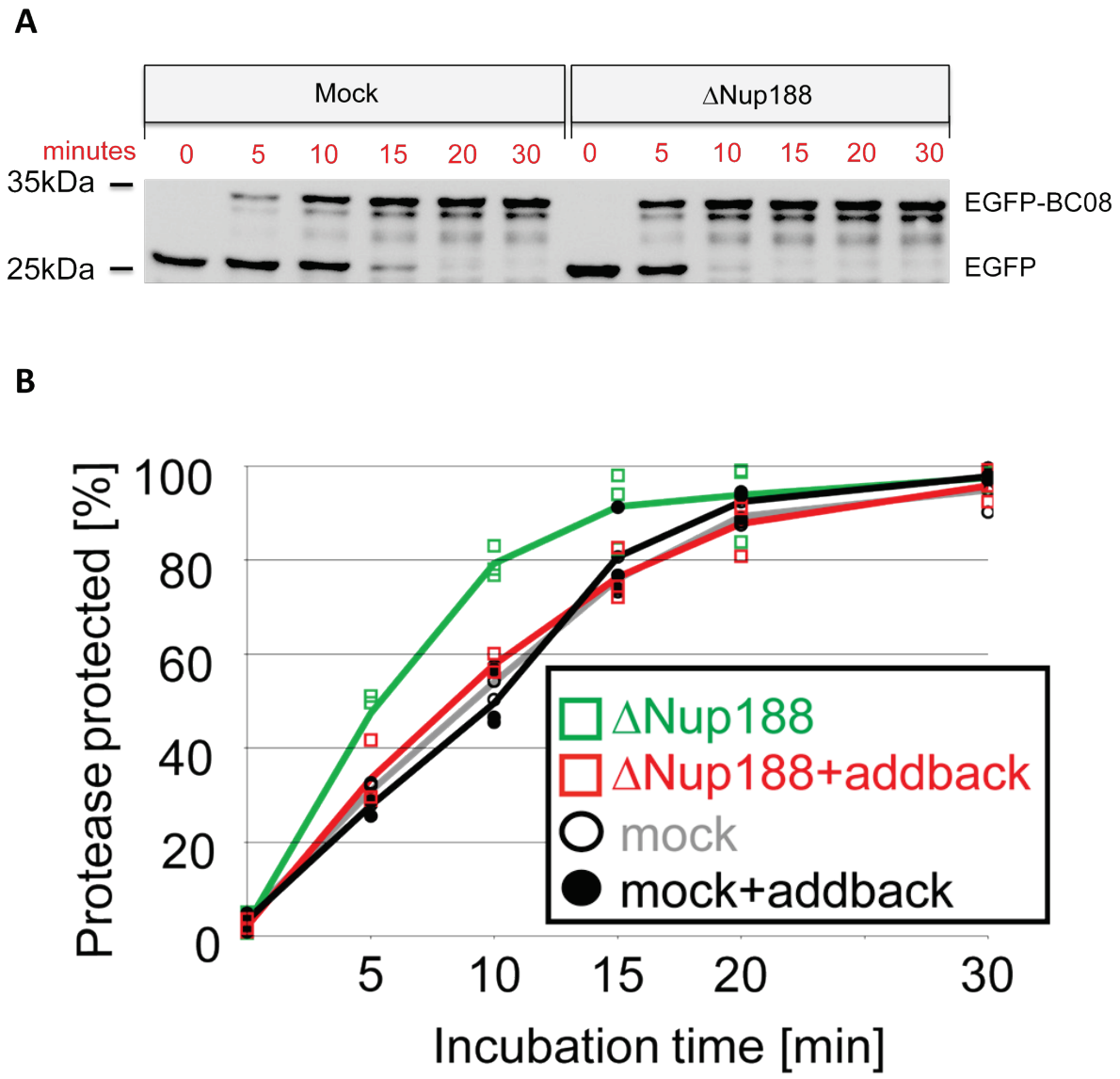

Figure 2.25. *The rate of transport of integral proteins to the inner nuclear membrane proteins is faster in Nup188-Nup93 depleted nuclei.* (A). Nuclei were assembled with mock and Nup188-Nup93 depleted extracts for 50 min, then proteoliposomes containing reporters were added. At the indicated time points, TEV protease fused with NusA was added, after 5 min the reaction was stopped using the addition of SDS sample buffer and boiling. Both the samples were run on a gel and western blotted with EGFP antibodies. The position of protease protected (EGFP-BC08) and the EGFP part of cleaved reporters (EGFP) were indicated. (B). A quantification from the three independent experiments performed in (A) were plotted in a graph together with the samples of mock, Nup188-Nup93 depleted nuclei with addition of in vitro translated Nup188-Nup93 (add-back). The green, red, gray and black colored boxes and lines represent the samples from Nup188-Nup93 depleted nuclei, Nup188-Nup93

depleted nuclei with add-back, mock depleted nuclei and mock depleted nuclei with add-back nuclei, respectively. The lines show the average of three independent experiments.

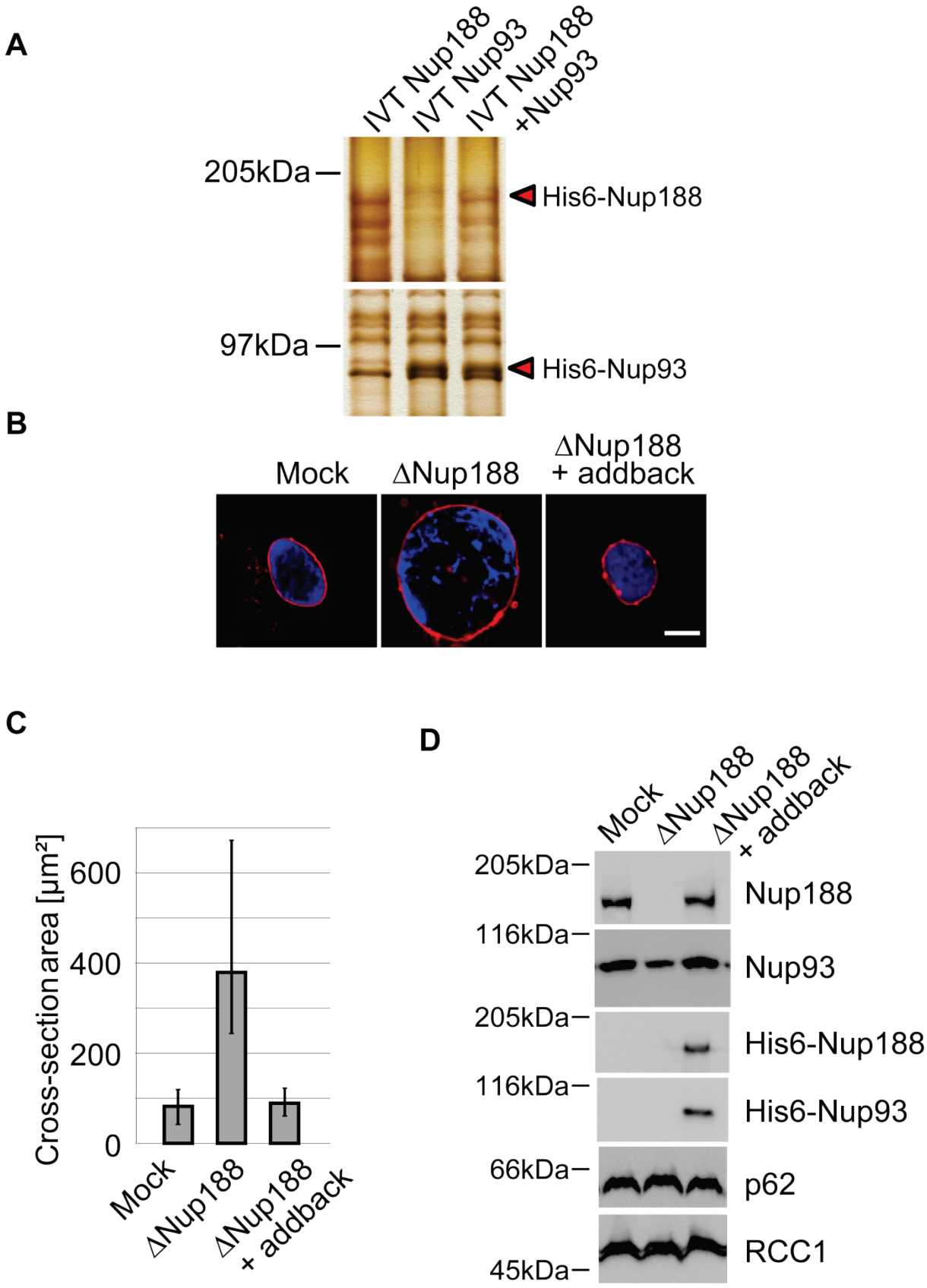

Figure 2.26. *Add-back of the recombinant Nup188-Nup93 to the Nup188-Nup93 depleted nuclei* (A). *In vitro* translated recombinant *Xenopus* Nup93, mouse Nup188 and co-translation of the both proteins were loaded on an 8% SDS-PAGE. After the run, the gel was silver stained and the position of full length recombinant Nup93 and Nup188 were marked. (B). Nuclei were assembled with *Xenopus* egg extracts of mock depleted, Nup188-Nup93 depleted and Nup188-Nup93 depleted with an addition of recombinant co-translated Nup188-Nup93 for 120 min, then fixed with 4% PFA and 0.5% gluteraldehyde and recorded at confocal microscopy (blue: DAPI, red: DiIC18).Scale bar: 20 µm. (C). Quantification of the cross section of more than 30 nuclei assembled in (B). An average of three independent experiments was shown. Error bars indicate the total variation. (D). Nuclei were assembled as in (B) but they were isolated at 1 hr (for an approximate equal estimate of NPCs) and analyzed in western blot. The recombinant Nup188-Nup93 was identified by anti-His6 antibody. Nucleoporin p62 was detected with mAb414 and chromatin binding protein RCC1 serves an equal loading control of the nuclei.

To rule out the possibility that only the BC08 reporter is transported quickly inside the Nup188-Nup93 depleted nuclei, a reporter containing the first transmembrane region of the Lamin B receptor (LBR) enough for INM targeting (Soullam and Worman, 1995) was also tested (Fig. 2.27A). This reporter was also expressed in *E.coli*, purified and reconstituted into proteoliposomes. These proteoliposomes were added to the nuclear assembly reactions of mock and Nup188-Nup93 depleted nuclei with or without the add-back of recombinant Nup188-Nup93 at 50 min. These nuclei were treated with TEV protease tagged with NusA at different time points and analyzed in western blot for the protease protection and the reporter cleavage of the reporters. The results show that the reporters are delivered to INM much earlier in the Nup188-Nup93 depleted nuclei than the controls. Also, the add-back of recombinant Nup188-Nup93 shows the similar behavior for both the conditions. This results show that any of the INM proteins would be delivered faster into the Nup188-Nup93 depleted nuclei.

We also tested whether this faster delivery of the INM proteins into the nuclei is specific only of the Nup188-Nup93 depleted nuclei. As done above, we did a depletion of Nup205-Nup93, assembled nuclei and checked whether these would cause a faster transport of INM proteins into the nuclei (Fig. 2.27B and C). The results show that both the reporters (BC08 and LBR) behave similar to mock depleted nuclei. Therefore, the enlarged nuclei phenotype of Nup188-Nup93 depleted nuclei is caused by the faster delivery of the INM proteins into the nuclei.

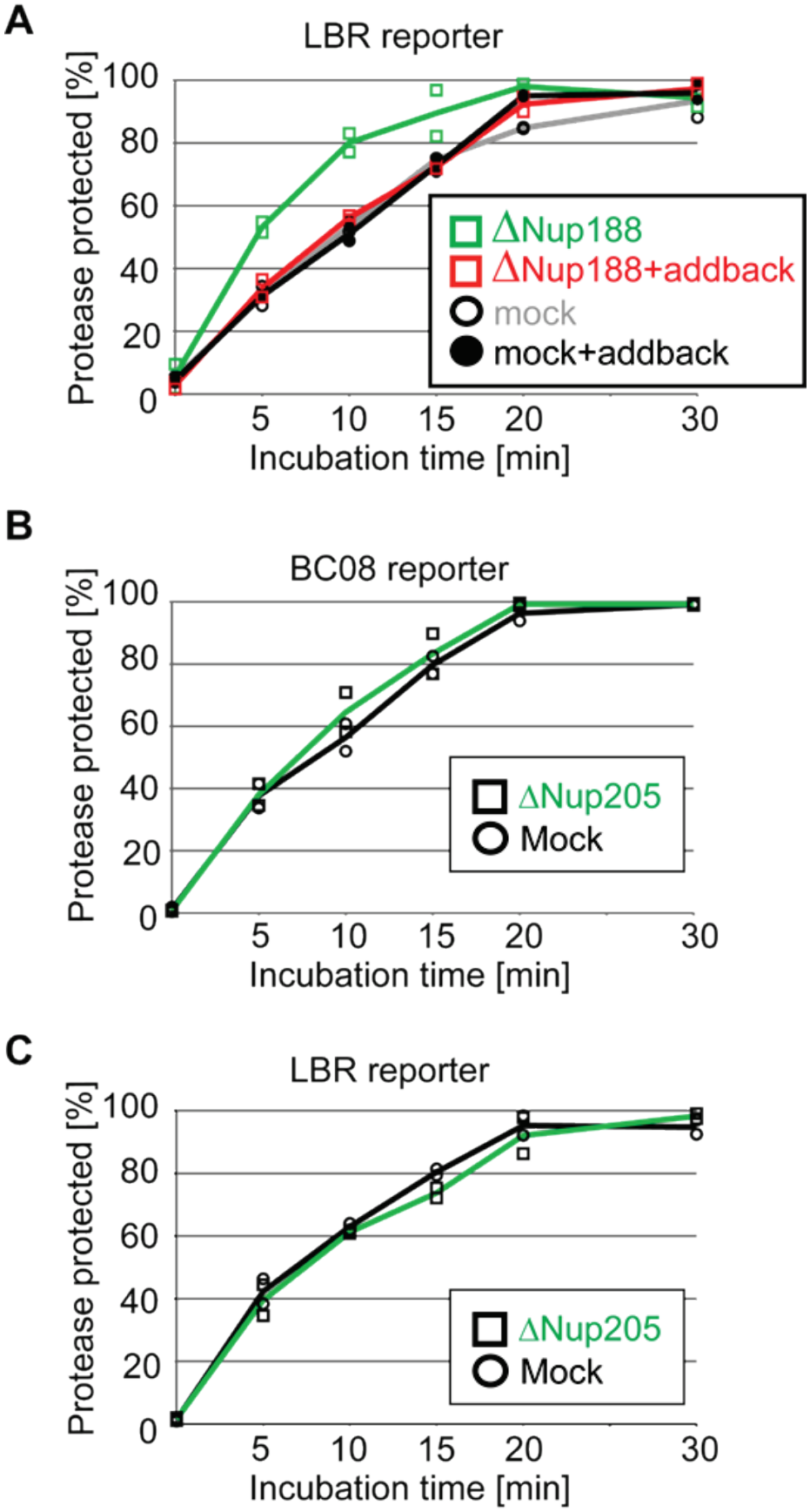
A
LBR reporter
Protease protected [%]
100
80
60
40
20
0
5
10
15
20
30
Incubation time [min]
ΔNup188
ΔNup188+addback
mock
mock+addback
B
BC08 reporter
Protease protected [%]
100
80
60
40
20
0
5
10
15
20
30
Incubation time [min]
ΔNup205
Mock
C
LBR reporter
Protease protected [%]
100
80
60
40
20
0
5
10
15
20
30
Incubation time [min]
ΔNup205
Mock

Figure 2.27. *The transport of INM reporters in Nup188-Nup93 and Nup205-Nup93 depleted nuclei.* Quantification of INM targeting of LBR reporters in Nup188-Nup93 depleted nuclei (A), BC08 and LBR reporters in Nup205-Nup93 depleted nuclei (B) and (C), respectively. The quantification was done for two independent experiments for Nup188-Nup93 and Nup205-Nup93 depleted nuclei.

2.1.16. Only INM proteins could travel into the Nup188-Nup93 depleted nuclei

The INM reporters reach inside the nuclei much faster in Nup188-Nup93 depleted nuclei than in mock depleted nuclei showing that some control of the flow of membrane components was lost. We asked whether the proteins of ER and ONM could be transported inside the nuclei and mis-localized in INM if Nup188-Nup93 was lost. For testing this, we used two ER membrane proteins as reporters in the previously mentioned assay: SPC18, a single-spanning membrane subunit of signal peptidase complex (Shelness et al., 1993) and Calnexin, a C-terminal fragment containing transmembrane region of the chaperone protein localized in ER (Bergeron et al., 1994). Both reporters contain a TEV protease cleavage site. When these reporters were added to the Nup188-Nup93 depleted nuclei, even after 60 min the reporters were not protease protected (Fig. 2.28). This means that both ER reporter proteins were not mis-localized to the INM. The cytoplasmic part for SPC18 and Calnexin are 31 and 41 kDa, respectively. These domain sizes were similar to the nucleoplasmic domain sizes of BC08 and LBR reporters described previously. These results shows, in Nup188-Nup93 depleted nuclei the mis-localization of ONM and ER proteins into the INM has not occurred.

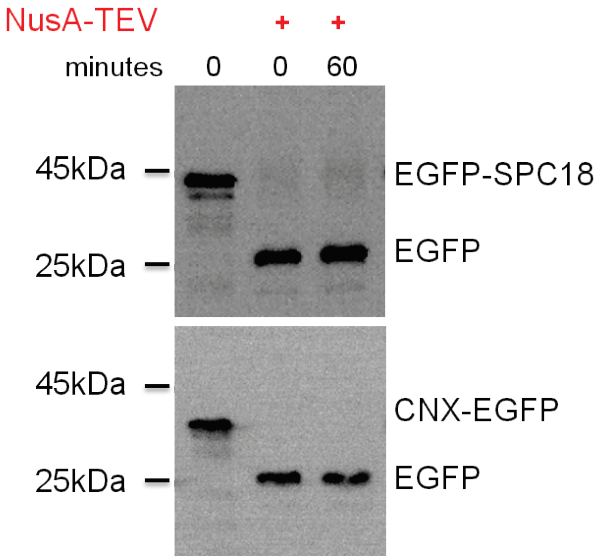

Figure 2.28. *ER protein reporters are not mislocalized in Nup188-Nup93 depleted nuclei.* Transmembrane containing fragments of SPC18 and Calnexin were assayed in Nup188-Nup93 depleted extracts. At the indicated time points, at mentioned places, NusA TEV protease was added, samples were analyzed in western blot using anti-EGFP antibodies.

2.1.17. Size limitation of the INM proteins to travel into the Nup188-Nup93 depleted nuclei is still valid

Most of the INM proteins have a nucleoplasmic domain less than 40 kDa. Previously, it was shown that an increase in nucleoplasmic size to 47 kDa prevents the INM targeting of those proteins (Ohba et al., 2004). As there is a faster flow of the membrane components to the INM in Nup188-Nup93 depleted nuclei, we tested whether these nuclei still follow the restricted size limit of nucleoplasmic domains. BC08 reporter was increased to 94 kDa and 64 kDa by fusing with NusA or GST protein moieties, respectively. INM targeting of these reporters were done on mock and Nup188 depleted nuclei as mentioned above. The results show that both 94 kDa and 64 kDa reporters were not able to traverse into the INM (Fig. 2.29). Nup188-Nup93 depleted nuclei still restricts the size of nucleoplasmic domain of INM proteins.

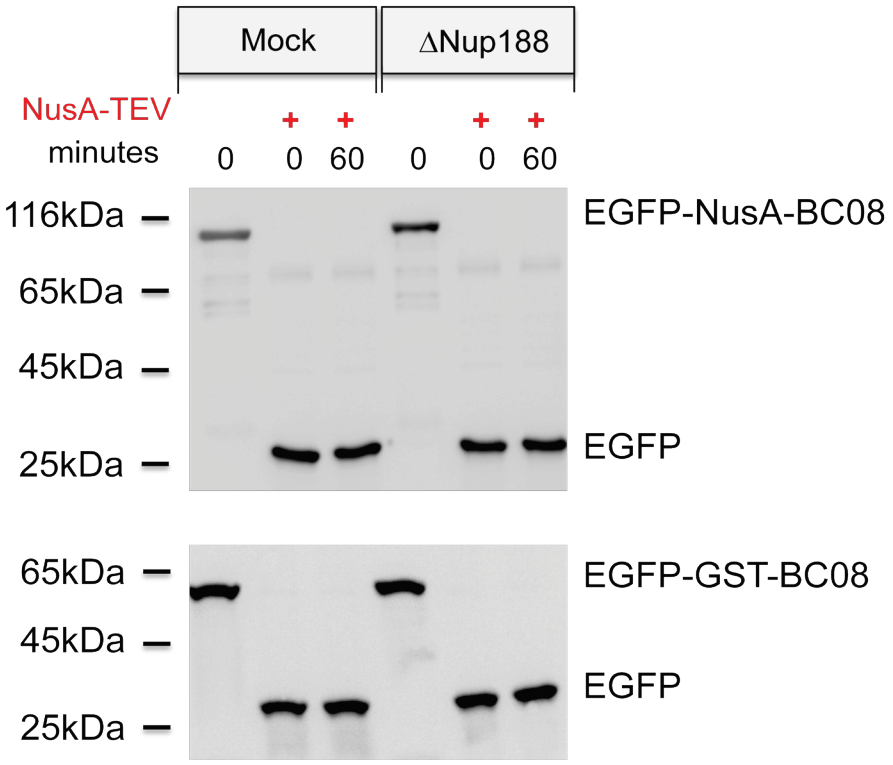

Figure 2.29. *Nup188-Nup93 depleted NPCs allow normal size exclusion limit for targeting of INM proteins into the nuclei.* The nucleoplasmic domain of BC08 reporter was increased to 94 kDa or 64 kDa by fusing NusA or GST proteins. These reporters were treated on mock and Nup188-Nup93 depleted nuclei. At 0 or 60 min, where indicated, NusA-TEV protease was added to the samples and analyzed by western blot.

2.1.18. Faster transport of proteins to INM is not caused by the increased number of NPCs.

The results on the depletion of Nup188-Nup93 show that the passage of INM proteins through the pore is increased and the transport of membrane components are rate limiting for the nuclear growth. Given the size of the Nup188-Nup93 depleted nuclei, we could imagine two possible scenarios:

1. Nup188-Nup93 is a critical component of NPCs and carries out the function of restriction of the flow of membrane components through the NPCs (Fig. 2.30; scenario 1).

2. During the depletion of Nup188-Nup93, NPC assembly could be increased causing more NPCs. With more NPCs, the total transport capacity of the Nup188-Nup93 depleted nuclei is increased and the expansion in the NE area would be a secondary effect (Fig. 2.30; scenario 2).

To distinguish between the above two scenarios, we blocked the de novo NPC assembly into the intact NE by treating 2 μM importin β, as done previously (D'Angelo et al., 2006). This excessive importin β hinders NPC formation during its early stage by inhibiting Nup107-Nup160 complex, an essential early component of NPC formation (Franz et al., 2007; Harel et al., 2003; Rasala et al., 2006; Walther et al., 2003). Two μM importin β was added to the nuclear assembly reaction of mock and Nup188-Nup93 depleted extracts at 50 min (when the NE is formed and both the nuclei is of similar size and NPCs are already formed).

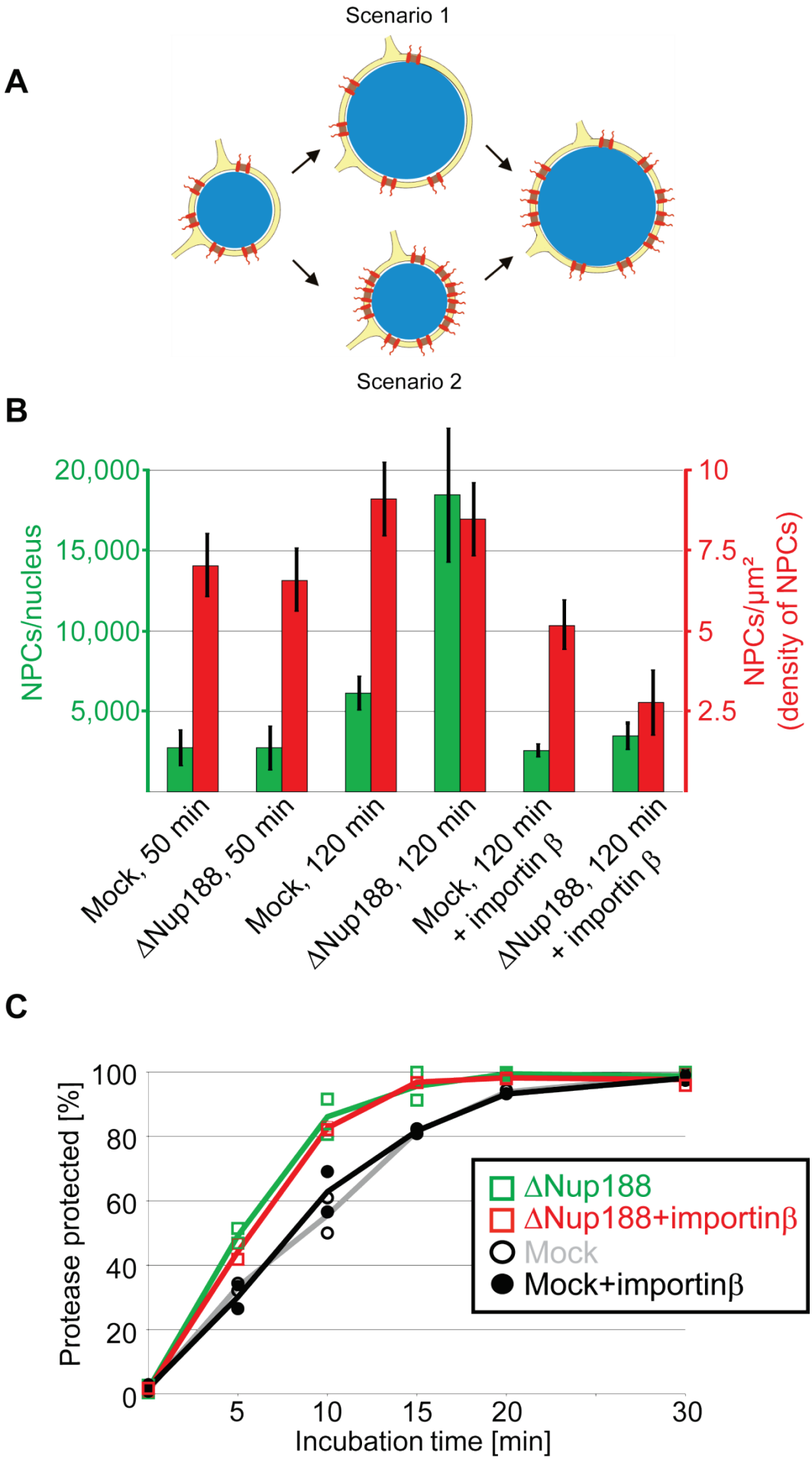
A
Scenario 1
Scenario 2
B
NPCs/nucleus
20,000
15,000
10,000
5,000
NPCs/µm²
(density of NPCs)
10
7.5
5
2.5
Mock, 50 min
ΔNup188, 50 min
Mock, 120 min
ΔNup188, 120 min
Mock, 120 min
+ importin β
ΔNup188, 120 min
+ importin β
C
Protease protected [%]
100
80
60
40
20
0
5
10
15
20
30
Incubation time [min]
ΔNup188
ΔNup188+importinβ
Mock
Mock+importinβ

Figure 2.30. *The enlarged growth and faster delivery of INM proteins of Nup188-Nup93 depleted nuclei are not dependent on the total number of NPCs.* (A). Schematic view of the two possible scenarios of nuclear expansion and increase in the number of NPCs during Nup188-Nup93 depletion. Scenario 1 shows that during Nup188-Nup93 depletion, a faster growth of the NE allows recruiting more NPCs. In scenario 2, the Nup188-Nup93 depletion causes an increased NPC formation, this result an increase in total transport capacity and allowing nuclear volume and NE expansion. (B). Mock and Nup188-Nup93 depleted egg extracts were used for nuclear assembly for 50 min and 120 min. Where mentioned, 2 μM importin β treatment blocked the de novo NPC assembly after 50 min (when the NE is formed), after the treatment the nuclei were allowed to assemble 70 min more (a total of 120 min). Total NPC numbers for an individual nucleus (green bars) and the density of NPCs (red bars) were quantified and plotted in a graph. (C). A quantification from two independent nuclear assembly reactions using mock and Nup188-Nup93 depleted egg extracts. Nuclei were assembled for 50 min, at the indicated places 2 μM importin β was added to stop the de novo NPC assembly. EGFP-BC08 reporter was used for INM targeting analysis on these nuclei. Squared boxes are from Nup188-Nup93 depleted nuclear samples (red and green represent with and without a treatment of 2 μM importin β, respectively) and circles from mock depleted nuclear samples (filled and open circles represent with and without a treatment of 2 μM importin β, respectively). The lines show the average of two independent experiments.

At the point of importin β addition, the total number and the density NPCs in mock and Nup188 depleted nuclei are almost same (Fig 2.31B, green and red bars, respectively). The nuclear assembly reaction was continued for another 70 min (a total of 120 min). During this time the Nup188-Nup93 depleted nuclei had grown significantly faster than the mock depleted nuclei. After 120 min, there is no significant difference in the total number of NPCs in mock and Nup188-Nup93 depleted nuclei (Fig. 2.30B; green bars). After the treatment of importin β to mock and Nup188-Nup93 depleted nuclei at 50 min (when the NE is complete around the chromatin and the sizes of both mock and Nup188-Nup93 depleted nuclei are same) and allowed to the nuclei to grow until 120 min. The number of NPCs in mock and Nup188-Nup93 depleted nuclei were similar (Fig. 2.30B; two green bars at the complete right end) and density of latter is decreased because of the increase in the total NE area (Fig. 2.30B; two red bars at the complete right end). The protease protection was measured on mock and Nup188-Nup93 depleted nuclei after the treatment with importin β at 50 min. The BC08 reporters were still protease protected much earlier than in control (Fig 2.31C). These data indicate that the rapid increase in size of the nuclei is not because of the increase in the total number of NPCs in Nup188-Nup93 depleted nuclei. Considering all the above experiments, Nup188-Nup93 depletion cause an increase in the flow of integral membrane proteins destined for INM through NPCs, showing the importance of Nup188-Nup93 in NPCs in controlling the flow of membrane components along the pore membrane.

2.1.19. INM reporters are not targeted in the nuclei that do not contain NPCs

To understand whether the transport of INM reporters happen only through the NPC by passive diffusion along the plane of membrane, we used BC08 reporter in INM targeting assay in Nup107-Nup160 is depleted from the *Xenopus* egg cytosol (Fig. 2.31). The nuclei assembled with the Nup107-Nup160 depleted cytosol are devoid of NPCs (Harel et al., 2003; Walther et al., 2003). Even after 60 min, the BC08 reporters are protease protected (Fig. 2.31A) in the Nup107-Nup160 depleted nuclei. These results show that the INM reporters were not targeted into the INM in the nuclei that devoid of NPCs.

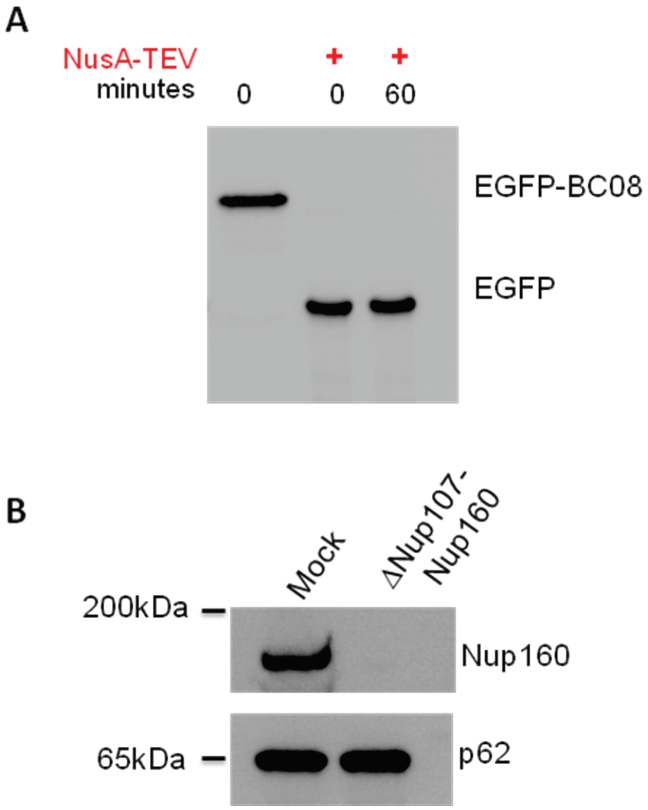

Figure 2.31: *No inner nuclear membrane targeting of the reporters in Nup107-Nup160 depleted nuclei*. (A). EGFP-BC08 reporter was used to test the INM targeting on Nup107-Nup160 depleted nuclei. The reporters are added and TEV protease containing NusA was added at the mentioned places, at mentioned time points. The protease reaction was stopped by adding SDS-sample buffer and boiling. The samples were western blotted with respective antibodies. (B). Immunodepletion of Nup107-Nup160 complex. The *Xenopus* egg cytosol that was immunodepleted for Nup107-Nup160

and used in (A) were probed for Nup160 and p62 specific antibodies. p62 serves as a control for equal loading of egg cytosol.

2.2. Nup98 is required for the maintenance of the diffusion barrier of NPCs.

2.2.1. Functional investigation of Nup98 in nuclear assembly

Nucleoporin Nup98 is a 98 kDa protein of the NPC. It is localized at both nuclear and cytoplasmic sides of the NPCs (Griffis et al., 2003). Nup98 is the only known vertebrate member of the GLFG repeat family (Powers et al., 1995) with additional functions that are still being explored. We planned to study a few functional aspects of Nup98 in the in vitro assembled nuclei.

2.2.2. Immunodepletion of Nup98

To understand the functional importance of Nup98, we planned to immunodeplete Nup98 from the *Xenopus* egg extracts and assemble nuclei using the immunodepleted extracts (4.2.3.4). The immunodepletion of Nup98 was done similar to the immunodepletions of Nup188-Nup93 and Nup205-Nup93 (2.1.3). We coupled an excessive amount of affinity purified antibodies specific for Nup98 to a protein A sepharose. The antibody bead containing column was blocked with 3% BSA to prevent unspecific binding of proteins. The *Xenopus* egg cytosol was incubated with the blocked Nup98 beads in the ratio of 1:1.5 for two rounds to efficiently deplete Nup98 from the egg extracts. Mock depleted egg extracts were obtained by incubating the rabbit IgG-protein A sepharose beads in the same ratio as the Nup98 depletion. An efficient depletion of Nup98 from the egg extracts was seen by western blotting (Fig. 2.32A) and immunofluorescence (Fig. 2.33; left side). The depletion of Nup98 is specific as the Nup205 was not depleted from the same cytosol. Immediately after the immunodepletion of Nup98, the egg cytosol was used to assemble nuclei *in vitro* (4.2.3.5). The NE assembly of the Nup98 looked similar to the mock depleted nuclei (Fig. 2.32B). The NE around the decondensed chromatin substrate looked continuous and smooth. A light microscopic analysis of the Nup98 depleted nuclei looks morphologically similar to the mock depleted nuclei. Immunofluorescence of Nup98 depleted nuclei was done to check the

presence of NPCs using monoclonal mAb414 antibodies, a widely used antibody to stain the NPCs that recognizes four different nucleoporins. Interestingly, NPC staining was very much reduced in the Nup98 depleted nuclei (Fig. 2.33; right side).

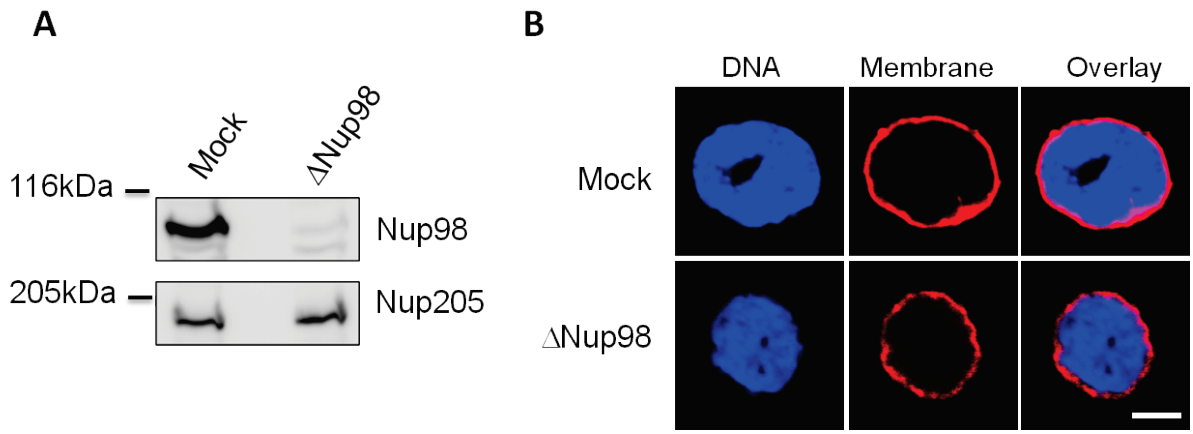

Figure 2.32: *Immunodepletion of Nup98*. (A) Western blot analysis of mock and Nup98 depleted *Xenopus* egg extracts. (B). Nuclei were assembled until 90 min using the mock and Nup98 depleted cytosol, fixed with 4% PFA and 0.5% glutaraldehyde. Nuclei were analyzed for chromatin and membrane staining using confocal microscopy (blue: DAPI, red: DiIC18). Scale bar: 20 µm.

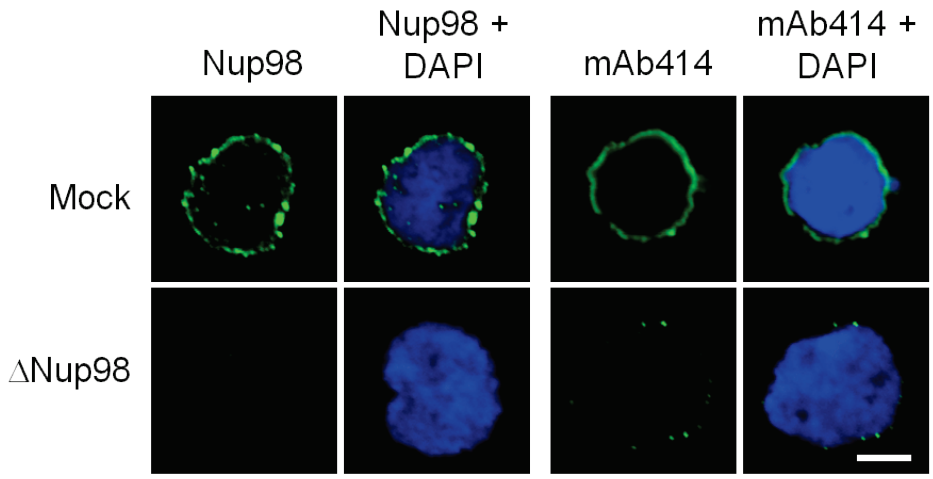

Figure 2.33: *NPCs are decreased in the Nup98 depleted nuclei*. Nuclei were assembled using the mock and Nup98 depleted cytosol until 90 min, fixed with 4% PFA and did immunofluorescence of Nup98 and mAb414 antibodies. Nuclei were analyzed and scanned using confocal microscopy (blue: DAPI, green: Nup98/mAb414). Scale bar: 20 µm.

2.2.3. The size exclusion limit of Nup98 depleted nuclei is altered

NPCs establish a diffusion barrier between cytoplasm and nucleus. Small molecules of size less than 30 kDa could diffuse across the barrier (Mohr et al., 2009) and larger molecules need active transport machinery. We suspected this size exclusion limit of Nup98 depleted nuclei might have been lost as there was a severe reduction in the NPC staining. To check for the integrity of NPCs we did a size exclusion assay for Nup98 depleted nuclei. We assembled nuclei using mock and Nup98 depleted extracts for 90 min and treated these nuclei with fluorescently labeled dextrans of different size (Fig. 2.34). The results show that Nup98 depleted nuclei excluded 500 kDa dextrans but not the 70 kDa dextran. This means that the NPC were assembled but only the exclusion limit of Nup98 depleted nuclei is impaired. This result is consistent with the previous results were we used Nup98 as a control (Fig. 2.16).

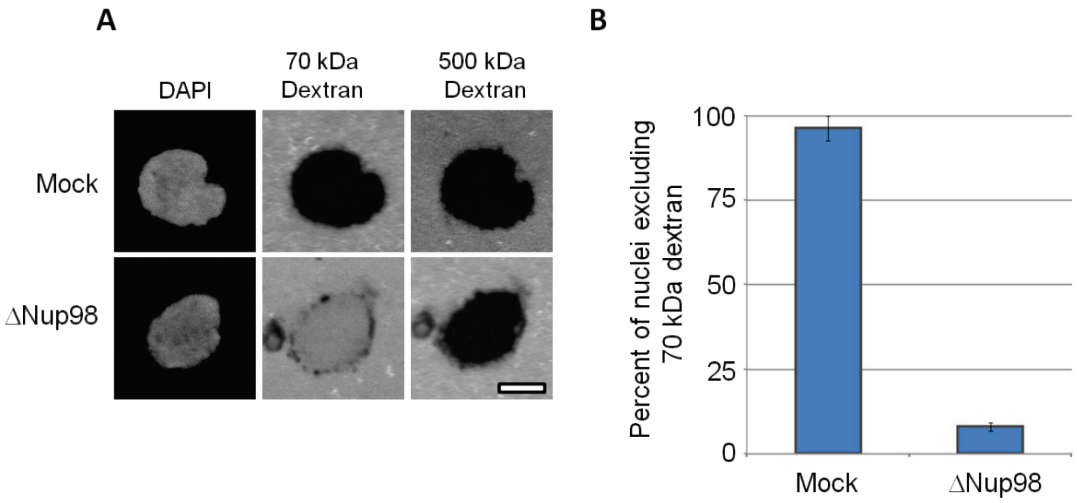

Figure 2.34: *The size exclusion limit of Nup98 depleted nuclei is altered*. (A). The mock and Nup98 depleted cytosol were used for nuclear assembly, after 90 min, these nuclei were treated with fluorescently labeled 70 kDa (middle column) and 500 kDa dextrans (right column). Immediately after 5 min, nuclei were analyzed for the size exclusion using confocal microscopy. Only the nuclei that excluded 500 kDa dextrans, showing the NE is intact, were considered for analysis. Scale bar: 20 µm. (B). Quantification of the exclusion of 70 kDa from (A) was plotted in a graph. Samples from three independent experiments with at least 100 nuclei in each condition with intact NE were considered (judged by the exclusion of 500 kDa). Error bars mark the standard deviation.

2.2.4. Immunofluorescence on Nup98 depleted nuclei reveals that levels of the p62 complex and other complexes are reduced

After we realized that the size exclusion barrier of Nup98 depleted nuclei was lost, we did immunofluorescence of many nucleoporins to check for their presence. We did immunofluorescence of nucleoporins those were the representative candidates of each sub-complexes in NPC (Fig. 2.35). The central channel of the NPC is lined by the Nup62 complex, we checked for the presence of two members of this subcomplex, p62 and Nup58. The results show that the amount of Nup62 complex is decreased. We also tested for the two distinct Nup93 complexes (one with Nup188 and the other with Nup205), Nup155 and Nup53. We found a reduction in the staining of all the proteins of the Nup93 complex tested. Interestingly, we found that the staining of Nup107, a representative of Nup107-Nup160 complex and Mel-28/ELYS, a binding partner of Nup107 complex (Franz et al., 2007) were not reduced. Previously, it was shown that Nup107-Nup160 complex initiates the NPC assembly by its recruitment to chromatin (Walther et al., 2003) and Mel-28 acts as a seeding point for the NPC assembly (Franz et al., 2007).

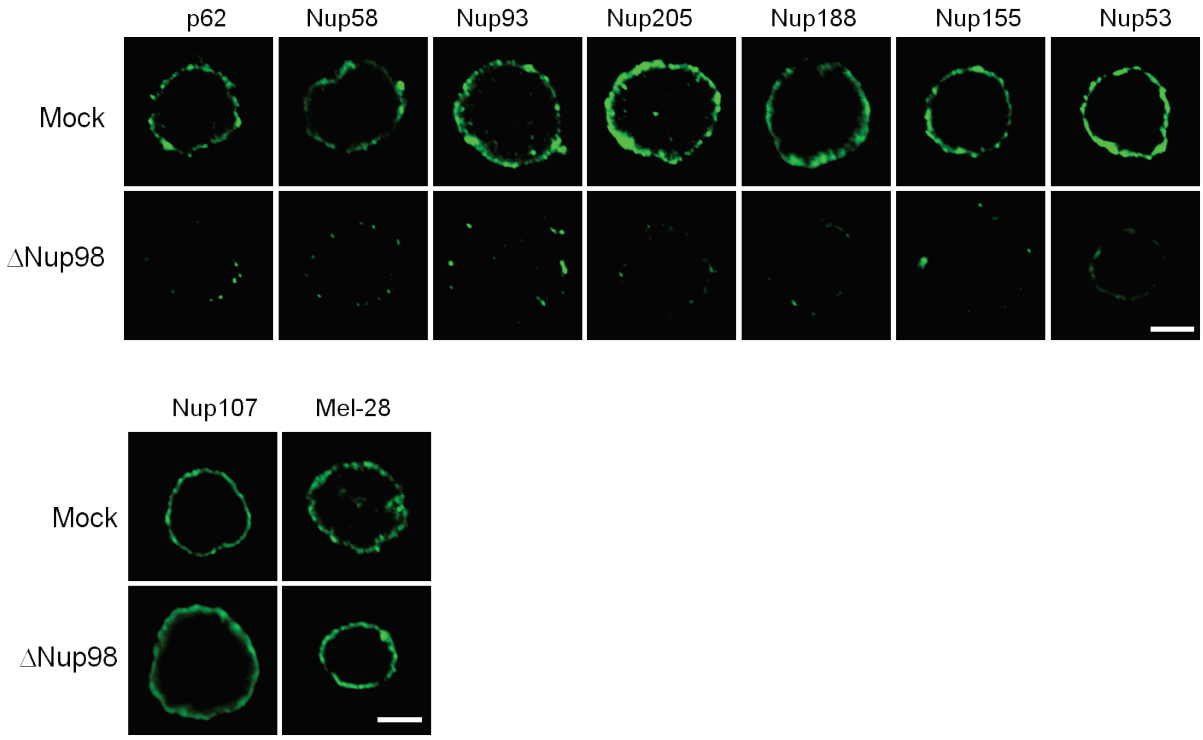

Figure 2.35. *Immunofluorescence of nucleoporins on Nup98 depleted nuclei.* Nucleoporins p62, Nup58, Nup93, Nup205, Nup188, Nup155, Nup53, Nup107 and Mel-28 were stained on mock

and Nup98 depleted nuclei, assembled for 90 min and fixed using 4% PFA and analyzed using respective antibodies (green) by immunofluorescence. The antibody staining was scanned using confocal microscopy. Scale bar: 20 µm.

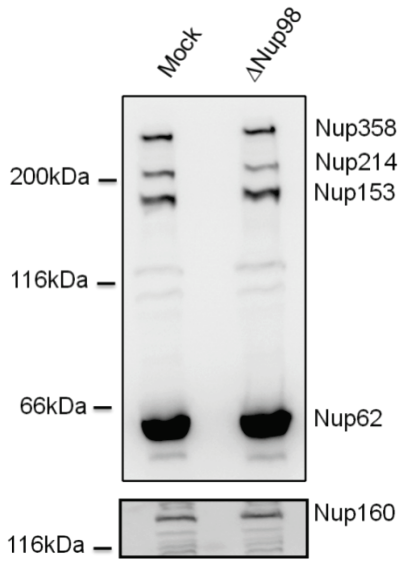

Figure 2.36. *Nup98 depletion does not co-deplete other nucleoporins in the cytosol*. After two rounds of depletion of mock and Nup98 from the *Xenopus* egg cytosol, the cytosol were analyzed in western blotting for the detection of Nup358, Nup214, Nup153 and Nup62 using mAb414 antibodies and Nup160 using a specific antibody.

The central channel of NPC is composed of Nup62 complex, consists of p62, Nup54 and Nup58 (Finlay et al., 1991). The members of Nup62 complex consist of unstructured FG-repeats, these contribute an establishment of permeability barrier and also mediate the receptor mediates transport through the NPCs (Alber et al., 2007; Rout et al., 2000). Putting together, we could imagine that the reduction of Nup62 complex would impair the permeability barrier in Nup98 depleted nuclei. We checked whether there is any decrease in the amount of p62 and other reduced nucleoporins in the cytosol after the depletion of Nup98 (Fig. 2.36). Western blotting analysis of the antibodies mAb414 and Nup160 shows that the nucleoporins (Nup358, Nup214, Nup153, Nup62 and Nup160) are present the Nup98 depleted cytosol in equal amounts to the mock depleted cytosol but are not efficiently recruited to the nuclei during nuclear assembly.

3. Discussions

3.1. Nup188 controls passage of membrane proteins across the NPC

3.1.1. Nup93 exists in two distinct complexes

Although Nup93 complex was known for more than a decade, in *Xenopus* it was recognized as a complex of three proteins; Nup93, Nup205 and Nup188 (Miller et al., 2000). In this thesis, we show that Nup93 is a part of two distinct subcomplexes; one with Nup188 and another with Nup205. *Xenopus* Nup93 complex has been shown to be essential for the proper assembly of NPC (Grandi et al., 1997) and acts as one of the major building blocks of NPC. The yeast orthologue of Nup93 is Nic96p, also shown to be an important factor for the assembly of NPCs (Zabel et al., 1996).

3.1.2. Nup188 and Nup205 are not essential for NE and NPC assembly

After showing the existence of Nup188-Nup93 and Nup205-Nup93, in this thesis, a functional analysis of Nup188-Nup93 in the NPC is investigated. To understand the function of Nup188-Nup93 and Nup205-Nup93 in NE formation and NPC assembly, we immunodepleted these two subcomplexes from the *Xenopus* egg cytosol and assembled nuclei. Chromatin and the membrane staining of the nuclei assembled on these depleted extracts show that there is no impairment in the NE assembly (Fig. 2.5B and 2.8B). A transmission electron microscopic analysis on the Nup188-Nup93 depleted nuclei also confirmed the same. Immunofluorescence of mAb414 on these nuclei showed that the NPCs could assemble without Nup188 and Nup205 (Fig. 2.6 and 2.9). Both Nup188 and Nup205 are not essential of NE formation and NPC assembly. Surprisingly, we found that nuclei depleted of Nup188-Nup93 grew enormous in size (at least 3-4 folds more than the mock depleted nuclei). These bigger sized nuclei upon any nucleoporin depletion were not seen any time before. After an understanding that the nuclear growth is rapid only after the NE is completely formed in Nup188-Nup93 depletion, we tested whether there is an increased DNA content by uncontrolled DNA replication causing this enormous size. The DNA replication is controlled by a licensing machinery and allows the DNA to replicate only once in a cell cycle (Blow and Sleeman, 1990), we thought

that during the depletion of Nup188-Nup93 some of the components of the DNA licensing machinery might have lost its function causing an impairment in licensing in turn led to this increase in nuclear size. A mass spectrometric analysis of an immunoprecipitation of Nup188 showed MCM5 as an interaction partner (data not shown), MCM is a six membered protein complex and component of the licensing machinery (Lei and Tye, 2001), By blocking the DNA replication on Nup188-Nup93 depleted nuclei we could not reduce the nuclear size showing that an increased amount of DNA is not the reason for the nuclear enlargement.

3.1.3. Transport of soluble cargos in Nup188-Nup93 depleted nuclei is normal

Our analysis then focused on the transport of soluble cargos through the NPCs. Nucleoporins containing FG repeats establish a permeability barrier and promote the receptor mediated transport through NPC. These FG repeats containing proteins are localized in center of the NPC (Alber et al., 2007; Rout et al., 2000). Molecules less than 30 kDa can easily diffuse across the NPC. We initially checked on the defect in the passive diffusion in the pore causing larger molecules (> 30 kDa) to diffuse inside the Nup188-Nup93 depleted nuclei. By testing with different sized fluorescently labeled dextrans (Fig. 2.16) we found that the NPCs in Nup188-Nup93 depleted nuclei are intact and there is no defect in the passive diffusion, also in Nup205-Nup93 depleted nuclei. Interestingly, a knock down of the *C.elegans* ortholog of Nup205 failed to exclude 70 kDa dextrans (Galy et al., 2003). Surprisingly, *C. elegans* ortholog of Nup188 was not found as yet. Probably, the worm could still make up for the function of Nup188 using Nup205, this argues for a possibility of a redundant function of Nup188-Nup93 and Nup205-Nup93 in vertebrates.

We then studied the rate of import of proteins by importin α/β and transportin mediated pathways in the Nup188-Nup93 depleted nuclei using specific reporters (Fig. 2.18). This study revealed that the rate of import of proteins is not altered in Nup188-Nup93 depleted nuclei. We also tested the export of proteins from the nuclei, we found that nuclear export is also working normal (Fig. 2.19). Blocking the export of mRNAs in these nuclei was not able

to reduce the size of Nup188-Nup93 depleted nuclei. Putting together, the transport of soluble cargos is not impaired in Nup188-Nup93 depleted nuclei.

3.1.4. Nup188-Nup93 controls the passage of membrane proteins through NPC

We then blocked the NPCs on Nup188-Nup93 depleted nuclei with excess amount of WGA, a lectin that interact with many nucleoporins and block the NPCs. This WGA treatment reduced the size of Nup188-Nup93 depleted nuclei. Previously, it was reported that WGA also hinders the transport of integral membrane proteins that are destined to INM from ONM may be by blocking the passageways (Ohba et al., 2004). After this, we fragmented the ER network by shaking the assembling mock and Nup188-Nup93 depleted nuclei. This ER fragmentation as well reduced the size of Nup188-Nup93 depleted nuclei. The enlargement of Nup188-Nup93 depleted nuclei requires more membrane to be utilized. ER is continuous with ONM and in turn continuous with INM, we suspected that when ER network is fragmented, supply of the membrane components is limited and does not allow the Nup188-Nup93 nuclei to grow further. As we have tested most of the other reasons for a nuclear growth and our promising results on the WGA treatment and ER fragmentation led us to focus on analyzing the flow of membrane components into the nuclei. To understand the mechanism of membrane flow in to the nuclei we developed a novel assay using INM protein reporters. Using this novel assay, we identified that the bigger nuclei is due to the effect of integral membrane proteins and other membrane components that are delivered faster to INM upon Nup188-Nup93 depletion. We think that the faster flow of membrane components cause a rapid expansion of the NE. This could provide a larger surface area and helps in integration of more NPCs. An increase in the total number of NPCs would secondarily cause the nuclear growth of Nup188-Nup93 depleted nuclei by a gain in overall transport capacity for the soluble cargos and the membrane components.

The transport of the soluble factors in and out of the NPCs across the NE is thoroughly studied (Suntharalingam and Wente, 2003). Several of the integral membrane proteins of INM have been shown to bind lamins that form an intermediate filament polymer and chromatin.

These transmembrane proteins of INM should be transported into the nuclei for performing their functions. Thus the INM proteins must be continuously transported to the INM after their synthesis in the ER. Recently, a few models have been proposed on the transport of integral membrane proteins to INM. Based on the vesicle fusion events of ER, golgi and plasma membranes it was hypothesized that ONM and INM could fuse to form transient channels allowing the transfer of membrane proteins, although this model was not yet experimentally proved. Another model is based on the observation of how the Herpes virus makes it the way to come out of nuclei. Nucleocapsids of the virus in the nucleus contacts the INM, then buds into the perinuclear space, from there on a fusion with ONM results the delivery of nascent nucleocapsids into the cytosol (Mettenleiter et al., 2009). A reversal of this process was conceived as a model of transport of INM proteins, through the vesicle budding of ONM into the perinuclear space and subsequent fusion with the INM would deliver the integral membrane proteins of INM to its destiny. Apart from the egression of herpes virus from the nucleus there is a little evidence supporting this model.

One of the most likely models is the lateral diffusion model which is based on an observation of peripheral channels on the outer face of the NPC (Hinshaw et al., 1992). In this model, transmembrane proteins are transported from the ONM to the INM via channels between the NPC and the pore membrane. Antibodies to the transmembrane nucleoporin gp210 and the treatment of WGA led to the block of the transport of integral membrane proteins from ONM to INM likely by blocking the passageways (Ohba et al., 2004). The deletion of Nup170 in yeast, one of the orthologues of vertebrate Nup155, causes the mis-localization of two of the integral membrane proteins of INM, Heh1p and Heh2p (King et al., 2006). The delivery of Heh1p and Heh2p to the INM requires importin α/β import receptors this strongly supports the involvement of NPC in the transport of integral membrane proteins from ONM to the INM. Also, when the Nup107-Nup160 is depleted from the *Xenopus* egg cytosol, the nuclei assembled with the depleted cytosol are devoid of NPCs (Harel et al., 2003; Walther et al., 2003). Our results also show on the Nup107-Nup160 depleted nuclei the INM reporters were not targeted to the INM (Fig. 2.31).

Our results on the depletion of Nup188-Nup93 show that the INM reporters are delivered faster into the nuclei implying the importance of Nup188-Nup93 in NPCs as the control of passage of membrane proteins from ONM to the INM (Fig. 3.1). Also the ER protein reporters are not mislocalized to the INM in the Nup188-Nup93 depleted nuclei. The depletion of Nup188p (a yeast ortholog of vertebrate Nup188) in yeast or Pom152p, a transmembrane nucleoporin reduced the INM localization of Doa10p, a yeast transmembrane ubiquitin ligase (Deng and Hochstrasser, 2006). Doa10p modifies substrates in ER membrane and it was also found in INM for the degradation of nuclear substrates (Swanson et al., 2001). During the NE proliferation, Doa10p is present in INM and the Nup188 depletion causes a redistribution of Doa10p to the ER, probably through an enhanced passage through the NPCs.

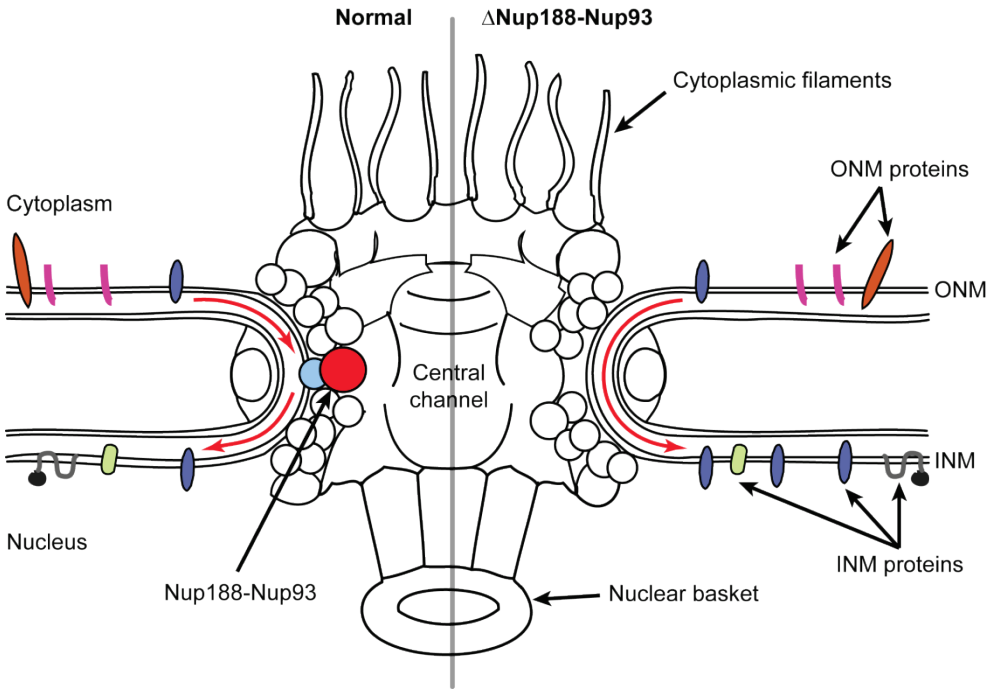

Figure 3.1: *Schematic representation of the normal and Nup188-Nup93 depleted NPCs*. The left half and right half of a NPC are showing a part of normal and Nup188-Nup93 depleted nuclei, respectively. The outer nuclear membrane (ONM) and inner nuclear membrane (INM) proteins are marked in their respective places. The red arrows show the direction of transport of INM proteins into the nuclei. The transport of INM proteins are controlled by Nup188-Nup93 in a normal nuclei (shown by red arrows at left side) and this control was lost in Nup188-Nup93 depleted nuclei (shown by an uninterrupted red arrow at right side).

NPCs are proposed to have eight peripheral channels, which were thought to be involved in passive diffusion of metabolites and ions (Hinshaw and Milligan, 2003; Kramer et al., 2007;

Naim et al., 2007; Stoffler et al., 2003). The cryo electron tomography of NPCs from *Dictyostelium discoideum*, a soil-living amoeba confirmed that the presence of peripheral channels ~9 nm in diameter (Beck et al., 2007). Presence of these peripheral channels is in contrast to the most accepted model in which FG repeat containing proteins form a common barrier for both the passive and active mediated transport (Ribbeck and Gorlich, 2001; Rout and Aitchison, 2001). Passive diffusion is sensitive to many of the same ligands and inhibitors of active transport through NPC, this concedes for a single permeability barrier for soluble transport factors through NPCs (Mohr et al., 2009). The peripheral channels could be involved in the transport of integral membrane proteins passing the NPCs (King et al., 2006; Powell and Burke, 1990; Zuleger et al., 2008). The nucleoplasmic domains of the most INM proteins are limited to approximately 40 kDa (Ohba et al., 2004) and these peripheral channels could be enough to accommodate and traverse them and we think that structural rearrangements within the NPC are necessary to allow for integral membrane passage without disrupting the diffusion barrier. We could imagine that depletion of Nup188-Nup93 might increase the conformational flexibility within NPCs causing an enhanced passage of integral membrane proteins without a hindering the size limitation that was observed by Ohba et al (Ohba et al., 2004).

As mentioned earlier, our analysis shows that Nup93 precipitates two distinct subcomplexes and weaker stability of Nup93 complex. Although Nup93 complex is a major building block of NPC, association of Nup93 complex members are less stable, it was previously reported that Nup155 and Nup53 precipitated as individual proteins (Franz et al., 2005; Hawryluk-Gara et al., 2008) but not precipitated with Nup93.However, the interaction of Nup188-Nup93 and Nup205-Nup93 seem to be stable. During the rescue of Nup188-Nup93 phenotype, an add-back of Nup188 alone could not rescue the phenotype. Only when the Nup188-Nup93 complex is pre-formed using the *in vitro* co-translation the phenotype could be rescued. The Nup188-Nup93 depletion caused a 50 % loss of Nup93, a large portion of the other 50 % of the Nup93 is with Nup205 and a small fraction is not bound with either Nup188 or Nup205 (Fig. 2.3). If the Nup205-Nup93 complex was not stable, the add-back of Nup188 alone could have rescued the phenotype.

Our immunodepletion results show that *Xenopus* egg cytosol devoid of Nup188-Nup93 or Nup205-Nup93 could assemble nuclei with closed NE and intact NPCs. The depletion of Nup205-Nup93 together with the depletion of Nup188-Nup93 was not technically possible as this double depletion would require four rounds of depletion of the *Xenopus* cytosol. After a four rounds of depletion, egg cytosol is unfit to assemble the nuclei because of a harsh treatment and dilution of the extracts that occurred during depletion.

Interestingly, the depletion of Nup93 complexes in *Xenopus* egg extracts could not assemble NPCs (Grandi et al., 1997). The subfraction of Nup93 (~5%), which was not a part of Nup188 or Nup205, could be interacting with p62, a FG repeat containing nucleoporin (Zabel et al., 1996). This argues for the possibility of other functions of Nup93 despite of Nup188-Nup93 and Nup205-Nup93. Other nucleoporins of Nup93 complex, Nup155 and Nup53 are essential for both NE and NPC assembly (Franz et al., 2005; Hawryluk-Gara et al., 2008).

In summary, this study suggests that Nup93 is present in two distinct complexes, one with Nup188 and the other with Nup205. Depletion of these two complexes show that they are not required for NE and NPC assembly. Functional analysis on Nup188-Nup93 complex reveals that it is rather responsible for controlling the passage of integral membrane proteins and membrane components through NPC. For a complete understanding of the control of INM proteins we have to understand how the integral membrane proteins of INM are selected at NPC. Nup188-Nup93 depletion led to a loss control of passage of membrane proteins, but the integral membrane proteins of ER are still not allowed to INM showing an existence of a selection mechanism at NPC that prevent mis-localization of ONM and ER integral membrane proteins. For understanding this selection mechanism, an understanding and functions of the nucleoporins that are involved in the transport of membrane components from ONM to INM have to be studied. On the other hand the function of Nup205-Nup93 is still to be understood. Although it was not found to be essential for NE assembly and NPC assembly, ablation of Nup205 in *C.elegans* was also shown to induce abnormal chromatin condensation (Galy et al., 2003). Nup205-Nup93 could be involved in structural maintenance of NPC.

3.2. Nup98 is an essential component for the establishment of diffusion barrier of NPC

Nup98 is one of the peripheral FG nucleoporins and in vertebrates it is located at both the cytoplasmic and the nuclear sides of the central channel of the NPC (Griffis et al., 2003). NPCs constitute a diffusion barrier at the NE, with only small molecules of size less than 30 kDa could diffuse across the barrier (Mohr et al., 2009) and larger molecules needed to be actively transported. In Nup98, the GLFG-repeat region takes part in the nuclear transport (Radu et al., 1995). In this thesis, we addressed the importance of Nup98 in the transport capabilities of NPCs.

3.2.1. Depletion of Nup98 alters the size exclusion limit of NPCs

The immunodepletion of Nup98 in *Xenopus* egg cytosol, followed by *in vitro* nuclear assembly and treatment of different sized fluorescently labeled dextrans showed the failure of the exclusion of 70 kDa dextran (Fig. 2.34). The GLFG-repeat regions of Nup98 are inclined to self associate (Patel et al., 2007), this self association might underlie in the formation of the diffusion barrier at the central channel of the NPCs. Also, the permeability barrier reconstituted by GLFG repeats containing hydrogels can also restrict passive diffusion of proteins as FG/FxFG repeat hydrogel (Frey and Gorlich, 2009). The immunofluorescence of a variety of nucleoporins showed a reduction of the many nucleoporins including FG-repeat containing Nup62 complex at the NPCs (Fig. 2.35), which was also seen earlier by (Wu et al., 2001). Although, western blotting analyses (Fig. 2.36) revealed that reduction in the nucleoporins levels happen only at the NE. Moreover, the depletion of Nup98 caused a reduction of FG-repeat containing Nup62 complex at the NPC. So, the disruption of the diffusion barrier could either be because of lack of Nup98 itself or an indirect effect on the failure of incorporation of FG-repeats containing nucleoporins in the central channel of the NPCs e.g. of the Nup62 complex. Together, these results suggest that Nup98 is not only important for various transport pathways but also for the establishment and maintenance of the diffusion barrier of NPCs. However, currently it cannot be decided whether this is a

function of Nup98 itself or other nucleoporins which are not assembled into the NPC upon Nup98 depletion.

4. Materials and Methods

4.1. Materials

4.1.1. Chemicals

Rotiphores® gel 30 37.5:1	Carl Roth, Germany
Agarose	Invitrogen, Germany
Ammonium chloride	Carl Roth, Germany
Ammonium sulfate	Merk, Germany
BCA™ Protein Assay Kit	Thermo Scientific, USA
Bovine serum albumin (BSA)	Calbiochem, Germany
4’,6-Diamidino 2-phenyindole (DAPI)	Roche, Germany
1,1'-Dioctadecyl-3,3,3',3' tetramethylindocarbocyanine perchlorate (DiIC18)	Invitrogen, Germany
1,4-Dithio L-threitol (DTT)	Carl Roth, Germany
Ethanol	Carl Roth, Germany
Ethylenediamine-N,N,N',N'-tetraacetic acid (EDTA)	Merk, Germany
Glutaraldehyde (50% aqueous solution)	Sigma-Aldrich, Germany
Glutathione Sepharose 4 Fast Flow	GE Healthcare, Sweden
Glycerol (87% aqueous solution)	Sigma-Aldrich, Germany
Glycine	Carl Roth, Germany
Glycogen (source: oyster)	Sigma-Aldrich, Germany
4-(2-Hydroxyethyl)piperazine-1-ethansulfonic acid (HEPES)	Carl Roth, Germany
Imidazole	Carl Roth, Germany
Immersion oil	Olympus, Japan
Kanamycin	Carl Roth, Germany
Magnesium chloride	J.T.Baker, Netherlands
Milk powder	Applichem, Germany
Paraformaldehyde	ACROS organics, Belgium
Piperazine 1,4-bis(2-ethanesulfonic acid) (PIPES)	Carl Roth, Germany
Phenylmethylsulfonyl fluoride (PMSF)	Carl Roth, Germany
Poly-L-Lysine solution	Sigma-Aldrich, Germany

Protein A Sepharose TM CL-4B	GE Healthcare, Sweden
QIAquick® PCR Purification Kit	Qiagen, Germany
QIAquick Gel Extraction Kit	Qiagen, Germany
Restriction enzymes	NEB or Fermentas, Germany
Sodium chloride	Merk, Germany
Sodium dodecylsulfate	Carl Roth, Germany
Sucrose	Carl Roth, Germany
N,N,N′,N′-Tetramethylethylenediamine (TEMED)	Carl Roth, Germany
Thrombin	ICN biomedicals, USA
Tris(hydroxymethyl)amino methane (Tris)	Carl Roth, Germany
Tween®-20	Carl Roth, Germany
Vectashield® mounting medium H-1000	Vector Laboratories, USA
Western LightningTM Chemiluminiscence reagent	PerkinElmer, USA
Fluorescently labeled dextrans	Invitrogen, Germany
Leptomycin B	Alexis, Germany
Aphidicolin	Alexis, Germany
Detergents	Calbiochem, Germany
Lipids	Avanti polar lipids
Sodium acetate	Merk, Germany
Sodium carbonate	Merk, Germany
Cysteine	Calbiochem, Germany
Ni-NTA agarose	Qiagen, Germany
Serva unstained SDS-PAGE protein marker	Serva, Germany
Complete™ Protease Inhibitor Cocktail Tablet, EDTA-free	Roche, Germany

4.1.2. Commonly used buffers and solutions

All solutions were prepared with double de-ionised or distilled water. The solutions were sterile filtered and stored at room temperature unless otherwise indicated in braces.

30% Sucrose (4 °C)	30% (w/v) Sucrose in PBS

Dejellying buffer (4 °C)	2% cysteine (w/v) in 0.25x MMR adjusted to pH 7.8 with 5M NaOH.
Energy mix (-20 °C)	100 mM Creatine phosphate, 5 mM GTP, 5 mM ATP, 0.5 mg/ml Creatin kinase
MMR	100 mM NaCl, 10 mM $MgCl_2$, 20 mM $CaCl_2$, 1 mM EDTA, 50 mM Hepes, pH 8.0
Ni-elution buffer	20mM TRIS pH7.4, 500mM NaCl, 400mM Imidazole, 10% (v/v) Glycerol.
Ni-wash buffer	20mM TRIS pH7.4, 500mM NaCl, 8mM Imidazole.
PBS (phosphate buffered saline)	130 mM NaCl, 100 mM Na_2HPO_4, pH 7.4
Resolving gel (8%) (modified accordingly for the other percentages)	375 mM Tris pH 8.8, 8% (w/v) acrylamide/bisacrylamide, 0.1 % (w/v) SDS.
S250 (4 °C)	250mM Sucrose, 50mM KCl, 2.5mM $MgCl_2$, 10mM Hepes pH 7.5
SDS sample buffer (6x)	0.6% (w/v) Bromophenol blue, 12% (w/v) SDS, 60% (v/v) glycerol, 300 mM Tris, pH 6.8
Stacking gel (3%)	125 mM Tris, pH 6.8, 3% (w/v) acrylamide/bisacrylamide, 0.1 % (w/v) SDS.
Vikifix	80mM Pipes pH 6.8, 1mM MgCl2, 150mM sucrose, 2% PFA
Western blotting buffer	25mM Tris base, 92 mM Glycine

4.1.3. Commonly used material

1.5 ml, 2 ml reaction tubes	Sarstedt, Germany
24-well plates	Greiner Bio-One, Germany
Bottle top filters, 0.22 µm pore size	Millipore, Germany
Filter paper	Whatman, England
General glass ware	Schott, Germany
MoBiCol columns	MoBiTec, Germany
SDS-PAGE Minigel system	Biorad, Germany

Ultracentrifuge tubes	Beckman, Germany
Coverslips (12 mm diameter)	Marienfeld, Germany
Microscope slides	Marienfeld, Germany
SDS-PAGE Miniprotean system	Biorad, Germany
Powerpac HC	Biorad, Germany
Syringes (Omnifix)	Braun, Germany
Diagnostic slides (3 well)	Menzel, Germany

4.1.4. Instrumental Equipments

Centrifuges:

Heraeus® Multifuge® 1L-R	Thermo (USA)
Eppendorf® centrifuge 5415 R	Eppendorf (Germany)
OptimaTM L-60 Ultracentrifuge	Beckman (USA)
Rotor SW40 TI	Beckman (USA)
Rotor SW55 TI	Beckman (USA)
OptimaTM TLX Ultracentrifuge	Beckman (USA)
Sorvall Evolution RC	Thermo (USA)

4.1.5. Plasmids

pEGFP-TEV-BC08: Generated by Dr. Wolfram Antonin. Full length *Xenopus* BC08 was fused to an N-terminal MISTIC fragment, a Bacillus subtilis integral membrane protein that folds independently into the membrane bypassing the cellular translocon machinery (Roosild et al., 2005). This is followed by a thrombin protease cleavage site, an EGFP domain, and a TEV protease cleavage site are cloned into a modified pET28a vector allowing purification via a C-terminal His_6 tag.

pEGFP-NusA-BC08: Generated by Dr. Wolfram Antonin. Full length *Xenopus* BC08 was fused to an N-terminal MISTIC fragment (Roosild et al., 2005). This is followed by a thrombin protease cleavage site, an EGFP domain, a TEV protease cleavage site and NusA (used to increase the size of the reporter) are cloned into a modified pET28a vector allowing purification via a C-terminal His_6 tag.

pEGFP-GST-BC08: Generated by Dr. Wolfram Antonin. Full length *Xenopus* BC08 was fused to an N-terminal MISTIC fragment (Roosild et al., 2005). This is followed by a thrombin protease cleavage site, an EGFP domain, a TEV protease cleavage site and GST (used to increase the size of the reporter) are cloned into a modified pET28a vector allowing purification via a C-terminal His_6 tag.

pEGFP-TEV-LBR (146-258): Generated by Dr. Wolfram Antonin. A part of the N-terminal region of *Xenopus* Lamin-B receptor which includes the first transmembrane region (146-258aa) was fused to an N-terminal MISTIC fragment (Roosild et al., 2005). This is followed by a thrombin protease cleavage site, an EGFP domain, and a TEV protease cleavage site are cloned into a modified pET28a vector allowing purification via a C-terminal His_6 tag.

pEGFP-TEV-SPC18: Generated by Dr. Wolfram Antonin. *Xenopus* SPC18, a membrane spanning subunit of the signal peptidase complex, was fused to an N-terminal MISTIC fragment (Roosild et al., 2005). This is followed by a thrombin protease cleavage site, an EGFP domain, and a TEV protease cleavage site are cloned into a modified pET28a vector allowing purification via a C-terminal His_6 tag.

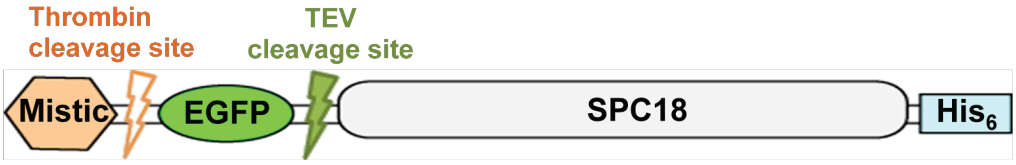

pEGFP-TEV-CNX: Generated by Dr. Wolfram Antonin. A part of the C-terminal region including the transmembrane region (aa 485–608) of *Xenopus* Calnexin, an ER localized chaperone protein, was fused to an N-terminal MISTIC fragment (Roosild et al., 2005) followed by a thrombin cleavage. Calnexin fragment is followed by a TEV protease cleavage site and an EGFP domain is cloned into a modified pET28a vector allowing purification via a C-terminal His_6 tag.

pNusA-TEV: Generated by Dr. Wolfram Antonin. TEV protease was fused with NusA (a solubility tag for protein expression) are cloned into a modified pET28a vector allowing purification via a C-terminal His_6 tag.

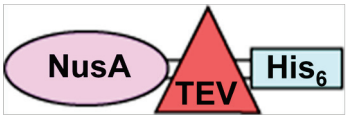

pTEV: Generated by Dr. Wolfram Antonin. TEV protease was cloned into a pET28a vector, expressed and purified through His_6 tag. Purified TEV protease was cross-linked to a synthetic peptide containing SV40 large T antigen NLS as described previously (Palacios et al., 1996).

pEGFP-TEV-NPM2: Generated by Dr. Wolfram Antonin. A full length Nucleoplasmin (NPM2), an importin α/β dependent nuclear import substrate, was fused to an N-terminal EGFP fragment and a TEV protease cleavage site are cloned into a modified pET28a vector allowing purification via a C-terminal His_6 tag.

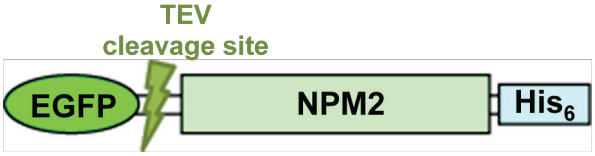

pEGFP-TEV- Nplc-M9-M10: Generated by Dr. Wolfram Antonin. A fusion protein that consists of the nucleoplasmin core domain (1-149aa of *Xenopus* Nucleoplasmin; Nplc), M9 domain (255-320aa) of hnRNP A1 (a transportin dependent nuclear import substrate) and M10 domain (an inactive M10 mutant version of Nuclear export signal; PLQLPPDLRLTLD), were fused to an N-terminal EGFP fragment and a TEV protease cleavage site are cloned into a modified pET28a vector allowing purification via a C-terminal His_6 tag.

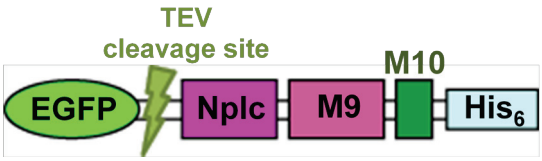

pEGFP-TEV- Nplc-M9-NES: Generated by Dr. Wolfram Antonin. A fusion protein that consists of nucleoplasmin core domain (1-149aa of *Xenopus* Nucleoplasmin; Nplc), M9

domain (255-320aa) of hnRNP A1 and nuclear export signal (a CRM1 recognized nuclear export signal; PLQLPPLERLTLD), were fused to an N-terminal EGFP fragment and a TEV protease cleavage site are cloned into a modified pET28a vector allowing purification via a C-terminal His_6 tag.

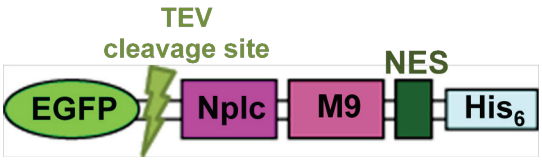

pMouse Nup188: Generated by Dr. Wolfram Antonin. The complete open reading frame of mouse Nup188 was amplified by PCR and cloned into modified pET28a vector containing a stem loop forming sequence derived from the 5'UTR of gene 10 of the T7 bacteriophage (AGGGAGACCACAACGGUUUCCCU) 5' of the in vitro transcribed/translated gene known to enhance in vitro transcription (O'Connor and Dahlberg, 2001).

p*Xenopus* Nup93: Generated by Dr. Wolfram Antonin. The complete open reading frame of mouse Nup188 was amplified by PCR and cloned into modified pET28a vector containing a stem loop forming sequence derived from the 5'UTR of gene 10 of the T7 bacteriophage (AGGGAGACCACAACGGUUUCCCU) 5' of the in vitro transcribed/translated gene known to enhance in vitro transcription (O'Connor and Dahlberg, 2001).

4.1.6. Antibodies

4.1.6.1. Primary antibodies

anti-Nup188: A fragment of *Xenopus laevis* Nup188 corresponding to 1573-1731 aa of the mouse sequence were expressed as GST fusion proteins in BL21(DE3) and purified using Glutathion Sepharose (GE-Healthcare). The purified protein were dialysed against PBS and injected into rabbits for antibody production. Following is the schematic view of the antibody recognizing region (in orange) in the full length protein.

anti-Nup205: A N-terminal fragment of *Xenopus laevis* Nup205 (aa 1-283) was fused to NusA as a solubility tag, cloned into pET28a vector and expressed as a His_6 tagged fusion protein in BL21(DE3). The purified protein were dialysed against PBS and injected into rabbits for antibody production. Following is the schematic view of the antibody recognizing region (in orange) in the full length protein.

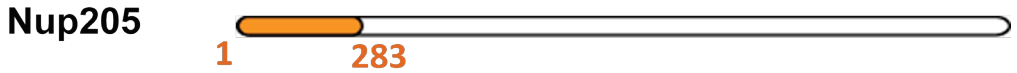

anti-Nup93: A N-terminal fragment of *Xenopus laevis* Nup93 (aa 1-230) was cloned into pET28a vector and expressed as a His_6 tagged fusion protein in BL21(DE3) as described previously (Franz et al., 2007). The purified protein were dialysed against PBS and injected into rabbits for antibody production. Following is the schematic view of the antibody recognizing region (in orange) in the full length protein.

anti-Nup155: A N-terminal fragment of *Xenopus laevis* Nup155 (aa 1-1389) was cloned into pET28a vector and expressed as a His_6 tagged fusion protein in BL21(DE3) as described previously (Franz et al., 2005). The purified protein were dialysed against PBS and injected into rabbits for antibody production. Following is the schematic view of the antibody recognizing region (in orange) in the full length protein.

anti-Nup53: A fragment of *Xenopus laevis* Nup53 (aa 78-310) was fused to NusA as a solubility tag, cloned into pET28a vector and expressed as a His_6 tagged fusion protein in BL21(DE3). The purified protein were dialysed against PBS and injected into rabbits for antibody production. Following is the schematic view of the antibody recognizing region (in orange) in the full length protein.

anti-Nup98: A fragment of *Xenopus laevis* Nup98 corresponding to 1-185 aa were expressed as GST fusion proteins in BL21(DE3) and purified using Glutathion Sepharose (GE-Healthcare). The purified protein were dialysed against PBS and injected into rabbits for antibody production. Following is the schematic view of the antibody recognizing region (in orange) in the full length protein.

anti-Nup160: A fragment of *Xenopus laevis* Nup160 (aa 1-414) was cloned into pET28a vector and expressed as a His_6 tagged fusion protein in BL21(DE3) as described previously (Franz et al., 2007). The purified protein were dialysed against PBS and injected into rabbits for antibody production. Following is the schematic view of the antibody recognizing region (in orange) in the full length protein.

anti-His: anti-His_6 antibody was purchased from Roche.

anti-EGFP: anti-EGFP antibody was purchased from Roche.

anti-Lamin B: anti-Lamin B antibody (X223) was purchased from ImmuQuest.

mAb414: Mouse monoclonal antibody was obtained from BabCO (Richmond, USA).

4.1.6.2. Secondary antibodies

Alexa Fluor 488 goat α-rabbit IgG, Cy3 goat α-rabbit IgG were bought from Invitrogen. Anti-rabbit IgG linked horseradish peroxidase and anti-mouse IgG linked horseradish peroxidase from goat (Calbiochem, Germany).

4.2. Methods

4.2.1. Microbiological methods and molecular cloning

4.2.1.1. PCR reactions

PCR reactions to generate DNA fragments for subcloning were routinely set up in a total reaction volume of 50 µl containing: 1 ng of DNA template, 2 mM of dNTP mix, forward and reverse primers at 0.5 µM each, 10x KOD reaction buffer and KOD Polymerase (1 µl). A typical PCR termocycle was comprised of 30 cycles. DNA strands were separated for 30 sec at 95 °C in the first cycle and in all subsequent cycles. For next 5 cycles, annealing temperature of the primers was set at 54 °C for 30 sec. Product elongation by KOD polymerase occurred at 75 °C for 1 min per 2.5 kilobase template. Then for the next 25 cycles, the annealing temperature of the primers was set at 58 °C for 30 sec and the elongation was done as earlier. The final extension step of a PCR cycle was continued for 5 min. All PCR reactions were carried out in a DNA Engine® Thermal cycler (MJ Research). After ensuring the correct fragment size on an agarose gel, the amplified PCR product was either purified with a PCR purification kit (Qiagen) following the manufacturer's instructions, or completely loaded it on an agarose gel and purified by gel extraction kit (Qiagen) following the manufacturer's instructions.

4.2.1.2. Preparation of chemically competent cells

BL21(DE3) were grown overnight on LB-Plate containing adequate antibiotics. A single colony was picked and inoculated in 100 ml LB medium containing antibiotics and grown at 37 °C for overnight. A 10 ml of the overnight culture was inoculated into two 500 ml LB medium separately with antibiotics. The cells were grown at 37°C until OD600. The flasks were chilled on ice water for 10 min. Then the culture was spun at 4000 rpm for 10 min at 4 °C in pre-cooled Sorvall Evolution RC centrifuge. The pellet was carefully resuspended in

ice-cold 100 ml $CaCl_2$ (50 mM) and kept in ice for 20 min. Then this suspension was spun at 4000 rpm for 10 min at 4 °C in pre-cooled Sorvall Evolution RC centrifuge. The pellet was resuspended in 16 ml ice cold $CaCl_2$ (50 mM) and 15% glycerol. Then cells were aliquoted, snap frozen in liquid nitrogen and stored at -80 °C.

4.2.1.3. Transformation of plasmid DNA into chemically competent cells

Transformation of E.coli $CaCl_2$ competent cells was done by gently mixing 50 µl of cells with 1 µl of plasmid DNA (10 ng – 1 µg). After incubation for 20 min on ice, bacteria were heat-shocked for 40 sec at 42 °C in a water bath, cooled for 5 min on ice and 300 µl LB medium (without any drug) was added. Bacteria were incubated for 1 hr at 37 °C to allow the expression of antibiotic resistance and were plated out on LB agar containing plates containing 25 µg/ml kanamycin. The plates were incubated overnight at 37 °C.

4.2.1.4. Preparation of DNA from *E.coli*

DNA was prepared using QIAPrep (Qiagen) kits following the manufacturer's instructions.

4.2.2. Biochemical standard methods

4.2.2.1. Expression and purification of EGFP-TEV-NPM2, EGFP-TEV- Nplc-M9-M10 and EGFP-TEV- Nplc-M9-NES

The plasmids for the above mentioned proteins are transformed in *E. coli* strain Bl21de3 to enhance the expression of eukaryotic proteins. Transformants were plated on LB-agar plates containing 25 µg/ml Kanamycin and incubated overnight at 37 °C. A single colony was picked to inoculate LB culture (containing 25 µg/ml Kanamycin) that was grown overnight to saturation. From this culture 1 liter LB-medium was inoculated for protein expression and cultures were grown to an OD of 0.8 at 600 nm wavelength. Protein expression was induced by addition of 0.2 mM IPTG for 3 h at their respective expressing temperatures. Cells were harvested by centrifugation at 4000 rpm for 15 min at 4 °C in a Sorvall Evolution RC centrifuge. The bacteria pellet corresponding to 1 liter culture was resuspended in 25 ml Ni-wash buffer. Cells were lysed in an EmulsiFlex homogenizer and 1 mM $MgCl_2$, 400 µl of 10 mg/ml DnaseI in PBS, 2 ml 0.2M PMSF was added and incubated for 10 minutes on ice. The lysate was cleared by centrifugation at 12000 rpm for 15 min at 4 °C in a Sorvall Evolution RC centrifuge. The supernatant was applied to Ni-NTA-Agarose ([Qiagen] 1ml 50% slurry per bacterial supernatant derived from 1 l culture) and incubated for 2 h at 4 °C under rotation. The resin was transferred to a plastic chromatography column and was washed twice with 10 bed volumes of cold Ni-wash buffer. Then the His_6 tagged proteins are eluted with Ni- elution buffer (e.g. 1ml per 1ml Ni-NTA-Agarose) after the incubation for 2 min. To the final eluate 1 mM DTT and 1 mM EDTA was added and dialysed overnight.

4.2.2.2. Purification of proteins by size exclusion chromatography

Further purification of EGFP-TEV-NPM2, EGFP-TEV- Nplc-M9-M10 and EGFP-TEV-Nplc-M9-NES fusion proteins were done by size exclusion chromatography on a Sepharose 200 column (GE-Healthcare).

4.2.2.3. Expression and purification of EGFP-TEV-BC08, EGFP-NusA-BC08, EGFP-GST-BC08, EGFP-TEV-LBR (146-258), EGFP-TEV-SPC18 and EGFP-TEV-CNX

Plasmids for these proteins were transformed to *E. coli* BL21de3 as mentioned above and expressed as above in the 1% (w/v) cetyltrimethylammonium bromide with the exception of purifying on magnetic Ni-loaded agarose beads (Novagen). The eluates were dialysed for 16 h against PBS containing 1mM EDTA. The MISTIC fragments from the reporters were cleaved off using thrombin protease.

4.2.2.4. Expression of recombinant *Xenopus* Nup93 and Mouse Nup188

Nup188-Nup93 complex were made by expressing Nup188 and Nup93 together at 37°C using the PURExpress™ in vitro protein synthesis kit (NEB) following the manufacturer's instructions, the incubation time for the protein expression was extended to 4h.

4.2.2.5. Sodium dodecyl sulfate polyacrylamide gel electrophoresis and Western blotting

SDS-PAGE was performed as described earlier (Laemmli, 1970) on 8% or 12% gels. For Western blotting, the proteins were transferred to a Nitrocellulose membrane (Whatman, Germany) after SDS-PAGE. The membrane was then probed with rabbit polyclonal antibodies or mouse monoclonal antibodies to detect respective proteins. Anti-rabbit or anti-mouse IgG antibodies linked horseradish peroxidase from goat (Amersham Bioscience) was used to detect the antibody that is bound to the corresponding protein.

4.2.2.6. Determination of protein concentration

The protein concentration of a solution was determined using BCA™ Protein Assay Kit (Pierce) following manufacturer's instructions. Briefly, Bovine serum albumin (BSA) protein standard dilutions were made in triplicates and several dilutions of the protein solution in 5 µl water. 95 µl BCA working solution were added and samples incubated for 30 min at 37 °C. Optical density was determined at a wavelength of 562 nm and the protein concentration was calculated via a standard curve.

4.2.2.7. Generating polyclonal antibody generation in rabbits

All antigens used for rabbit immunization were recombinant proteins, purified either under native conditions or from inclusion bodies. One milliliter antigen solution (0.5mg/ml) is mixed well with 1ml Freud complete in syringes and connector till a highly viscous. For the initial immunizations four subcutaneous injection (23G x 1¼ needle) and two intramuscular injections (20G x 1½ needle) of the viscous mixture were given per rabbit. After the primary immunization, rabbits were boosted three times with first two boosts in a 14 day rhythm and the third after 28 days of the second boost. For the first boost, a mixture of 1 ml antigen solution (0.2mg/ml) with Freud incomplete and for the second and third boost, 1 ml antigen solution (0.1mg/ml) with Freud incomplete was injected. Rabbit bleeds were then coagulated then it was spun down at 4000 rpm for 30 min in a Heraeus Multifuge 1L-R, the serum was collected, frozen in liquid Nitrogen and stored at -80 °C.

4.2.2.8. Affinity purification of antibodies

For affinity purification of antibodies from serum, an antigen column was first prepared. For this, the antigen for the specific antibody was expressed and purified in bacteria. The purified proteins were dialyzed against 20mM HEPES, 500mM NaCl pH7.4. One milliliter of 100 % Affigel resin (BioRad, Affigel 10 for neutral, basic proteins and Affigel 15 for acidic proteins)

was taken and washed with ice cold water. The resin then was incubated with 30 mg of the dialyzed antigen and incubated for 4 hrs at 4 °C on a turning wheel. The supernatant was recovered and the efficiency of binding was calculated by measuring the protein concentration (should be 10% of the starting concentration). The reaction was stopped by the addition of 3 ml 1 M ethanolamine pH 8 for 1 hr at 4 °C (this quenches non-reacted active sites on the resin). Then washed sequentially with 100mM $NaHCO_3$ pH 8.3, 500mM NaCl and 100mM Sodium acetate pH 4.2; 500mM NaCl twice. The antigen resin was washed with 200mM glycine pH 2.3, 150mM NaCl to remove unbound material. Then the resin was washed with PBS for 3 times. 10 ml of the respective serum was incubated with the resin over night at 4 °C. The resin was washed 3 times with PBS containing 0.1% Tween 20 followed by extensive washing with ice cold PBS. The resin was transferred into a column and washed with PBS. Antibodies were eluted with 3 times 1ml 200mM glycine pH 2.7, 150mM NaCl and 5 times 1ml 200mM glycine pH 2.2, 150mM NaCl. The eluted antibodies were neutralized with a small amount of 1.5M TRIS pH 8.8. The affinity purified antibodies are immediately dialyzed against PBS.

4.2.2.9. Preparation of antibody beads

To the 4 ml of affinity purified antibody 1 ml of 50% protein A sepharose was added and incubated over night on a rotating wheel at 4 °C. For control beads rabbit IgGs were incubated with protein A sepharose. The beads were washed twice with coupling buffer (200mM $NaHCO_3$, 100mM NaCl pH 9.3) and crosslinked for 20 min with 10mM DMP in coupling buffer. The beads were once washed with coupling buffer and once again crosslinked as above. The crosslinked beads were washed once with 0.1M ethanolamine pH 8.2 and incubated in the same for 1 hr in room temperature. The beads were washed twice with 100mM Sodium acetate, 500mM NaCl pH4.2 and then washed twice with 100mM $NaHCO_3$, 500mM NaCl, pH 8.3. This consecutive washing step was repeated 4 times, finally washed with PBS and blocked with 3% BSA in PBS.

4.2.3. Biochemical methods related to the *X. laevis* egg extract system

4.2.3.1. Preparation of *X. laevis* egg extract

Female *X. laevis* frogs were primed by injection with pregnant mare serum gonadotropin (PMSG) and 4-14 days later ovulation of mature eggs was stimulated by injection of human chorionic gonadotropin (hCG) (0.5 ml of 2000 U/ml water). The frogs were transferred into plastic boxes containing MMR and kept in dark for 16 hrs at 16 °C. Eggs laid in MMR buffer were collected damaged eggs (mostly white) were selected and discarded and only good quality eggs were selected, pooled washed extensively in MMR. The jelly coat of the eggs was removed by incubation in a freshly prepared 0.25x MMR supplemented with 2% cystein, soon the eggs started to become closely packed (~10 min). The collected eggs were arrested in metaphase of meiosis II. Following dejellying, exposure to air was avoided since the eggs were very fragile and lysed easily after removal of the jelly coat. Eggs were released from cell cycle arrest at metaphase of meiosis II by addition of the calcium ionophore A23187 (8 µl (2mg/ml in ethanol) per 100 ml MMR) that mimics fertilization. Animal cap contraction was visible after 10 min, as judged by an upturn of the vegetal, black pole. Activation was stopped after 7-10 min by thorough washing with MMR buffer which removed the ionophore. Eggs were incubated at room temperature for 20 min and subsequently washed twice with S250 buffer. Damaged eggs were removed with a pasteur pipette and the remaining eggs were transferred with a cut plastic pasteur pipette to SW55 plastic centrifuge tubes and centrifuged in low speed centrifugation for 2 min at 800 rpm (Heraeus, Multifuge 1L-R). The eggs were packed, removed additional buffer and centrifuged for 20 min 15000 rpm at 4 °C in a Optima™ L-60 Ultracentrifuge with a SW55Ti rotor. The tubes were broached with a syringe and nuclear material, organelles and glycogen were removed, leaving lipids, yolk and pigment behind and supplemented with 1 mM DTT, 44 µg/ml cycloheximide (inhibitor of protein synthesis), 5 µg/ml cytochalasin B (inhibitor of actin polymerization), and 1x Complete™ EDTA-free Proteinase Inhibitor Cocktail. This 'low speed extract' was centrifuged for 40 min at 45000 rpm at 4 °C to separate soluble and lipid components. The cytosolic phase was collected by a syringe, diluted with 0.3 fold 50mM KCl, 2.5mM $MgCl_2$, 10mM Hepes pH 7.5 and spun again at the same centrifugation settings. The cytosolic phase 'high speed extract'

(cytosol) was collected with a syringe and glycerol was added to the final concentration of 3% (v/v), snap frozen and stored in liquid nitrogen.

4.2.3.2. Preparation of the total membrane fraction from *X. laevis* egg extracts

For preparation of total membranes, the membrane fraction was diluted in 10 volumes S250 buffer, 1 mM DTT and 1x Complete™ EDTA-free Proteinase Inhibitor Cocktail. Then homogenized in a dounce homogenizer, placed on top of 1ml S500, 1mM DTT and 1x Complete™ EDTA-free Proteinase Inhibitor Cocktail in SW40 tubes, spun in SW40 for 20min at 11000 rpm at 4 °C. The obtained pellets were resuspended in S250, 1mM DTT and 1x Complete™ EDTA-free Proteinase Inhibitor Cocktail to 20% volume of the cytosol. Then the total membrane fraction is stored at in liquid nitrogen.

4.2.3.3. Preparation of the floated membranes

For preparation of floated membranes, during the interphasic high speed extracts preparation the membranes were removed on top of the mitochondria and pigments. This membrane fraction is mixed with 4 volumes of S2100 with 1 mM DTT, 1x Complete™ EDTA-free Proteinase Inhibitor Cocktail and homogenized twice in a 30 ml dounce homogenizer. 5 ml of the membrane solution were added into a Beckman centrifuge tube suitable for SW40Ti rotor and overlaid with 1.4 ml S1400, S1300, S1100, S900, S700 cushion and on top of the gradient 0.2ml S250 buffer was added. Membranes were floated for 4 h at 38000 rpm at 4 °C. The upper 3 membrane fractions were taken and diluted with 3 volumes of S250, 1 mM DTT and 1x Complete™ EDTA-free proteinase inhibitor cocktail. This mixture is then pelleted in an Optima™ TLX Ultracentrifuge at 100000 rpm for 30 min in TLA100.4. The pellet was resuspended in S250, 1 mM DTT and 1x Complete™ EDTA-free proteinase inhibitor cocktail to bring the volume to 50% of the cytosol and frozen in liquid nitrogen.

4.2.3.4. Immunodepletion of nucleoporins from the egg extracts

The blocked antibody beads (4.2.2.9) were taken washed twice with S250 and incubated with freshly prepared cytosol (4.2.3.1) in the following ratio (Nup188 – 1:1.2, Nup205 – 1:1.5, Nup98 – 1:1.5 to the extracts and respective amount of control antibody beads) for 30 min at 4 °C under rotation. The flow through was collected and the depletion step repeated on fresh, preblocked antibody resin. Depleted cytosol was recovered and immediately used for *in vitro* nuclear reconstitution reactions.

4.2.3.5. *In vitro* nuclear assembly

For a typical nuclear assembly reaction, 1 µl sperm chromatin (3000 sperm heads/µl) was incubated for 10 min at 20 °C in 20 µl cytosol. To start the NE assembly reaction, 2 µl floated membranes (either with DiIC18 or unstained floated membranes for immunofluorescence or transmission electron microscopy), 0.4 µl 10x energy mix and 0.4 µl glycogen (20 mg/ml) were added. NE assembly took place for 1.5 - 2 hrs at 20 °C.

4.2.3.6. Immunofluorescence of *in vitro* reconstituted nuclei

An NE assembly reaction was fixed in 0.5 ml 4% PFA in PBS and incubated for 20 min on ice. Cover slips (round, 11 mm in diameter) were coated with poly-L lysine solution for 5 min at RT. Poly-L-lysine solution was removed and cover slips dried and transferred to scintillation vials. Fixed NE assembly reactions were applied to 0.8 ml 30% sucrose in S250 buffer. The reaction was spun through the cushion onto lysine coated cover slips at 4000 rpm for 15 min (4 °C) in a Heraeus Multifuge 1L-R Cover slips were lifted by puncturing the vials from the bottom with a syringe needle and then removed with forceps. Immunofluorescence staining was performed in a 24-well plate. The fixative was quenched with 50 mM NH_4Cl in PBS for 10 min at RT. Blocking solution contained 3% BSA in 0.1% Triton-X100 in PBS and was applied to the cover slips for 30 min at RT. Antibodies were diluted in blocking solution.

Primary antibodies were incubated with the nuclei on the cover slips for 2 hrs in a humid chamber followed by 3 washes with 0.1% Triton-X100 in PBS. Secondary antibodies coupled to fluorophors (Alexa Fluor® 488/Cy3 goat anti-mouse/rabbit IgG were diluted 1:2000 in blocking solution and applied for 1 hr. After labeling with secondary antibodies, cover slips were washed 3 times with 0.1% Triton-X100 in PBS and with PBS. To stain the chromatin, DAPI (1 mg/ml) was diluted 1:1000 in PBS and reactions on cover slips were stained for 10 min at RT. After two additional washes with PBS and water, cover slips were removed from solutions and remaining liquid was removed. Samples were mounted on a drop of Vectarshield® mounting media on glass slides. Liquid was removed from the rim of the cover slips with a tissue and the preparation was sealed with nail polish at the perimeter. Reactions were evaluated by confocal microscopy. A modified protocol was used when membranes were investigated. Vikifix with 0.5% glutaraldehyde yielded better conservation of nuclear membranes due to the presence of glutaraldehyde.

4.2.3.7. Immunoprecipitation on *Xenopus* egg extracts

Egg cytosol was diluted 1:1 with PBS supplemented with Complete™ EDTA free proteinase inhibitor cocktail and spun for 20 min at 100000 rpm in a TLA100.4 rotor. 50 µl antiserum were added to 300 µl cytosol after centrifugation and incubated for 2 h at 4 °C. 60 µl Protein A sepharose was added as 50% slurry and incubation continued for 1 hr. Beads were sedimented, supernatant removed and the resin was washed 5 times with 500 mM NaCl in PBS and next 5 times with PBS. Bound proteins were eluted in 40 µl 1x SDS-sample buffer supplemented with 100 mM DTT. 10 µl of the eluates were separated on 8%/12% polyacrylamide gels and analyzed by immunostaining on Western blots.

4.2.3.8. DNA replication assay

DNA replication on the nuclear assembly was tested by the addition of 43.5 µM Fluorescein-12-dUTP in the presence and the absence of 16 µM aphidicolin. Then the samples were fixed with vikifix with 0.5 % gluteraldehyde, processed and recorded at the confocal microscopy.

4.2.3.9. Size exclusion assay

The nuclei were assembled until 90 min with unlabelled floated membranes. For the immunodepletion of Nup188, Nup205 and Nup98, the nuclei were incubated with 10µg/ml of 10kDa dextran labeled with Texas red, 30µg/ml of 70kDa Dextran with Fluorescein and 40µg/ml of 2MDa with Tetramethylrhodamine. Nup98 depleted nuclei were also incubated with 40µg/ml of 70kDa Dextran with Texas red and 30µg/ml of 500kDa with Tetramethylrhodamine. The dextrans are incubated for 5 min then mixed with equal amount of squash fix and immediately analyzed at the confocal microscopy.

4.2.3.10. Testing of nuclear import of proteins

To test importin α/β and transportin dependent nuclear import function, a full length NPM2 (Nucleoplasmin) or Nplc-M9-M10 from (Englmeier et al., 1999), respectively, was fused to EGFP followed by a TEV protease recognition site and cloned into a modified pET28a vector allowing the purification via C-terminal hexa histidin tag. After Ni-NTA purification, both the substrates were purified size exclusion chromatography on a Sepharose 200 column (GE-Healthcare). Nuclei were assembled on a 50 µl, as the volume ratio described previously (Franz et al., 2005). The nuclear assembly was allowed until 50 min after the addition of membranes then, 1 µg of the respective reporters was added. At the indicated time points, 10 µl of the samples were added to 1 µl of 5 µg/µl NusA-TEV protease and incubated for 1 min at 20ºC. The TEV protease cleavage was stopped by the addition of SDS sample buffer and boiling at 95ºC for 5 min, then the samples were ran on a 12% SDS-PAGE and Western blotted.

4.2.3.11. Testing of nuclear export of proteins and block of nuclear export

Nuclear export of proteins was tested using a reporter called 'shuttling substrate' that contains both NLS and NES (Nplc-M9-NES) and a control reporter (Nplc-M9-M10) as reported previously (Englmeier et al., 1999). The export reporters (0.1mg/ml) were added to a nuclear assembly reaction and incubated for 90 min, fixed and processed for microscopy. The nuclear export was blocked by the addition of 100 nM of Leptomycin B (Englmeier et al., 1999) along with the reporters.

4.2.3.12. Counting of NPCs on the *in vitro* nuclei

The assembled nuclei were stained with mAb414 and fixed without gluteraldehyde on the cover slips for counting the NPCs, as mentioned earlier. These nuclei were scanned along the z-axis using the confocal microscope mentioned below (4.2.4), the numbers of Z-stacks were suggested by Fluoview software are recorded and saved in '.oif' format. These files were then imported to Imaris 6.1.5® from Bitplane Scientific Solutions. After the import, a dialogue box was open, clicked 'Surpass' then selected 'Volume.' This made the 3D reconstruction of the scanned nuclei. To count the NPCs, I selected the 'Add new spots' on the properties tab (top left). Then, selected 'Different Spot Sizes (Region growing)' and the channel to Alexa Flour 488 (secondary antibody used for mAb414). The estimated diameter for each spot was set to '0.12µm' as the recorded diameter of a NPC is 120 nm (Akey and Radermacher, 1993). On the next step selected Filter type 'Intensity Max Ch=2.' At the bottom of the panel it showed the 'Selected 1427 out of 3688' meaning 1427 high-confidence NPCs and the 3688 total NPCs.

4.2.3.13. Counting the Density of NPCs

The assembled nuclei were stained with mAb414 and fixed without gluteraldehyde on the cover slips for counting the density of NPCs, as mentioned earlier. These nuclei were scanned along the z-axis and saved as mentioned above. The files were then imported to Imaris 6.1.5®

from Bitplane Scientific Solutions. After opening the 3D reconstructed nuclei, a new 'Surface' was added then selected 'Segment only a Region of Interest' and unselected 'Process entire Image finally.' A homogenous NPC stained area and a plane surface was selected (use 'Esc' key to go from selecting the surface to rotating the surface, vice versa). In the next step, a small portion of DAPI channel was selected and reconstructed (selected portion should be a thin surface). After clicking next steps with the default parameters clicked 'Stastistics' menu and 'detailed' tab, this gave me the entire selected area of the DAPI (Say 50 μm^2). Since only the top region of the DAPI is required we divided the area by two (25 μm^2). From the properties menu added the 'new spots,' then selected 'Segment only a Region of Interest' (unchecked 'Process entire Image finally') and 'Different Spot Sizes (Region growing).' Now the same selected area of DAPI was again selected, in the next step Alexa Flour 488 (secondary for mAb414) was selected. The estimated diameter for each spot was set to '0.12µm' as the recorded diameter of a NPC is 120 nm (Akey and Radermacher, 1993). On the next step the filter type was selected to 'Intensity Max Ch=2.' At the bottom of the panel it showed 'Selected 169 out of 294' meaning 169 high-confidence NPCs and the 264 total NPCs. There are 169 NPCs on the selected DAPI area (25 μm^2). The total number of NPCs per square micrometer is 169 NPCs/25 μm^2 that is 6.76 NPCs/μm^2.

4.2.3.14. An assay for targeting of INM proteins

A full length of *Xenopus* BC08 construct (4.1.5) was expressed in *E.coli* and purified. The MISTIC fragments were cleaved-off using thrombin and the reporters are reconstituted into liposomes. This reconstitution was done by adding around 10 µg of the reporter with 20 µl of a lipid mix containing 3 mg/ml cholesterol, 3 mg/ml Na-phosphatidylserine, 3 mg/ml Na-phosphatidylinositol, 6 mg/ml phosphatidylethanolamin, 15 mg/ml phosphatidylcholine (all solubilzed in 10% octylglucopyranoside) and 2 µl of 1 mg/ml DiIC18 in DMSO. Detergent was removed by passing the sample over a G-50 column equilibrated in S250 buffer. The proteoliposome (the liposomes with the reporters) containing fraction (identified by the color) was collected and the liposomes pelleted by centrifugation for 30 min at 200,000 g (OptimaTM TLX Ultracentrifuge). The pellets were resuspended in 40 µl S250 buffer. Proteins were correctly oriented within the liposomes with the EGFP unit facing the exterior as judged by their sensitivity to TEV protease cleavage. 50 µl nuclear assembly reactions

were assembled in the volume ratio as described previously (4.2.3.5). At indicated time points 10 µl of the samples were added to 1 µl of 5 µg/µl NusA-TEV protease in S250 buffer and incubated for 5 min at 20ºC. The cleavage reaction was stopped by fixation with 4% paraformaldehyde and processed for microscopy as described. For Western blot analysis TEV cleavage was stopped by addition of SDS sample buffer and immediate incubation at 95ºC for 5 min followed by SDS-PAGE and Western blotting.

4.2.4. Light microscopy

The samples from the experiments below were recorded using Olympus FV1000 confocal microscope with 405-, 488- and 559-nm laser lines and a 60x NA 1.35 oil immersion objective lens using the Olympus Fluoview software. Overlaps between the channels were avoided by scanning different channels sequentially in the Fluoview. The physical measurements of the samples were done using the Fluoview. All the images were processed using ImageJ (NIH, Bethesda, USA) and Adobe® Photoshop® CS4.

References

Akey, C.W. (1989). Interactions and structure of the nuclear pore complex revealed by cryo-electron microscopy. J Cell Biol *109*, 955-970.

Akey, C.W., and Radermacher, M. (1993). Architecture of the *Xenopus* nuclear pore complex revealed by three-dimensional cryo-electron microscopy. J Cell Biol *122*, 1-19.

Alber, F., Dokudovskaya, S., Veenhoff, L.M., Zhang, W., Kipper, J., Devos, D., Suprapto, A., Karni-Schmidt, O., Williams, R., Chait, B.T.*, et al.* (2007). Determining the architectures of macromolecular assemblies. Nature *450*, 683-694.

Alberts, B., Johnson, A., Lewis, J., Raff, M., Roberts, K., and Walther, P. (2002). Molecular Biology of the Cell, 4th edn (Garland Science).

Anderson, D.J., and Hetzer, M.W. (2007). Nuclear envelope formation by chromatin-mediated reorganization of the endoplasmic reticulum. Nat Cell Biol *9*, 1160-1166.

Antonin, W., Ellenberg, J., and Dultz, E. (2008). Nuclear pore complex assembly through the cell cycle: regulation and membrane organization. FEBS Lett *582*, 2004-2016.

Antonin, W., Franz, C., Haselmann, U., Antony, C., and Mattaj, I.W. (2005). The integral membrane nucleoporin pom121 functionally links nuclear pore complex assembly and nuclear envelope formation. Mol Cell *17*, 83-92.

Beck, M., Forster, F., Ecke, M., Plitzko, J.M., Melchior, F., Gerisch, G., Baumeister, W., and Medalia, O. (2004). Nuclear pore complex structure and dynamics revealed by cryoelectron tomography. Science *306*, 1387-1390.

Beck, M., Lucic, V., Forster, F., Baumeister, W., and Medalia, O. (2007). Snapshots of nuclear pore complexes in action captured by cryo-electron tomography. Nature *449*, 611-615.

Bergeron, J.J., Brenner, M.B., Thomas, D.Y., and Williams, D.B. (1994). Calnexin: a membrane-bound chaperone of the endoplasmic reticulum. Trends Biochem Sci *19*, 124-128.

Blow, J.J., and Laskey, R.A. (1986). Initiation of DNA replication in nuclei and purified DNA by a cell-free extract of *Xenopus* eggs. Cell *47*, 577-587.

Blow, J.J., and Sleeman, A.M. (1990). Replication of purified DNA in *Xenopus* egg extract is dependent on nuclear assembly. J Cell Sci *95 (Pt 3)*, 383-391.

Brohawn, S.G., Leksa, N.C., Spear, E.D., Rajashankar, K.R., and Schwartz, T.U. (2008). Structural evidence for common ancestry of the nuclear pore complex and vesicle coats. Science *322*, 1369-1373.

Burke, B., and Ellenberg, J. (2002). Remodelling the walls of the nucleus. Nat Rev Mol Cell Biol *3*, 487-497.

Chen, P.W., Lin, S.J., Tsai, S.C., Lin, J.H., Chen, M.R., Wang, J.T., Lee, C.P., and Tsai, C.H. (2010). Regulation of microtubule dynamics through phosphorylation on stathmin by Epstein-Barr virus kinase BGLF4. J Biol Chem *285*, 10053-10063.

Colaiacovo, M.P., Stanfield, G.M., Reddy, K.C., Reinke, V., Kim, S.K., and Villeneuve, A.M. (2002). A targeted RNAi screen for genes involved in chromosome morphogenesis and nuclear organization in the Caenorhabditis elegans germline. Genetics *162*, 113-128.

Cremer, T., and Cremer, C. (2001). Chromosome territories, nuclear architecture and gene regulation in mammalian cells. Nat Rev Genet *2*, 292-301.

Cronshaw, J.M., Krutchinsky, A.N., Zhang, W., Chait, B.T., and Matunis, M.J. (2002). Proteomic analysis of the mammalian nuclear pore complex. J Cell Biol *158*, 915-927.

D'Angelo, M.A., Anderson, D.J., Richard, E., and Hetzer, M.W. (2006). Nuclear pores form de novo from both sides of the nuclear envelope. Science *312*, 440-443.

D'Angelo, M.A., and Hetzer, M.W. (2008). Structure, dynamics and function of nuclear pore complexes. Trends Cell Biol *18*, 456-466.

De Souza, C.P., Osmani, A.H., Hashmi, S.B., and Osmani, S.A. (2004). Partial nuclear pore complex disassembly during closed mitosis in Aspergillus nidulans. Curr Biol *14*, 1973-1984.

Deng, M., and Hochstrasser, M. (2006). Spatially regulated ubiquitin ligation by an ER/nuclear membrane ligase. Nature *443*, 827-831.

Denning, D.P., Patel, S.S., Uversky, V., Fink, A.L., and Rexach, M. (2003). Disorder in the nuclear pore complex: the FG repeat regions of nucleoporins are natively unfolded. Proc Natl Acad Sci U S A *100*, 2450-2455.

Devos, D., Dokudovskaya, S., Alber, F., Williams, R., Chait, B.T., Sali, A., and Rout, M.P. (2004). Components of coated vesicles and nuclear pore complexes share a common molecular architecture. PLoS Biol *2*, e380.

Dundr, M., and Misteli, T. (2001). Functional architecture in the cell nucleus. Biochem J *356*, 297-310.

Ellenberg, J., Siggia, E.D., Moreira, J.E., Smith, C.L., Presley, J.F., Worman, H.J., and Lippincott-Schwartz, J. (1997). Nuclear membrane dynamics and reassembly in living cells: targeting of an inner nuclear membrane protein in interphase and mitosis. J Cell Biol *138*, 1193-1206.

Englmeier, L., Olivo, J.C., and Mattaj, I.W. (1999). Receptor-mediated substrate translocation through the nuclear pore complex without nucleotide triphosphate hydrolysis. Curr Biol *9*, 30-41.

Fabre, E., and Hurt, E. (1997). Yeast genetics to dissect the nuclear pore complex and nucleocytoplasmic trafficking. Annu Rev Genet *31*, 277-313.

Fahrenkrog, B., Koser, J., and Aebi, U. (2004). The nuclear pore complex: a jack of all trades? Trends Biochem Sci *29*, 175-182.

Fernandez-Martinez, J., and Rout, M.P. (2009). Nuclear pore complex biogenesis. Curr Opin Cell Biol *21*, 603-612.

Finlay, D.R., Meier, E., Bradley, P., Horecka, J., and Forbes, D.J. (1991). A complex of nuclear pore proteins required for pore function. J Cell Biol *114*, 169-183.

Franz, C., Askjaer, P., Antonin, W., Iglesias, C.L., Haselmann, U., Schelder, M., de Marco, A., Wilm, M., Antony, C., and Mattaj, I.W. (2005). Nup155 regulates nuclear envelope and nuclear pore complex formation in nematodes and vertebrates. EMBO J *24*, 3519-3531.

Franz, C., Walczak, R., Yavuz, S., Santarella, R., Gentzel, M., Askjaer, P., Galy, V., Hetzer, M., Mattaj, I.W., and Antonin, W. (2007). MEL-28/ELYS is required for the recruitment of nucleoporins to chromatin and postmitotic nuclear pore complex assembly. EMBO Rep *8*, 165-172.

Frey, S., and Gorlich, D. (2009). FG/FxFG as well as GLFG repeats form a selective permeability barrier with self-healing properties. EMBO J *28*, 2554-2567.

Frey, S., Richter, R.P., and Gorlich, D. (2006). FG-rich repeats of nuclear pore proteins form a three-dimensional meshwork with hydrogel-like properties. Science *314*, 815-817.

Fried, H., and Kutay, U. (2003). Nucleocytoplasmic transport: taking an inventory. Cell Mol Life Sci *60*, 1659-1688.

Gall, J.G. (2000). Cajal bodies: the first 100 years. Annu Rev Cell Dev Biol *16*, 273-300.

Galy, V., Mattaj, I.W., and Askjaer, P. (2003). Caenorhabditis elegans nucleoporins Nup93 and Nup205 determine the limit of nuclear pore complex size exclusion in vivo. Mol Biol Cell *14*, 5104-5115.

Gerace, L., and Blobel, G. (1980). The nuclear envelope lamina is reversibly depolymerized during mitosis. Cell *19*, 277-287.

Glavy, J.S., Krutchinsky, A.N., Cristea, I.M., Berke, I.C., Boehmer, T., Blobel, G., and Chait, B.T. (2007). Cell-cycle-dependent phosphorylation of the nuclear pore Nup107-160 subcomplex. Proc Natl Acad Sci U S A *104*, 3811-3816.

Goldberg, M.W., and Allen, T.D. (1993). The nuclear pore complex: three-dimensional surface structure revealed by field emission, in-lens scanning electron microscopy, with underlying structure uncovered by proteolysis. J Cell Sci *106 (Pt 1)*, 261-274.

Goldberg, M.W., and Allen, T.D. (1996). The nuclear pore complex and lamina: three-dimensional structures and interactions determined by field emission in-lens scanning electron microscopy. J Mol Biol *257*, 848-865.

Gomez-Ospina, N., Morgan, G., Giddings, T.H., Jr., Kosova, B., Hurt, E., and Winey, M. (2000). Yeast nuclear pore complex assembly defects determined by nuclear envelope reconstruction. J Struct Biol *132*, 1-5.

Grandi, P., Dang, T., Pane, N., Shevchenko, A., Mann, M., Forbes, D., and Hurt, E. (1997). Nup93, a vertebrate homologue of yeast Nic96p, forms a complex with a novel 205-kDa protein and is required for correct nuclear pore assembly. Mol Biol Cell *8*, 2017-2038.

Griffis, E.R., Xu, S., and Powers, M.A. (2003). Nup98 localizes to both nuclear and cytoplasmic sides of the nuclear pore and binds to two distinct nucleoporin subcomplexes. Mol Biol Cell *14*, 600-610.

Harel, A., Orjalo, A.V., Vincent, T., Lachish-Zalait, A., Vasu, S., Shah, S., Zimmerman, E., Elbaum, M., and Forbes, D.J. (2003). Removal of a single pore subcomplex results in vertebrate nuclei devoid of nuclear pores. Mol Cell *11*, 853-864.

Hawryluk-Gara, L.A., Platani, M., Santarella, R., Wozniak, R.W., and Mattaj, I.W. (2008). Nup53 is required for nuclear envelope and nuclear pore complex assembly. Mol Biol Cell *19*, 1753-1762.

Hawryluk-Gara, L.A., Shibuya, E.K., and Wozniak, R.W. (2005). Vertebrate Nup53 interacts with the nuclear lamina and is required for the assembly of a Nup93-containing complex. Mol Biol Cell *16*, 2382-2394.

Hetzer, M., Gruss, O.J., and Mattaj, I.W. (2002). The Ran GTPase as a marker of chromosome position in spindle formation and nuclear envelope assembly. Nat Cell Biol *4*, E177-184.

Hetzer, M.W., Walther, T.C., and Mattaj, I.W. (2005). Pushing the envelope: structure, function, and dynamics of the nuclear periphery. Annu Rev Cell Dev Biol *21*, 347-380.

Hinshaw, J.E., Carragher, B.O., and Milligan, R.A. (1992). Architecture and design of the nuclear pore complex. Cell *69*, 1133-1141.

Hinshaw, J.E., and Milligan, R.A. (2003). Nuclear pore complexes exceeding eightfold rotational symmetry. J Struct Biol *141*, 259-268.

Holmer, L., and Worman, H.J. (2001). Inner nuclear membrane proteins: functions and targeting. Cell Mol Life Sci *58*, 1741-1747.

Hu, T., Guan, T., and Gerace, L. (1996). Molecular and functional characterization of the p62 complex, an assembly of nuclear pore complex glycoproteins. J Cell Biol *134*, 589-601.

Jarnik, M., and Aebi, U. (1991). Toward a more complete 3-D structure of the nuclear pore complex. J Struct Biol *107*, 291-308.

King, M.C., Lusk, C.P., and Blobel, G. (2006). Karyopherin-mediated import of integral inner nuclear membrane proteins. Nature *442*, 1003-1007.

Kiseleva, E., Rutherford, S., Cotter, L.M., Allen, T.D., and Goldberg, M.W. (2001). Steps of nuclear pore complex disassembly and reassembly during mitosis in early Drosophila embryos. J Cell Sci *114*, 3607-3618.

Kramer, A., Ludwig, Y., Shahin, V., and Oberleithner, H. (2007). A pathway separate from the central channel through the nuclear pore complex for inorganic ions and small macromolecules. J Biol Chem *282*, 31437-31443.

Krull, S., Thyberg, J., Bjorkroth, B., Rackwitz, H.R., and Cordes, V.C. (2004). Nucleoporins as components of the nuclear pore complex core structure and Tpr as the architectural element of the nuclear basket. Mol Biol Cell *15*, 4261-4277.

Kuersten, S., Ohno, M., and Mattaj, I.W. (2001). Nucleocytoplasmic transport: Ran, beta and beyond. Trends Cell Biol *11*, 497-503.

Laemmli, U.K. (1970). Cleavage of structural proteins during the assembly of the head of bacteriophage T4. Nature *227*, 680-685.

Lamond, A.I., and Sleeman, J.E. (2003). Nuclear substructure and dynamics. Curr Biol *13*, R825-828.

Lei, M., and Tye, B.K. (2001). Initiating DNA synthesis: from recruiting to activating the MCM complex. J Cell Sci *114*, 1447-1454.

Lohka, M.J., and Maller, J.L. (1985). Induction of nuclear envelope breakdown, chromosome condensation, and spindle formation in cell-free extracts. J Cell Biol *101*, 518-523.

Lohka, M.J., and Masui, Y. (1983). Formation in vitro of sperm pronuclei and mitotic chromosomes induced by amphibian ooplasmic components. Science *220*, 719-721.

Loiodice, I., Alves, A., Rabut, G., Van Overbeek, M., Ellenberg, J., Sibarita, J.B., and Doye, V. (2004). The entire Nup107-160 complex, including three new members, is targeted as one entity to kinetochores in mitosis. Mol Biol Cell *15*, 3333-3344.

Lusk, C.P., Blobel, G., and King, M.C. (2007). Highway to the inner nuclear membrane: rules for the road. Nat Rev Mol Cell Biol *8*, 414-420.

Lutzmann, M., Kunze, R., Buerer, A., Aebi, U., and Hurt, E. (2002). Modular self-assembly of a Y-shaped multiprotein complex from seven nucleoporins. EMBO J *21*, 387-397.

Makio, T., Stanton, L.H., Lin, C.C., Goldfarb, D.S., Weis, K., and Wozniak, R.W. (2009). The nucleoporins Nup170p and Nup157p are essential for nuclear pore complex assembly. J Cell Biol *185*, 459-473.

Mans, B.J., Anantharaman, V., Aravind, L., and Koonin, E.V. (2004). Comparative genomics, evolution and origins of the nuclear envelope and nuclear pore complex. Cell Cycle *3*, 1612-1637.

Mansfeld, J., Guttinger, S., Hawryluk-Gara, L.A., Pante, N., Mall, M., Galy, V., Haselmann, U., Muhlhausser, P., Wozniak, R.W., Mattaj, I.W.*, et al.* (2006). The conserved transmembrane nucleoporin NDC1 is required for nuclear pore complex assembly in vertebrate cells. Mol Cell *22*, 93-103.

Marheineke, K., and Hyrien, O. (2001). Aphidicolin triggers a block to replication origin firing in *Xenopus* egg extracts. J Biol Chem *276*, 17092-17100.

Mattaj, I.W. (2004). Sorting out the nuclear envelope from the endoplasmic reticulum. Nat Rev Mol Cell Biol *5*, 65-69.

Meier, E., Miller, B.R., and Forbes, D.J. (1995). Nuclear pore complex assembly studied with a biochemical assay for annulate lamellae formation. J Cell Biol *129*, 1459-1472.

Mettenleiter, T.C., Klupp, B.G., and Granzow, H. (2009). Herpesvirus assembly: an update. Virus Res *143*, 222-234.

Miller, B.R., Powers, M., Park, M., Fischer, W., and Forbes, D.J. (2000). Identification of a new vertebrate nucleoporin, Nup188, with the use of a novel organelle trap assay. Mol Biol Cell *11*, 3381-3396.

Mohr, D., Frey, S., Fischer, T., Guttler, T., and Gorlich, D. (2009). Characterisation of the passive permeability barrier of nuclear pore complexes. EMBO J *28*, 2541-2553.

Murray, A.W. (1991). Cell cycle extracts. Methods Cell Biol *36*, 581-605.

Naim, B., Brumfeld, V., Kapon, R., Kiss, V., Nevo, R., and Reich, Z. (2007). Passive and facilitated transport in nuclear pore complexes is largely uncoupled. J Biol Chem *282*, 3881-3888.

Nehrbass, U., Rout, M.P., Maguire, S., Blobel, G., and Wozniak, R.W. (1996). The yeast nucleoporin Nup188p interacts genetically and physically with the core structures of the nuclear pore complex. J Cell Biol *133*, 1153-1162.

Newmeyer, D.D., Lucocq, J.M., Burglin, T.R., and De Robertis, E.M. (1986). Assembly in vitro of nuclei active in nuclear protein transport: ATP is required for nucleoplasmin accumulation. EMBO J *5*, 501-510.

O'Connor, M., and Dahlberg, A.E. (2001). Enhancement of translation by the epsilon element is independent of the sequence of the 460 region of 16S rRNA. Nucleic Acids Res *29*, 1420-1425.

Ohba, T., Schirmer, E.C., Nishimoto, T., and Gerace, L. (2004). Energy- and temperature-dependent transport of integral proteins to the inner nuclear membrane via the nuclear pore. J Cell Biol *167*, 1051-1062.

Onischenko, E.A., Crafoord, E., and Hallberg, E. (2007). Phosphomimetic mutation of the mitotically phosphorylated serine 1880 compromises the interaction of the transmembrane nucleoporin gp210 with the nuclear pore complex. Exp Cell Res *313*, 2744-2751.

Ottaviano, Y., and Gerace, L. (1985). Phosphorylation of the nuclear lamins during interphase and mitosis. J Biol Chem *260*, 624-632.

Palacios, I., Weis, K., Klebe, C., Mattaj, I.W., and Dingwall, C. (1996). RAN/TC4 mutants identify a common requirement for snRNP and protein import into the nucleus. J Cell Biol *133*, 485-494.

Patel, S.S., Belmont, B.J., Sante, J.M., and Rexach, M.F. (2007). Natively unfolded nucleoporins gate protein diffusion across the nuclear pore complex. Cell *129*, 83-96.

Powell, L., and Burke, B. (1990). Internuclear exchange of an inner nuclear membrane protein (p55) in heterokaryons: in vivo evidence for the interaction of p55 with the nuclear lamina. J Cell Biol *111*, 2225-2234.

Powers, M.A., Macaulay, C., Masiarz, F.R., and Forbes, D.J. (1995). Reconstituted nuclei depleted of a vertebrate GLFG nuclear pore protein, p97, import but are defective in nuclear growth and replication. J Cell Biol *128*, 721-736.

Rabut, G., Doye, V., and Ellenberg, J. (2004). Mapping the dynamic organization of the nuclear pore complex inside single living cells. Nat Cell Biol *6*, 1114-1121.

Radu, A., Moore, M.S., and Blobel, G. (1995). The peptide repeat domain of nucleoporin Nup98 functions as a docking site in transport across the nuclear pore complex. Cell *81*, 215-222.

Rakowska, A., Danker, T., Schneider, S.W., and Oberleithner, H. (1998). ATP-Induced shape change of nuclear pores visualized with the atomic force microscope. J Membr Biol *163*, 129-136.

Rasala, B.A., Orjalo, A.V., Shen, Z., Briggs, S., and Forbes, D.J. (2006). ELYS is a dual nucleoporin/kinetochore protein required for nuclear pore assembly and proper cell division. Proc Natl Acad Sci U S A *103*, 17801-17806.

Ribbeck, K., and Gorlich, D. (2001). Kinetic analysis of translocation through nuclear pore complexes. EMBO J *20*, 1320-1330.

Ribbeck, K., Lipowsky, G., Kent, H.M., Stewart, M., and Gorlich, D. (1998). NTF2 mediates nuclear import of Ran. EMBO J *17*, 6587-6598.

Ris, H. (1991). The three-dimensional structure of the nuclear pore complex as seen by high voltage electron microscopy and high resolution low voltage scanning electron microscopy. EMSA Bull, 54-56.

Ris, H. (1997). High-resolution field-emission scanning electron microscopy of nuclear pore complex. Scanning *19*, 368-375.

Ris, H., and Malecki, M. (1993). High-resolution field emission scanning electron microscope imaging of internal cell structures after Epon extraction from sections: a new approach to correlative ultrastructural and immunocytochemical studies. J Struct Biol *111*, 148-157.

Roosild, T.P., Greenwald, J., Vega, M., Castronovo, S., Riek, R., and Choe, S. (2005). NMR structure of Mistic, a membrane-integrating protein for membrane protein expression. Science *307*, 1317-1321.

Rout, M.P., and Aitchison, J.D. (2001). The nuclear pore complex as a transport machine. J Biol Chem *276*, 16593-16596.

Rout, M.P., Aitchison, J.D., Suprapto, A., Hjertaas, K., Zhao, Y., and Chait, B.T. (2000). The yeast nuclear pore complex: composition, architecture, and transport mechanism. J Cell Biol *148*, 635-651.

Rutherford, S.A., Goldberg, M.W., and Allen, T.D. (1997). Three-dimensional visualization of the route of protein import: the role of nuclear pore complex substructures. Exp Cell Res *232*, 146-160.

Sanford, J.R., Ellis, J., and Caceres, J.F. (2005). Multiple roles of arginine/serine-rich splicing factors in RNA processing. Biochem Soc Trans *33*, 443-446.

Schwartz, T.U. (2005). Modularity within the architecture of the nuclear pore complex. Curr Opin Struct Biol *15*, 221-226.

Shelness, G.S., Lin, L., and Nicchitta, C.V. (1993). Membrane topology and biogenesis of eukaryotic signal peptidase. J Biol Chem *268*, 5201-5208.

Shulga, N., Mosammaparast, N., Wozniak, R., and Goldfarb, D.S. (2000). Yeast nucleoporins involved in passive nuclear envelope permeability. J Cell Biol *149*, 1027-1038.

Sonnichsen, B., Koski, L.B., Walsh, A., Marschall, P., Neumann, B., Brehm, M., Alleaume, A.M., Artelt, J., Bettencourt, P., Cassin, E.*, et al.* (2005). Full-genome RNAi profiling of early embryogenesis in Caenorhabditis elegans. Nature *434*, 462-469.

Soullam, B., and Worman, H.J. (1995). Signals and structural features involved in integral membrane protein targeting to the inner nuclear membrane. J Cell Biol *130*, 15-27.

Stoffler, D., Feja, B., Fahrenkrog, B., Walz, J., Typke, D., and Aebi, U. (2003). Cryo-electron tomography provides novel insights into nuclear pore architecture: implications for nucleocytoplasmic transport. J Mol Biol *328*, 119-130.

Stoffler, D., Goldie, K.N., Feja, B., and Aebi, U. (1999). Calcium-mediated structural changes of native nuclear pore complexes monitored by time-lapse atomic force microscopy. J Mol Biol *287*, 741-752.

Straube, A., Weber, I., and Steinberg, G. (2005). A novel mechanism of nuclear envelope break-down in a fungus: nuclear migration strips off the envelope. EMBO J *24*, 1674-1685.

Suntharalingam, M., and Wente, S.R. (2003). Peering through the pore: nuclear pore complex structure, assembly, and function. Dev Cell *4*, 775-789.

Swanson, R., Locher, M., and Hochstrasser, M. (2001). A conserved ubiquitin ligase of the nuclear envelope/endoplasmic reticulum that functions in both ER-associated and Matalpha2 repressor degradation. Genes Dev *15*, 2660-2674.

Ulbert, S., Platani, M., Boue, S., and Mattaj, I.W. (2006). Direct membrane protein-DNA interactions required early in nuclear envelope assembly. J Cell Biol *173*, 469-476.

van Deursen, J., Boer, J., Kasper, L., and Grosveld, G. (1996). G2 arrest and impaired nucleocytoplasmic transport in mouse embryos lacking the proto-oncogene CAN/Nup214. EMBO J *15*, 5574-5583.

Walther, T.C., Alves, A., Pickersgill, H., Loiodice, I., Hetzer, M., Galy, V., Hulsmann, B.B., Kocher, T., Wilm, M., Allen, T.*, et al.* (2003). The conserved Nup107-160 complex is critical for nuclear pore complex assembly. Cell *113*, 195-206.

Walther, T.C., Fornerod, M., Pickersgill, H., Goldberg, M., Allen, T.D., and Mattaj, I.W. (2001). The nucleoporin Nup153 is required for nuclear pore basket formation, nuclear pore complex anchoring and import of a subset of nuclear proteins. EMBO J *20*, 5703-5714.

Walther, T.C., Pickersgill, H.S., Cordes, V.C., Goldberg, M.W., Allen, T.D., Mattaj, I.W., and Fornerod, M. (2002). The cytoplasmic filaments of the nuclear pore complex are dispensable for selective nuclear protein import. J Cell Biol *158*, 63-77.

Weis, K. (2003). Regulating access to the genome: nucleocytoplasmic transport throughout the cell cycle. Cell *112*, 441-451.

Wen, W., Meinkoth, J.L., Tsien, R.Y., and Taylor, S.S. (1995). Identification of a signal for rapid export of proteins from the nucleus. Cell *82*, 463-473.

Williams, R.R. (2003). Transcription and the territory: the ins and outs of gene positioning. Trends Genet *19*, 298-302.

Worman, H.J. (2005). Components of the nuclear envelope and their role in human disease. Novartis Found Symp *264*, 35-42; discussion 42-50, 227-230.

Worman, H.J., Yuan, J., Blobel, G., and Georgatos, S.D. (1988). A lamin B receptor in the nuclear envelope. Proc Natl Acad Sci U S A *85*, 8531-8534.

Wu, X., Kasper, L.H., Mantcheva, R.T., Mantchev, G.T., Springett, M.J., and van Deursen, J.M. (2001). Disruption of the FG nucleoporin NUP98 causes selective changes in nuclear pore complex stoichiometry and function. Proc Natl Acad Sci U S A *98*, 3191-3196.

Yang, L., Guan, T., and Gerace, L. (1997). Integral membrane proteins of the nuclear envelope are dispersed throughout the endoplasmic reticulum during mitosis. J Cell Biol *137*, 1199-1210.

Yang, Q., Rout, M.P., and Akey, C.W. (1998). Three-dimensional architecture of the isolated yeast nuclear pore complex: functional and evolutionary implications. Mol Cell *1*, 223-234.

Ye, Q., and Worman, H.J. (1996). Interaction between an integral protein of the nuclear envelope inner membrane and human chromodomain proteins homologous to Drosophila HP1. J Biol Chem *271*, 14653-14656.

Zabel, U., Doye, V., Tekotte, H., Wepf, R., Grandi, P., and Hurt, E.C. (1996). Nic96p is required for nuclear pore formation and functionally interacts with a novel nucleoporin, Nup188p. J Cell Biol *133*, 1141-1152.

Zipperlen, P., Fraser, A.G., Kamath, R.S., Martinez-Campos, M., and Ahringer, J. (2001). Roles for 147 embryonic lethal genes on C.elegans chromosome I identified by RNA interference and video microscopy. EMBO J *20*, 3984-3992.

Zuleger, N., Korfali, N., and Schirmer, E.C. (2008). Inner nuclear membrane protein transport is mediated by multiple mechanisms. Biochem Soc Trans *36*, 1373-1377.

Publication

Curriculum Vitae

Personal:	**Name:**	**Boopathy Gandhi Theerthagiri Kuppusamy**
	Date of birth:	27th January 1979
	Place of Birth:	Dharmapuri, Tamil Nadu, India.
	Nationality:	Indian
	Permanent address:	19/17, Annamalai Street Dharmapuri – 636701 Tamil Nadu, India.

Education and training:

2007-2010	*Ph.D* in Biochemistry and Cell biology, Friedrich Miescher Laboratory of the Max Planck Society, Germany
2005-2006	*Research Trainee*, McKusick-Nathans Institute of Genetic Medicine, Johns Hopkins University, USA
2002-2006	*Research Scientist*, Institute of Bioinformatics, Bangalore, India
1999-2001	*M.Sc in Biotechnology*, University of Madras, Chennai, India
1996-1999	*B.Sc in Biotechnology*, Bharathiar University, Coimbatore, India
1994-1996	*Higher secondary education*, Dharmapuri, India
1989-1994	*Secondary education*, Dharmapuri, India
Until 1989	*Primary education*, Dharmapuri, India

Publications:

1. Laurell, E., Beck, K., Krupina, K., **Gandhi, T**., Bodenmiller, B., Horvath, P., Abersold, R., Antonin, W. and Kutay, U. Phosphorylation of Nup98 by multiple kinases is crucial for NPC disassembly during mitotic entry. (*Submitted*). (Publication related to this thesis)

2. **Gandhi, T**., Eisenhardt, N., Schwarz, H. and Antonin, W.; The nucleoporin Nup188 controls membrane flow through the nuclear pore complex. ***Journal of Cell Biology*** (2010) 189 (7). (Publication related to this thesis)

3. **Gandhi, T. K. B**., Zhong, J., Suresh, M., Karthick, L., Chandrika, K. N., Mohan, S., Sharma, S., Pinkert, S., Shilpa, N., Bala, P., Mishra, G., Kannabiran, N., Shen, B., Deshpande, N., Nayak, R., Sarker, S., Boeke, J. D., Parmigiani, G., Schultz, J., Bader, J. and Pandey, A; Analysis of the Human Protein Interactome and its Comparison with Yeast, Worm and Fly Interaction Datasets. ***Nature Genetics***. (2006) 38(3):285-93.

4. Mathivanan, S., Periaswamy, B., **Gandhi, T. K. B.**, Kandasamy, K., Suresh, S., Mohmood, R., Ramachandra, Y. L. and Pandey, A. An evaluation of human protein-protein interaction data in the public domain. ***BMC Bioinformatics***. (2006) 7, S19.

5. **Gandhi, T. K. B**., Chandran, S., Peri, S., Saravana, R., Amanchy, R., Prasad, T. S. K and Pandey, A.; A bioinformatics analysis of protein tyrosine phosphatases in humans. ***DNA Research***. (2005) 12, 79-89.

6. Muthusamy, B., Hanumanthu, G., Reshmi, R., Sriranjini, S., Suresh, S., Rekha, B., Srinivas, D., Karthick, L., Vrushabendra, B. M., Sharma, S., Mishra, G., Rashmi, B. P., Kadekar, S., Chatterjee, P., Mangala, K. S., Shivashankar, H. N., Chandrika, K. N., Deshpande, N., Suresh, M., Kannabiran, N., Niranjan, V., Nalli, A., Prasad, T. S. K., Arun, K. S., Reddy, R., Chandran, S., Jadhav, T., Julie, D., Mahesh, M., John, S. L., Palvankar, K., Sudhir, D., P. Bala., Jithesh, M. K., Rashmi, N. S., Vishnupriya, G., Dhar, K., Reshma, S., Raghothama, C., Prasad, C. K. **Gandhi, T. K. B**., Harsha, H. C., Mohan, S. S., Deshpande, K. S., Sarker, M. and Pandey, A; Plasma proteome database as a resource for proteomics research. ***Proteomics.*** (2005) 5(13):3531-6.

7. Ping, P., Vondriska, T. M., Creighton, C. J., **Gandhi, T. K. B**., Yang, Z., Menon, R., Kwon, M. S., Cho, S. Y., Drwal, G., Kellmann, M., Peri, S., Suresh, S., Gronborg, M., Molina, H., Chaerkady, R., Rekha, B., Muthusamy, B., Shet, A. S., Gerszten, R. E., Wu, H., Raftery, M., Wasinger, V., Schulz-Knappe, P., Hanash, S. M., Paik, Y. K., Hancock, W. S., States, D. J., Omenn, G. S. and Pandey, A.; A functional annotation of subproteomes in human plasma. ***Proteomics.*** (2005) 5(13):3506-19.

8. Harsha, H. C., Suresh, S., Amanchy, R., Deshpande, N., Shanker, K., Yatish, A. J., Muthusamy, B., Vrushabendra, B. M., Rashmi, B. P., Chandrika, K. N., Padma, N., Sharma, S., Badano, J. L, Ramya, M. A., Shivashankar, H.N., Peri, S., Choudhury, D. R., Kavitha, M. P., Saravana, R., Niranjan, V., **Gandhi, T. K. B.**, Ghosh, N., Chandran, S., Menezes, M., Joy, M., Mohan, S. S., Katsanis, N., Deshpande, K. S., Raghothama, C., Prasad, C. K., and Pandey, A; A manually curated functional annotation of the human X chromosome. ***Nature Genetics***. (2005) 37, 322-323.

9. Peri, S., Navarro, J.D., Kristiansen T.Z., Amanchy, R., Surendranath, V., Muthusamy, B., **Gandhi, T.K.B**., Chandrika, K.N., Deshpande, N., Suresh, S., Rashmi, B.P., Shanker, K., Padma, N., Niranjan, V., Harsha, H.C., Talreja, N., Vrushabendra, B.M., Ramya, M.A., Yatish, A.J., Joy, M., Shivashankar, H.N., Kavitha, M.P., Menezes, M., Choudhury, D.R., Ghosh, N., Saravana, R., Chandran, S., Mohan, S., Jonnalagadda, C.K., Prasad, C.K., Kumar-Sinha, C., Deshpande, K.S. and Pandey, A; Human Protein Reference Database as a Discovery Resource for Proteomics. ***Nucleic Acids Research***. (2004) 32, D497-501.

10. Peri, S., Navarro, J.D., Amanchy R., Kristiansen T.Z., Jonnalagadda C.K., Surendranath V., Niranjan V., Muthusamy B., **Gandhi T.K.B**., Gronborg M., Ibarrola N., Deshpande N., Shanker K., Shivashankar H.N., Rashmi B.P., Ramya M.A., Zhao, Z., Chandrika K.N., Padma N., Harsha H.C., Yatish A.J., Kavitha M.P., Menezes M., Choudhury D.R., Suresh S., Ghosh N., Saravana R., Chandran S., Krishna S., Joy M., Anand S.K., Madavan V., Joseph A., Wong G.W., Schiemann W.P., Constantinescu S.N., Huang L., Khosravi-Far R., Steen H., Tewari M., Ghaffari S., Blobe G.C., Dang C.V., Garcia J.G.N., Pevsner J., Jensen O.N., Roepstorff P., Deshpande K.S., Chinnaiyan A.M., Hamosh A., Chakravarti A. and Pandey A; Development of Human Protein Reference Database as an initial platform for approaching systems biology in humans. ***Genome Research***. (2003) 13, 2363-2371.

11. **Gandhi, T.K.B**. and Pandey, A; Using bioinformatics to identify *cis*-regulatory sequences. ***Trends in Biotechnology***. (2002) 20, 448.

Scholarships:

Max-Planck-Society PhD scholarship (2007-2010).